UNIVERSITA' DEGLI STUDI DI PADOVA

SCUOLA DI DOTTORATO DI RICERCA IN SCIENZE DELLE PRODUZIONI VEGETALI

INDIRIZZO AGROBIOTECNOLOGIE- CICLO XXI

Dipartimento di Agronomia Ambientale e Scienze delle Produzioni Vegetali

Genetic determination of aroma in grapevine (*Vitis vinifera* L.)

From QTL to gene expression analysis in aromatic and non-aromatic varieties

Direttore della Scuola: Ch.mo Prof. Andrea Battisti

Supervisore: Ch.mo Prof. Angelo Ramina

Dottorando: Juri Battilana

DATA CONSEGNA TESI

02 febbraio 2009

to Mattia and Silvia

Declaration

I hereby declare that this submission is my own work and that, to the best of my knowledge and belief, it contains no material previously published or written by another person nor material which to a substantial extent has been accepted for the award of any other degree or diploma of the university or other institute of higher learning, except where due acknowledgment has been made in the text.

Battilana Juri, 2-02-2009

A copy of the thesis will be available at *http://paduaresearch.cab.unipd.it/*

Dichiarazione

Con la presente affermo che questa tesi è frutto del mio lavoro e che, per quanto io ne sia a conoscenza, non contiene materiale precedentemente pubblicato o scritto da un'altra persona né materiale che è stato utilizzato per l'ottenimento di qualunque altro titolo o diploma dell'università o altro istituto di apprendimento, a eccezione del caso in cui ciò venga riconosciuto nel testo.

Battilana Juri, 2-02-2009

Una copia della tesi sarà disponibile presso *http://paduaresearch.cab.unipd.it/*

Table of Contents

Riassunto

L'interesse della ricerca sull'aroma è stato rivolto negli ultimi decenni soprattutto al chiarimento della struttura, della biosintesi, della distribuzione nella pianta e dell'evoluzione durante la maturazione dei composti che ne sono responsabili. Per contro, le conoscenze dei meccanismi molecolari (natura dei geni e degli enzimi coinvolti e loro regolazione) che controllano tale carattere sono ancora limitate.

Il percorso di ricerca svolto durante il dottorato è iniziato con l'identificazione, attraverso l'analisi QTL (Quantitative Trait Loci) dei composti di natura terpenica responsabili della sensazione aromatica, quali: linalolo, nerolo e geraniolo, delle regioni genomiche statisticamente coinvolte nella determinazione del carattere aroma Moscato in due popolazioni derivate dall'incrocio tra due varietà di *V. vinifera*: Italia e Big Perlon (300 piante F1); e dall'incrocio interspecifico di *V. vinifera* cultivar Moscato Bianco e *V. riparia* (175 piante F1).

Il peso maggiore nella determinazione del contenuto dei monoterpeni è stato attribuito ad una regione genomica di circa 1.3 cM del Cromosoma 5 di vite che arriva a spiegare, in alcune annate, fino al 90% della variazione fenotipica del carattere studiato. Approfondendo lo studio, si è visto che l'enzima 1-deoxy-D-xylulose 5-phosphate synthase (DXS) è codificato da un gene posizionato nell'intervallo di confidenza del QTL nel cromosoma 5. Da qualche anno si sa che questa proteina svolge un ruolo catalitico nel primo e limitante step della biosintesi plastidiale dell'Isopentenil difosfato, il precursore dei terpeni nelle cellule vegetali. Altri studi hanno dimostrato che è un enzima essenziale per i batteri ed è cruciale per la formazione della clorofilla e dei carotenoidi nelle piante. Nel genoma della vite abbiamo identificato diverse forme del gene *DXS* corrispondenti alle classi 1, 2 e 3 già descritte in altre specie vegetali**.**

Nel corso del dottorato è stata studiata la cinetica di espressione genica durante la maturazione delle uve rispetto all'evoluzione del profilo metabolico di alcune varietà aromatiche (Moscato Bianco e Chardonnay clone 809) e non aromatiche (Chardonnay clone 130), al fine di comprendere a quale livello eventualmente si esplica la funzione di controllo di questo gene sull'accumulo dei composti terpenici.

L'analisi chimica e le osservazioni in campo ripetute in tre anni consecutivi (2005, 2006 e 2007), ci ha permesso di caratterizzare in modo accurato le varietà considerate, sia dal punto di vista metabolico che dal punto di vista fisiologico. Interessanti differenze sono state evidenziate, non solo in termini di concentrazioni massime dei singoli composti identificati, ma soprattutto in termini di cinetiche di accumulo, in relazione alla varietà ed all'annata considerata. Alcuni monoterpeni identificati, infatti, mostrano differenze che si possono attribuire ad un effetto stagione, mentre altri composti evolvono in funzione dello stadio di sviluppo delle bacche. L'effetto dell'influenza di fattori ambientali e degli stress sull'espressione di *DXS1* e sull'attività dell'enzima che ne deriva sarà dunque un altro obiettivo da affrontare, magari con approcci di ingegneria metabolica.

Infine, lo studio di una parte del trascrittoma di vite, attraverso l'analisi Microarray, confrontando due fasi interessanti in termini di accumulo di monoterpeni, della maturazione delle bacche in due cloni della cultivar Chardonnay (aromatico e non), ci ha permesso di identificare alcuni pathway metabolici implicati nel normale sviluppo delle bacche, ma coinvolti anche nella regolazione della trascrizione dell'RNA, nel trasporto, nel metabolismo secondario (in particolare la via di biosintesi di fenilpropanoidi e lignine), nella formazione della parete cellulare ed infine nella risposta agli stress. Questo ci ha permesso di definire un set di geni candidati su cui varrà la pena approfondire gli studi futuri.

Dalle informazioni prodotte finora, sono stati generati marcatori del DNA con elevate capacità predittive che possono essere già applicati alla selezione dei semenzali in programmi di miglioramento genetico per le qualità aromatiche di varietà da vino o da tavola. Altre possibili ricadute di questo studio si intravedono per il settore viti-enologico, per esempio, nello sviluppo di test diagnostici dello stato metabolico delle uve in vigneto o in cantina e nel suggerimento di nuove pratiche colturali ed enologiche che garantiscano l'espressione elevata e costante del potenziale aromatico delle uve.

Summary

Major goals of plant functional genomics are the identification of genes underlying agriculturally important traits and to understand their biological functions. In recent years, progress in this field has been significantly supported by the study of the genetic determinism of phenotypic traits, however examples in grape are still very scarce. Currently consumers are looking for both aromatic presence in table grape and the persistence and complexity of aroma in wine. The flavour content (taste and aroma) influence directly on wine microstructure by playing an essential role in high-quality winemaking. The many compounds contributing to flavour are determined in vineyards through complex interactions among genotypes, environment and cultural practices. Enological processes and individual sensorial perception play also critical roles in determining flavour of the wine (Lund and Bohlmann, 2006). However, the value of a wine is mainly related to the quality of the grape berries. Gene interaction and biochemical mechanisms that enhance high-quality wines production during the biphasic growth of grape berries are for instance still unknown, though the economic relevance of the sector.

The first objective of the present PhD thesis was to identify the major genome regions controlling the variability of muscat aroma and monoterpenic odorant content in grape berries, through QTL detection in two mapping populations derived from the intra-specific cross Italia x Big Perlon (300 F1 individuals) and the inter-specific cross Moscato Bianco x *Vitis riparia* (175 F1 individuals). Experiments at IASMA Research Centre led to the co-localization of *DXS1* (1-deoxy-D-xylulose 5-phosphate synthase class 1 gene in both linkage maps and through the years of analysis with a major QTL explaining a high percentage of the total variance.

A second effort was oriented to the understanding of the role of candidate gene in the expression of Muscat aroma trait. This was carried out by evaluating the trascriptomic profile of *DXS1* during the whole maturation period of the berry, comparing grapes of two aromatic (Moscato Bianco and Chardonnay clone 809) and one non-aromatic grapevine varieties (Chardonnay clone 130). Volatiles of grape berries were monitored during ripening by analyzing the composition of the berries extracts at 13 different phenological stages for three years.

Berry development was considerably affected by the diverse climatic conditions occurred in the years. Ripening time was similar but not equal in 2005 and 2006. On the contrary, in the warm 2007 season, berries development was 10 to 20 days ahead of time, depending of the variety. This is reflected on some monoterpenoids accumulation that seems to be slightly dependent only by the growing stage, while other compounds seem to be significantly depending by environmental conditions.

The results of *DXS1* expression showed that a particular trend rather than the level of expression ratio could be responsible for this trait.

Finally, microarray experiments were performed by using two cDNA pools from different ripening stages of the two Chardonnay clones which differ for the aromatic metabolic profile. The functional categorization and biological function of the genes found differentially expressed were involved in RNA regulation of transcript, transport, secondary metabolism (phenylpropanoids and lignin biosynthesis), cell wall and stress signalling pathways that can overlap or converge at specific points during grape development and aroma biosynthesis.

This study increased our knowledge about the genetic determinism of aroma in grape since 1) the genome regions controlling the phenotypic variation were characterized and 2) the correlation of the level of metabolic compounds during grape maturation with candidate genes transcription profiling was described. The results presented here allow us to plan further functional genomics studies in order to clarify the gene networks that can be involved in this important and complex quality trait. However the available information is ready to be applied in marker assisted breeding programmes for the rapid screening of seedlings having the potential to express the desired fruit traits. Moreover this study is opening new perspectives for the management of grape quality also in the vineyards.

Capitolo I

The 1-deoxy-D-xylulose 5-phosphate synthase gene co-localizes with a major QTL affecting monoterpenes content in grapevine

1.1. Introduction

Aroma plays an essential role in high-quality winemaking and is greatly appreciated for fresh grape consumption as well. Different combinations and concentrations of several fruit compounds define the so-called 'varietal aroma', which, in turn, affects wine 'character' (Ribéreau-Gayon et al. 2000). Numerous studies have revealed that the typical flavor of Muscat grape varieties is closely related to the presence of C10 terpene molecules (monoterpenes). Each compound has distinct organoleptic features and interacts with the others, thus contributing to shape the final aroma of the mixture. In particular, linalool, geraniol, nerol, citronellol and α-terpineol are often described as the major aromatic determinants based on their high concentrations in Muscat cultivars and their low olfactory perception thresholds (Ribéreau-Gayon et al. 1975; Mateo and Jiménez 2000). Moderate concentrations of monoterpenes can be found also in aromatic but non-muscat varieties (i.e. Gewürztraminer, Rhine Riesling and relevant crosses, Sylvaner, some Malvasias). Monoterpenes have been found both in grape leaves and berries as free volatiles, free polyhydroxylated molecules (polyols) and glycosidic derivatives of the two former types. Only the free volatile compounds make a direct contribution to the aroma, whereas free polyols and glycosidic derivatives constitute a reserve of odorless precursors, which generate flavor upon hydrolysis. The distribution of monoterpenes within the berry is not uniform: free geraniol and nerol are concentrated in the skin, whereas free linalool is more evenly distributed, like the glycosidic forms (Strauss et al. 1986).

Monoterpenes belong to the terpenoid family, which is the largest and most diverse group of natural compounds including both primary and secondary metabolites with a great variety of biological functions. Monoterpenoids, sesquiterpenoids, diterpenoids and triterpenoids are considered secondary metabolites of ecological significance since many of them mediate plant–environment interactions (Mahmoud and Croteau 2002). Plants synthesize the precursors of all terpenoids, isopentenyl diphosphate (IPP) and dimethylallyl diphosphate (DMAPP), by two independent pathways: the mevalonic acid (MVA) and the methylerythritol phosphate (MEP) pathways, which are localized respectively in cytoplasm and plastids (Lichtenthaler 1999). Terpene synthases (TPS) are

the primary enzymes responsible for catalyzing the formation of hemiterpenes (C5), monoterpenes (C10), sesquiterpenes (C15) or diterpenes (C20). The biosynthesis of monoterpenes via the plastidial pathway was demonstrated both in grape leaves and berries (Luan and Wüst 2002). At least five complementary dominant genes plus a modifier gene have been proposed to be involved in the regulation of Muscat flavor (Wagner 1967). To date, only a few genetic studies concerning enzymes implicated in terpene biosynthesis have been reported for V. vinifera. Clastre et al. (1993) purified and characterized a geranyl diphosphate synthase. Lücker et al. (2004) identified two V. vinifera sesquiterpene synthases: (+)-valencene synthase and (−)-germacrene D synthase. Martin and Bohlmann (2004) functionally characterized a (−)-α terpineol synthase. Mathieu et al. (2005) identified a potential V. vinifera carotenoid cleavage dioxygenase (CCD) gene. However, having the complete sequence of the grape genome, several TPS genes were recently predicted, ranging in number between 35 (Velasco et al. 2007) and 89 (Jaillon et al. 2007).

With the aim of improving our knowledge about the genetic determinism of Muscat flavor in grape, we carried out QTL analysis on two F1 mapping populations, which were analyzed for the content of several aromatic compounds during more than one season. The genomic regions controlling the phenotypic variability under study were further characterized by applying the candidate gene approach (Pflieger et al. 2001). This method has been recognized, especially in plants with large genomes and long generation times, as a promising alternative to the money and labor-consuming positional cloning (reviewed in Remington et al. 2001; Paran and Zamir 2003) in order to identify and isolate genes governing important traits (Morgante and Salamini 2003; Salvi and Tuberosa 2005). In the most widespread version the candidate gene approach attempts to link, through mapping analysis, QTLs that are responsible for the studied variation with sequences that play a potential role in the measured phenotype or have a structural similarity to known genes, i.e. R-gene analogues. The availability of whole genome sequences and expressed sequence tag (EST) databases for important crops is accelerating the process of gene discovery. Grape can be placed among the best characterized plant species with respect to ESTs (Da Silva et al. 2005) and the genomic sequence of Pinot noir, a widely cultivated variety, has been recently made available (Jaillon et al. 2007; Velasco et al. 2007). In

three cases we observed co-segregation between the CG loci and QTLs for the content of the main aromatic monoterpene compounds. This represents an important advancement towards marker-assisted selection for crop improvement. The selection of new varieties based on key genes for flavor determination and the adoption of practices promoting their expression represent some of the perspectives of this research.

1.2. Materials and Methods

1.2.1. Plant material

Two mapping populations were considered in this study: Pop1 (163 F1 individuals, intraspecific) and Pop2 (174 F1 individuals, interspecific), which segregate for Muscat flavor and other traits. They derived respectively from the crosses Italia (*V. vinifera*) x Big Perlon (*V. vinifera*) and Moscato Bianco (*V. vinifera*) x *V. riparia* (accession Wr 63 from the IASMA Ampelographic Collection). Pop1 and Pop2 have been grown at the Experimental Station of the University of Bari and of IASMA (Italy) respectively. Good quality DNA was extracted from young leaves following the protocol described in Grando et al. (2003).

1.2.2. Candidate gene selection

Candidate gene choice was carried out in two steps. A first set of 19 V. vinifera ESTs was directly selected from the public database TGI (http://compbio.dfci.harvard.edu/tgi/cgi-bin/tgi/gimain.pl?gudb=grape, Release 3.1) by using keywords related to terpenoid metabolism (mevalonate and non-mevalonate pathways of IPP biosynthesis, monoterpenoid and diterpenoid metabolism). A second set of 51846 ESTs was extracted from the TGI database (Release 4.0) based on 650 gene ontology terms associated with berry composition and ripening. ESTs were checked for quality and assembled with cd-hit software (Li and Godzik 2006) in order to remove redundant sequences (identity > 80%). Functional characterization was available for 6637 ESTs after BLASTX alignment (E-value ≤ 1 e-6) against a UniProt (http://www.expasy.uniprot.org/) partition containing only proteins annotated by one of the selected GO terms. Ninety-three sequences with a

potential role in berry flavor (106 GO terms) were extracted from this characterized pool, clustered with CAP3 software (Huang and Madan 1999; terminal alignment ≥ 40 bases, identity ≥ 90%) and checked for belonging to TC (tentative consensus) sequences in TGI database. This procedure finally resulted in the selection of 53 putative CGs.

1.2.3. Amplification

Specific primers were designed for each EST by using the software Primer Express (Applied Biosystems, Foster City, CA, USA). In most cases, the polymerase chain reaction (PCR) mixture (12.5 µl) contained 5–10 ng of genomic DNA, 1.25 µl of 10X PCR buffer (QIAGENE, Valencia, CA, USA; 1.5 mM of MgCl2), 40 µM of each dNTP, 0.6 µM of each primer and 0.5 unit of HotStarTaq polymerase (QIAGENE). Amplification was carried out by using a GeneAmp PCR System 9700 (Perkin-Elmer, Norwalk, CT, USA) and a touchdown protocol (Don et al. 1991). Primer sequences and detailed amplification conditions are reported in Table 1.

Table 1 Nucleotidic sequence of the primers used for PCR amplification of the CG markers developed in this study.

Marker	Primer sequence	Primer conc.	MgCl2 conc.	Taq polymerase 0.04U/µl	Amplification program
G10H	Forward: GTGTTAAATAAACTCGGAAGTCTTT	0.6 µM	1.5 mM	HotStar	Program 1
	Reverse: TAATTTGCACTTAAATGGCTATCAA	0.6 µM			
PMVAK	Forward: ACCCAATGCAGGAATAGTGC	0.6 µM	1.5 mM	HotStar	Program 1
	Reverse: ACTGCTTGCTCAACGAAAGG	0.6 µM			
YGBB	Forward: CGAGTGTGCGCAAGTTGTAT	0.6 µM	1.5 mM	HotStar	Program 1
	Reverse: TGCATGAAGCAGGCTATGAG	0.6 µM			
ISPH	Forward: TCTTCTTCCTCGTCTGTGGC	0.6 µM	1.5 mM	HotStar	Program 1
	Reverse: TTTCGCTGTAACATTTCCCC	0.6 µM			
GGPP-S	Forward: TCCCGAGATTTCTCAATACCC	0.6 µM	1.5 mM	HotStar	Program 1
	Reverse: GGAAATTTGCCAGATGTATAGGG	0.6 µM			
DXS	Forward: TGAATCTCTTCCATCGCCG	0.6 µM	1.5 mM	HotStar	Program 1
	Reverse: TGGCAGTTCAACACCCACC	0.6 µM			
CDP-ME	Forward: TTCCATCAGAAGAACCACCC	0.6 µM	1.5 mM	HotStar	Program 1
	Reverse: ATCCTTTGTTTTTGATGGCG	0.6 µM			
CRTISO-sscp	Forward: AATCATTGCTCTTCATCCGC	1.0 µM	1.5 mM	HotStar	Program 2
	Reverse: TAATGGCACGTATGGACCAA	1.0 µM			
ACTRANS	Forward: GTTTGCATTGTTGGTGTTGC	0.6 µM	1.5 mM	HotStar	Program 1

	Reverse: TGTCTAGCAGGAGCCTGTCC	0.6 μM			
B-diox-II-sscp	Forward: GGAGAGTTTGTCAGGGTTG	0.6 μM	1.5 mM	HotStar	Program 1
	Reverse: AAGTACACCAAAACGAGCCT	0.6 μM			
IPPISOM	Forward: TGCACAAAGAAAGCTGTTGG	0.6 μM	1.5 mM	HotStar	Program 1
	Reverse: GCAACTTCATCAGGGTTTGG	0.6 μM			
HMGS	Forward: GGTCGGCTGGAAGTAGGC	0.6 μM	1.5 mM	HotStar	Program 1
	Reverse: AGCTGCTCCTCCAGTAGGC	0.6 μM			
Gib20ox	Forward: GTCTTCGGCACCAATCCAAC	0.6 μM	1.5 mM	HotStar	Program 1
	Reverse: TCACCAGATCGGTCCTGATG	0.6 μM			
DXR	Forward: GCACACTATCTGTTTGGGGC	0.6 μM	1.5 mM	HotStar	Program 1
	Reverse: AGAACTCCTGTCATGGTGCC	0.6 μM			
Gib2ox	Forward: TCCACCATGTTCAGAGCTTC	0.6 μM	1.5 mM	HotStar	Program 1
	Reverse: R TCTTGACTTGTAAGCAGACC	0.6 μM			
DHAP-s	Forward: GTGCCATGCAGAGAGTGTCA	0.6 μM	1.5 mM	HotStar	Program 1
	Reverse: GGCCAGTTGTTGAATCCTGT	0.6 μM			
DHAP-S-p	Forward: TGGCATCAAGGTGAGCAATA	1.0 μM	1.5 mM	HotStar	Program 2
	Reverse: AGATGAACTCCTCCAGGGTGG	2.0 μM			
FAH1	Forward: TGGATCTCTCGGTGGTTCAGT	0.6 μM	1.5 mM	HotStar	Program 1
	Reverse: GCATTGTCACGCAGTGTTGG	0.6 μM			
FAH	Forward: GGAAGAATCTTGCCTGAGCA	0.6 μM	1.5 mM	HotStar	Program 1
	Reverse: CGATCTCCTTGGAACTGGAA	0.6 μM			
HPD1-sscp	Forward: GGTGGATAAGGATGATCAAGG	0.6 μM	1.5 mM	HotStar	Program 1
	Reverse: GTCTACGATTCGCTTGGCTC	0.6 μM			
HPD	Forward: GATGGTGTTGCTGCCGTTG	0.6 μM	1.5 mM	HotStar	Program 1
	Reverse: TAAGTTGGTGGTGGCGAGG	0.6 μM			
PHEA-sscp	Forward: ACTCCAACACTGGAAGTGCC	0.6 μM	1.5 mM	HotStar	Program 1
	Reverse: TCCAAGATCCAGCATCATCA	0.6 μM			
IGPS	Forward: GCTTCTTGAAGGAGACGTGG	0.6 μM	1.5 mM	HotStar	Program 1
	Reverse: GATCCACTCCAATGCAGGTT	0.6 μM			
PAL	Forward: GCTCCATTCCACTCCTTCAA	0.6 μM	1.5 mM	HotStar	Program 1
	Reverse: AGGCAAGTCCTAGTCGAGCA	0.6 μM			
PAI1	Forward: CTATTTGAACGTGGTGACAA	0.6 μM	1.5 mM	HotStar	Program 1
	Reverse: ACAGCACTCCCAAAGGCACT	0.6 μM			
trpB	Forward: CTGGTTGCATGTGTAGGTGG	0.6 μM	1.5 mM	HotStar	Program 1
	Reverse: TCCAGGCCAGCACTAATAGAA	0.6 μM			
TAT	Forward: TCCATGGCTGTAATGGTGAA	1.0 μM	1.5 mM	HotStar	Program 2
	Reverse: AGGTCACTGCTGTTGGATGA	1.0 μM			
HGOb-sscp	Forward: TTGCGGTGGTAATAAGGAGG	0.6 μM	1.5 mM	HotStar	Program 1
	Reverse: GGTTGCTTGGCATGGTAACT	0.6 μM			
HGOa	Forward: TCCAGTACCAATTCGGCTTC	0.5 μM	2 mM	GoldTaq	Program 2
	Reverse: GTCTGGCAGATCAACAACGA	0.5 μM			
AIP	Forward: CTGCTTCCTTCCTTCACACC	0.6 μM	1.5 mM	HotStar	Program 1
	Reverse: AGGCATTGGAACTCTGGATG	0.6 μM			
pepA1	Forward: TTCTGATGGTGCTGCAATGT	0.6 μM	1.5 mM	HotStar	Program 1
	Reverse: GAGCATGTTCTGTGACGAGC	0.6 μM			

cnd41	Forward: CCAATGACGACAGATCCTGG Reverse: GAACGCCAAGCAGGTAAGAC	0.6 µM 0.6 µM	1.5 mM	HotStar	Program 1
conG-p	Forward: TCGACTCTGATCAGCACCAC, Reverse: GAGTTCCACGGAATAGCAGC,	0.6 µM 0.6 µM	1.5 mM	HotStar	Program 1
pDNAbP	Forward: TCTGGTTGTGCGTCCACTTG Reverse: CGACATCCGATCCGGTATCC	0.6 µM 0.6 µM	1.5 mM	HotStar	Program 1

Abbreviations: conc = concentration; U = unit; HotStar = HotStarTaq polymerase (QIAGENE); GoldTaq = AmpliTaq Gold DNA polymerase (Applied Biosystems)

Program 1: 10 min at 94 °C; 11 cycles of 45 sec at 94 °C, 45 sec at 62 °C with –0.5 °C/cycle, 1min at 72 °C; 24 cycles of 45 sec at 94 °C, 45 sec at 57 °C, 1min at 72 °C; 10 min at 72 °C

Program 2: 10 min at 94 °C; 11 cycles of 45 sec at 94 °C, 45 sec at 60 °C with –0.5 °C/cycle, 1min at 72 °C; 24 cycles of 45 sec at 94 °C, 45 sec at 55 °C, 1min at 72 °C; 10 min at 72 °C

1.2.4. Sequencing

Two to four nanograms of amplified DNA were employed for every 100 bp to be sequenced in both directions. PCR products were purified with ExoSapIT (Amersham Pharmacia Biotech, Uppsala, Sweden) and sequenced with the Big Dye ® Terminator v 3.1 Cycle Sequencing Kit (Applied Biosystems) in a GeneAmp PCR System 9700. After precipitation, the sequencing products were mixed with 15 µl of HiDiTM formamide and subjected to capillary electrophoresis in an ABI PRISM 3130xl Genetic Analyzer (Applied Biosystems). The resulting data were analyzed with the softwares Sequencing analysis v 3.7 (Applied Biosystems) and ChromasPro v 1.3 (http://www.technelysium.com.au).

1.2.5. Marker development and analysis

Markers for the CG sequences were generated by SSCP (single strand conformational polymorphism) and minisequencing methods.

SSCP: The gel was prepared between two glasses by mixing 7.5 ml of MDE gel solution (FCM BioProducts, Rockland, ME, U.S.A), 17.7 ml of H_2O, 3 ml of glycerol 50% v/v, 8 ml of TBE 10X, 18.8 µl of TEMED and 150 µl of APS 10% w/v. Five microlitres of PCR products were added with 7 µl of SSCP loading buffer and denatured for 3 min at 95 °C.

The electrophoresis run was performed for 15–16 h at a constant voltage of 135 V. The visualization of SSCP polymorphisms followed Sanguinetti et al. (1994).

Minisequencing with SnaPshot technique: The primers (Table 2) were designed with the software Primer Express (Applied Biosystems) and added with a variable length tail in order to multiplex the minisequencing products. PCR fragments were purified with ExoSapIT. The minisequencing reaction was performed in a GeneAmp PCR System 9700 following the recommendations of the manufacturer (Applied Biosystems). The minisequencing products (0.5 µl) were mixed with 9.45 µl of HiDiTM formamide and 0.05 µl of GeneScan-120 LIZ size standard (Applied Biosystems) and run in an ABI PRISM 3130xl Genetic Analyzer (Applied Biosystems). The resulting data were analyzed with the software GeneScanTM v 3.7 (Applied Biosystems).

Table 2 SNaPshot list primers

SNP marker	Primer sequence	
YGBB	Forward:	GACCTGATAGCCTCCTTGTG
DXS	Forward:	AATCAAATGCTATGGTATAA
DHAP-s	Reverse:	AGCCCATATTTTAGTAGTGT
DHAP-S-p	Reverse:	GGTAACCAATTTAATGCTGG
FAH1	Reverse:	TCAACAAGTTCTTGGGAATG
FAH	Forward:	GAAGCACCAAGACAATAAAC
HPD	Forward:	ACACTGCGGGAGATGAGGCG
IGPS	Forward:	CCTATGCTTCTCTGTGTTTA
PAL	Forward:	TCTCTTTCACCATTGATCAG
PAI1	Reverse:	ATTATTTTCCAGTCATCCCT
trpB	Reverse:	CAGCCTAACGTCTTCATCAT
TAT	Forward:	CACAGACAAAATTGTAGCAC
HGOa	Forward:	AGTTCAGGTAAACCTCGCTC
AIP	Forward:	GGCCATCAGAAAATCAAACA
pepA1	Reverse:	CACAATTGATTCTATCGATG
cnd41	Forward:	TTCAAGGGTAATCTCAAGGA
conG-p	Forward:	AACAACGTATGGAGGATTGT
pDNAbP	Reverse:	GTCACGGAGCTGCTAAAACC

1.2.6. Map construction

Parental and consensus linkage maps were constructed in Pop1 as described by Costantini et al. (2008). The same method was applied to Pop2, for which linkage maps were previously reported by Grando et al. (2003). An updated mapping set was used here based on 174 F1 individuals genotyped at 119 loci with SSR (Simple Sequence Repeat), EST and RGA (Resistance Gene Analog) markers.

1.2.7. Metabolite profiling and quantification

Berries were collected from each genotype when their sugar content was approximately 16 °Brix. This value was established in the framework of the EU-Project MASTER (Marker Assisted Selection for TablE gRape) in order to compare QTLs detected for the same trait in different genetic backgrounds, including the progeny described by Doligez et al. (2006). With the aim of minimizing the great variability among the different berries of the same cluster as well as among the berries of different clusters, sugar concentrations from 3 randomly taken berries per cluster and 2-3 representative clusters per genotype were averaged.

Pop1: The content of free linalool, geraniol and nerol was evaluated in three consecutive years (2002, 2003, 2004) in Pop1 and its parental varieties by using SPME (solid phase micro-extraction) method according to Doligez et al. (2006). One hundred grams of frozen berries were put in a glass jar (500 ml) to which were added 60 grams of $(NH_4)_2$ SO_4 in 50 ml of MilliQ water (Millipore, Bedford, MD, USA) and deuterated standards: 115 µg kg-1 of linalool-d5; 93.7 µg kg-1 of geraniol-d2 and 65.6 µg kg-1 of nerol- d2, these latter compounds as a mixture. All internal standards were supplied by INRA of Montpellier (France) and were synthesized as described in Doligez et al. (2006). After homogenization, forty millilitres of this solution and a magnetic stir were placed in a 50 ml vial, sealed and equilibrated for 10 min at 30 °C. A polyacrylate (PA)-coated fiber (85 µm; PA Codex: 57304, Supelco, Bellefonte, USA) was exposed in the headspace for 30 min and then desorbed at 250 °C for 5 min in a GC-injector by working in splitless mode. High-resolution gas chromatography-mass spectrometry was performed using a PerkinElmer gas chromatograph with a TurbomassGold Mass Spectrometer equipped

with a DBWax fused silica column (60 m x 0.32 mm I.D., 0.5 μm film thickness). Helium with a flow rate of 4 ml min-1 was used as carrier gas. The oven program was as follows: 50 °C, 4 °C min-1 to 190 °C, 10 °C min-1 to 220 °C, 220 °C for 10 min. Detector temperature was set to 220 °C. In 2002 a MS detector was employed; both *total ion chromatograms* (TIC) and *selection ion recording* (SIR) profiles were obtained. In 2003 and 2004 monoterpenic compounds, that were well detectable also by a flame ionization detector (FID), were quantified by GC-FID. Calibration curve was achieved using a neutral grape (Alphonse Lavalle); berries of similar size and color were added with linalool (22.4 μg ml-1), nerol (22.0 μg ml-1) and geraniol (22.2 μg ml-1) (Aldrich, > 97 %; checked as for the purity of each compound in respect of the other two) dissolved in MilliQ water and ethanol (1:1, v/v) to get a final concentration in the range of 0 to about 300 μg kg-1 (7 scores) but also to control the linearity of the curve until 1.5 mg kg-1 (1 score).

Pop2: In Pop2 and its female parent (Moscato Bianco) linalool, nerol and geraniol were quantified in two years (2002 and 2004) in their free and bound forms by using SPE (solid phase extraction) method. According to Versini et al. (1988) and Günata et al. (1989), the juice obtained by crushing 100 grams of frozen berries was submitted to a XAD-2 resin (particle size: 0.2–0.25 mm). The two adsorbed forms were separately eluted, the bound ones were hydrolyzed as aglycons after reaction with AR 2000 enzyme (Gist Brocades) and both fractions were enriched in an organic solvent solution. The analytical methodology was the same as in the cited papers; the quantification by HRGC-MS analysis was referred to the internal standard 1-heptano with response factor (RF) = 1.

1.2.8. Data and QTL analysis

Metabolic data were tested for normality with the Kolmorogov–Smirnov test. When not normally distributed, they were ln-transformed. Correlations between years within traits and between traits within years were determined with the non-parametric Spearman rank correlation test. Both tests were implemented in the software SPSS v 15.0.

QTL detection was carried out with the software MapQTL v 4.0 (Van Ooijen et al. 2002) on the four parental varieties by separately analyzing every year of phenotypic evaluation. Non-parametric Kruskal–Wallis (KW) rank-sum test and interval mapping (Lander and

Botstein 1989) methods were applied. In multiple QTL mapping (MQM) the markers closest to the QTLs found with either simple interval mapping (SIM) or KW were employed as cofactors. For SIM LOD thresholds at 0.95 of significance were determined through 1000 permutations at both chromosome-wide and genome-wide level (Churchill and Doerge 1994); for MQM the same values as for SIM were used, since this function is not available in MapQTL. One-LOD support interval was adopted for the confidence interval.

1.2.9. In silico analysis

The total number of genes underlying QTLs on LGs 5 and 10 was estimated through the procedure described in Velasco et al. (2007). Based on the results obtained from QTL analysis in Pop1, gene prediction was performed at 3 different magnification levels on the genomic sequence of Pinot Noir clone ENTAV115: 1) within the region encompassed by the two closest SSR markers to the LOD peak (on LG 10) or between the only microsatellite mapped on one side of the LOD peak and the end of the genomic metacontig on the other side (on LG 5), 2) within the region where the LOD values were above the genome-wide LOD threshold (P = 0.05) and 3) in the 1-LOD interval. Mean values across traits and years were calculated for the length of these regions.

In order to investigate *DXS* gene copy number and organization, the genomic sequence of grapevine (Jaillon et al. 2007; Velasco et al. 2007) was screened with BLASTN algorithm by using as query sequence the TGI tentative consensus on which marker DXS was developed (TC56417). Nucleotide and amino acid sequence analysis of the aligning genomic contigs was performed with online bioinformatic tools: the softwares FGENESH v 2.5 (Salamov and Solovyev 2000) for prediction of potential genes, FGENESH+ (Salamov and Solovyev 2000) and GeneWise v 2.0 (Birney et al. 2004) for analysis of gene structure, Predotar v 1.03 (Small et al. 2004) and SignalP v 3.0 (Bendtsen et al. 2004) for prediction of protein subcellular localization. Protein organization into functional domains was derived from Conserved Domain Database (http://www.ncbi.nlm.nih.gov/Structure/cdd/cdd.shtml).

1.3. Results

1.3.1. Marker development and analysis

Specific primer pairs were designed for 53 CG sequences and tested on the two parents of Pop1, Italia and Big Perlon (Figure 1). Forty-six of them produced a unique and reproducible band. They were initially assessed for single strand conformational polymorphisms in a six individual-subset of the Italia x Big Perlon progeny. Segregating polymorphisms were detected in 16 cases. The remaining 30 sequences produced monomorphic profiles and were thus sequenced in both parents in order to identify single nucleotide polymorphisms (SNPs). All of them were confirmed to correspond to the originally selected genes through BLASTN alignment against the database TGI. Twenty-one sequences contained SNPs, which were successfully detected in 18 cases with minisequencing. Altogether, 34 EST-derived markers were developed (Table 3).

Figure 1

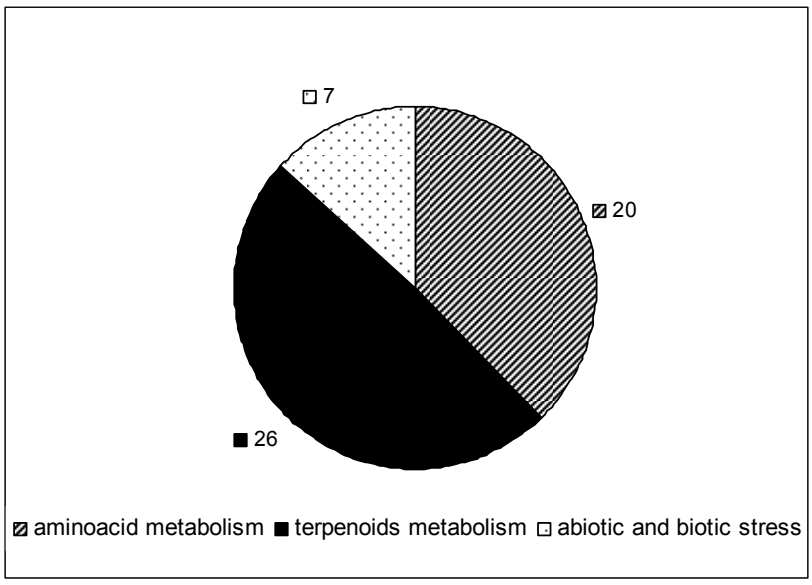

From 53 candidate genes selected, 26 are involved in the metabolism of terpenoids, 20 in the metabolism of aromatic amino acids and 7 in stress or regulation of chloroplast gene expression

Table 3 List of the CG markers positioned onto Italia and Big Perlon maps

A) Terpenoid metabolism

Marker	LG	cM	TC	Annotation	Method
G10H[a]	2	47.6	TC9597[b]	Geraniol 10-hydroxylase	SSCP
PMVAK[a]	2	50.6	TC34499	Phosphomevalonate kinase	SSCP
YGBB	2	92.0	TC58474	2-C-methyl-D-erythritol 2,4-cyclodiphosphate synthase, chloroplast precursor	SNP
ISPH	3	20.9	TC14300[b]	LYTB-like protein precursor	SSCP
GGPP-S	4	46.7	TC51973	Geranylgeranyl pyrophosphate synthetase, chloroplast precursor	SSCP
DXS	5	2.7	TC56417[c]	1-deoxy-D-xylulose 5-phosphate synthase	SNP
CDP-ME	6	14.4	TC14915[b]	4-diphosphocytidyl-2-C-methyl-D-erythritol kinase, chloroplast precursor	SSCP
CRTISO-sscp[d]	8	73.2	TC62553	Carotenoid isomerase, chloroplast precursor	SSCP
ACTRANS[a]	12	34.4	TC52127	Acetoacetyl-CoA thiolase	SSCP
B-diox-II-sscp	13	0.0	TC62780	9,10[9', 10']carotenoid cleavage dioxygenase	SSCP
IPPISOM	14	6.2	TC32368[b]	Isopentenyl-diphosphate delta-isomerase 1	SSCP
HMGS	14	26.2	TC68763	Hydroxymethylglutaryl coenzymeA synthase	SSCP
Gib20ox	16	22.6	TC11917[b]	Gibberellin 20-oxidase	SSCP
DXR	17	39.9	TC64939	1-deoxy-D-xylulose 5-phosphate reductoisomerase precursor	SSCP
Gib2ox	19	33.8	TC60763	Gibberellin 2-oxidase	SSCP

B) Aromatic amino acid metabolism

Marker	LG	cM	TC	Annotation	Method
DHAP-S	2	56.7	TC59396	3-deoxy-D-arabino-heptulosonate 7-phosphate synthase	SNP
DHAP-S-p	7	54.3	TC57642	3-deoxy-D-arabino-heptulosonate 7-phosphate synthase precursor	SNP
FAH1	10	91.3	TC53032	Fumarylacetoacetase	SNP
FAH	10	93.5	TC56398	Fumarylacetoacetase	SNP
HPD1-sscp[d]	12	1.2	TC58798[e]	4-hydroxyphenylpyruvate dioxygenase	SSCP
HPD	12	5.4	TC58798[e]	4-hydroxyphenylpyruvate dioxygenase	SNP
PHEA-sscp[d]	12	23.1	TC55648	Putative P-protein: chorismate mutase prephenate dehydratase	SSCP
IGPS	12	35.4	TC64485	Indole-3-glycerol phosphate synthase	SNP
PAL	13	43.0	TC60180	Phenylalanine ammonia lyase	SNP
PAI1	14	33.7	TC60070	NADH-ubiquinone oxidoreductase	SNP
trpB	19	60.1	TC62261	Tryptophan synthase beta subunit	SNP
TAT	19	75.0	TC53133	Tyrosine aminotransferase	SNP
HGOb-sscp	19	79.2	TC66094	Homogentisate 1,2-dioxygenase	SSCP
HGOa	19	81.6	CF518271	Homogentisate 1,2-dioxygenase	SNP

C) Stress and gene regulation

Marker	LG	cM	TC	Annotation	Method
AIP	3	0.0	TC53877	Putative auxin-regulated protein	SNP
pepA1	8	33.5	TC66643	Putative CND41, chloroplast nucleoid DNA binding protein Pepsin A	SNP
cnd41	10	84.0	TC57402	Putative chloroplast nucleoid DNA-binding protein cnd41	SNP
conG-p	14	3.6	TC51730	Putative CND41; conglutin gamma precursor Conglutin gamma precursor	SNP
pDNAbP	15	47.9	TC67994	Chloroplast nucleoid DNA binding protein putative	SNP

Abbreviations: LG = linkage group; cM = marker position on the Italia x Big Perlon consensus map (Costantini et al. 2008); TC = tentative consensus; SSCP = single strand conformational polymorphism; SNP = single nucleotide polymorphism

[a] Monomorphic markers in Pop1 were mapped for synteny after being analyzed in Pop2

[b] These TCs were split into two or more tentative consensus in TGI Database (Release 5.0, 21 June 2006, http://compbio.dfci.harvard.edu/tgi/cgi-bin/tgi/gimain.pl?gudb=grape)

[c] DXS was mapped also in Pop2 as SSCP marker

[d] A SNP marker (SnaPshot technique) within the same TC was additionally mapped in Costantini et al. (2008)

[e] These molecular markers were developed from two distinct ESTs belonging to the same TC

1.3.2. Map construction

The dataset of CG markers was used to genotype Pop1, along with the other marker types described in Costantini et al. (2008). By applying a similar procedure to that described in Costantini et al. (2008), linkage maps were also obtained for Moscato Bianco and *V. riparia* with the main goal to validate QTL results achieved in Pop1 (Fig 2B).

Four CG markers, which were monomorphic in Pop1 (ACTRANS, GAI, G10H and PMVAK), were analyzed in Pop2 and located for synteny in Italia x Big Perlon maps. *DXS* marker was mapped in both populations.

Figure 2

A)

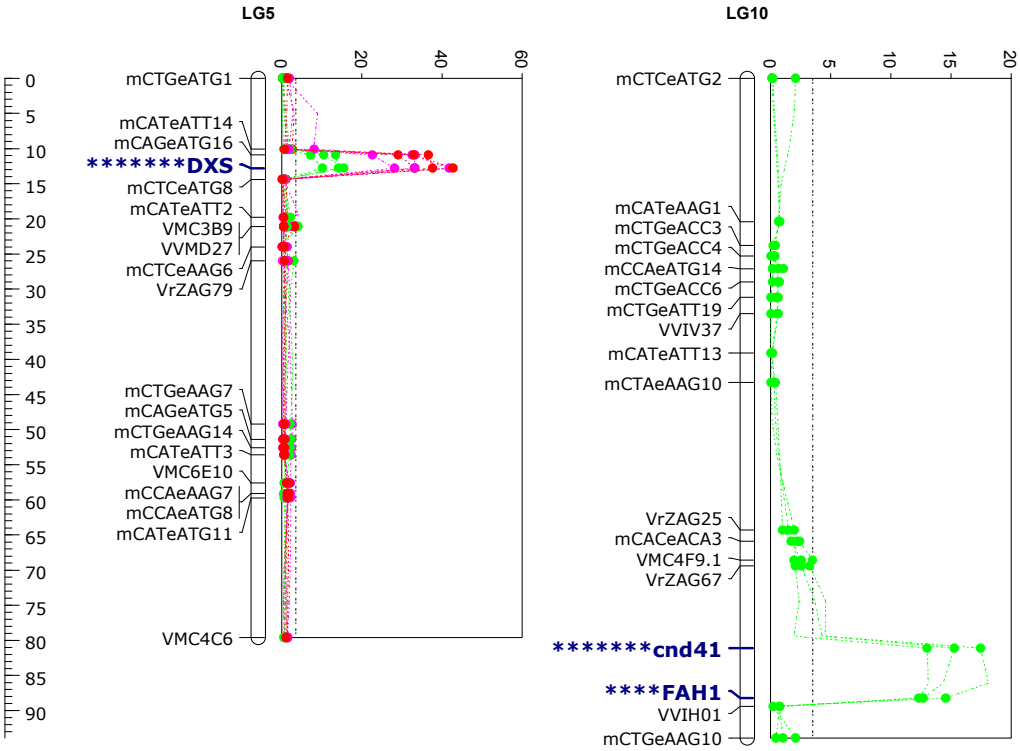
LG5
LG10
mCTGeATG1
mCATeATT14
mCAGeATG16
*******DXS
mCTCeATG8
mCATeATT2
VMC3B9
VVMD27
mCTCeAAG6
VrZAG79
mCTGeAAG7
mCAGeATG5
mCTGeAAG14
mCATeATT3
VMC6E10
mCCAeAAG7
mCCAeATG8
mCATeATG11
VMC4C6
mCTCeATG2
mCATeAAG1
mCTGeACC3
mCTGeACC4
mCCAeATG14
mCTGeACC6
mCTGeATT19
VVIV37
mCATeATT13
mCTAeAAG10
VrZAG25
mCACeACA3
VMC4F9.1
VrZAG67
*******cnd41
****FAH1
VVIH01
mCTGeAAG10

B)

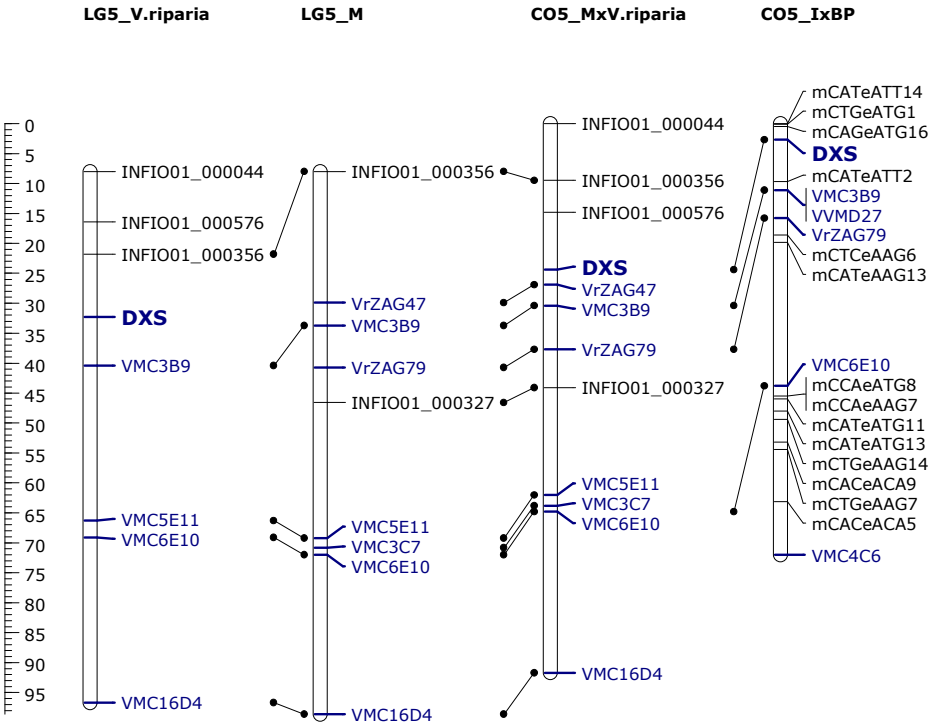
LG5_V.riparia
LG5_M
CO5_MxV.riparia
CO5_IxBP
INFIO01_000044
INFIO01_000576
INFIO01_000356
DXS
VMC3B9
VMC5E11
VMC6E10
VMC16D4
INFIO01_000356
VrZAG47
VMC3B9
VrZAG79
INFIO01_000327
VMC5E11
VMC3C7
VMC6E10
VMC16D4
INFIO01_000044
INFIO01_000356
INFIO01_000576
DXS
VrZAG47
VMC3B9
VrZAG79
INFIO01_000327
VMC5E11
VMC3C7
VMC6E10
VMC16D4
mCATeATT14
mCTGeATG1
mCAGeATG16
DXS
mCATeATT2
VMC3B9
VVMD27
VrZAG79
mCTCeAAG6
mCATeAAG13
VMC6E10
mCCAeATG8
mCCAeAAG7
mCATeATG11
mCATeATG13
mCTGeAAG14
mCACeACA9
mCTGeAAG7
mCACeACA5
VMC4C6

CG markers co-localizing with QTLs for monoterpene content. **A)** LGs 5 and 10 are from the Italia map; on the left are shown the Pinot Noir genomic contig containing the DXS marker and the domain architecture of the predicted DXS1 protein. Abbreviations: PPTS = putative plastid target sequence; TPP_DXS = thiamine pyrophosphate (TPP) family, DXS subfamily, TPP-binding module; Transket_pyr = transketolase, pyridine binding domain; Transket_C = transketolase C-terminal domain. **B)** From left to right are shown LG 5 in *V. riparia* map, in Moscato Bianco (M) map, in Moscato Bianco x *V. riparia* integrated map and in Italia (I) x Big Perlon (B) integrated map. INFIO01_000327, INFIO01_000356 and INFIO01_000044 represent SSCP markers developed on EST sequences (http://www.ncbi.nlm.nih.gov), whereas INFIO01_000576 is a SSR marker within a EST

1.3.3. Metabolite profiling and quantification

Linalool, nerol and geraniol content showed a continuous variation, which is typical of quantitative traits, and a transgressive segregation in both progenies (Figure 3).

Figure 3

A)

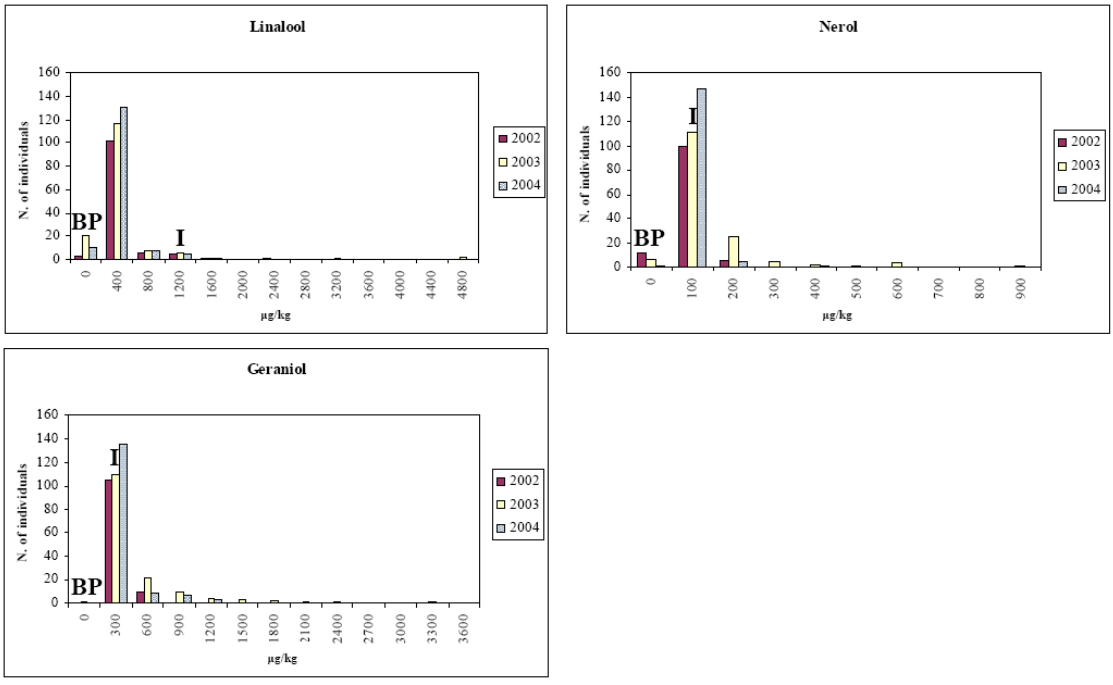

B)

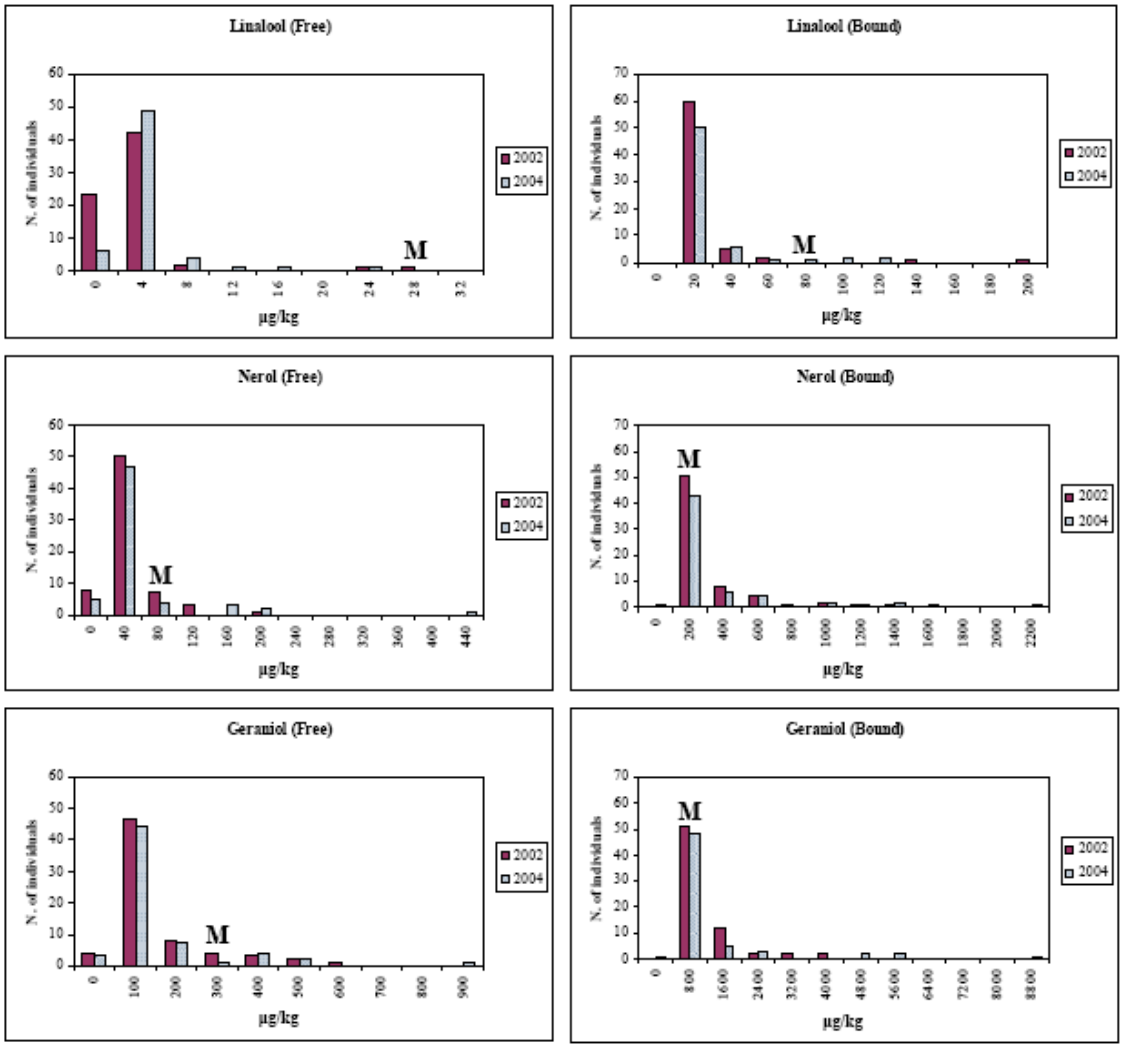

Monoterpenes content distribution in Pop1 (A) and Pop2 (B). Abbreviations: I = Italia, BP = Big Perlon, M = Moscato Bianco

1.3.4. Data and QTL analysis

The one-sample Kolmogorov–Smirnov test indicated departures from normality ($P < 0.05$) for the content of linalool, nerol and geraniol, which was highly skewed towards low values in both populations. Data were ln-transformed in the attempt to achieve normality, which is preferred for the QTL analysis based on interval mapping. However, some ln-transformed distributions were still significantly different from normal at $P = 0.05$ (Pop1: ln-linalool

2002, ln-nerol 2003 and 2004, ln-geraniol 2004; Pop2: free ln-nerol 2004, bound ln-nerol 2002 and 2004, free and bound ln-geraniol 2002).

In all years and both populations significant (P = 0.01) Spearman rank-order correlations were found among the three monoterpenes (except for bound geraniol in Pop2, 2004), and was always stronger between nerol and geraniol. In Pop1 they were significantly (P = 0.01) correlated only between 2002 and 2004, probably due to the uncommonly high temperatures measured during summer 2003; in Pop2 correlation between years was significant (P = 0.05) only for free nerol content.

Several QTLs were suggested by simple interval mapping (data not shown), but only some of them were confirmed with multiple QTL mapping and were significant at both the chromosome-wide and the genome-wide thresholds (Table 4).

Table 4 QTLs identified in Italia (A) and Moscato Bianco (B) for the content of linalool, nerol and geraniol

A)

Year	Compound	LG	Marker	Position (cM)	LOD peak	LOD threshold 0.95		% var expl	KW
						Chromosome-wide	Genome-wide		
2002	Free linalool	5	DXS	12.8	10.2	3.1	8.7	26.3	*******
	Free linalool	10	FAH1	86.1/88.2	13.1	6.7	8.7	36.4	*****
	Free nerol	5	DXS	12.8	28.1	2.9	5.9	68.7	*******
	Free geraniol	5	DXS	12.8	33.3	3.0	9.2	75.5	*******
2003	Free linalool	5	DXS	12.8	13.0	2.9	8.0	31.1	*******
	Free linalool	10	cnd41	81.1	15.3	6.0	8.0	34.8	*******
	Free nerol	5	mCAGeATG16	10.9	33.3	3.0	12.8	68.8	*******
	Free geraniol	5	DXS	12.8	37.7	3.0	10.8	68.9	*******
2004	Free linalool	5	DXS	12.8	15.5	3.1	5.5	36.4	*******
	Free linalool	10	FAH1	86.1/88.2	18.1	4.0	5.5	10.6	*******
	Free nerol	5	DXS	12.8	41.8	3.4	12.6	82.9	*******
	Free geraniol	5	DXS	12.8	42.8	3.1	12.6	83.7	*******

B)

Year	Compound	LG	Marker	Position (cM)	LOD peak	LOD threshold 0.95		%var expl	KW
						Chromosome-wide	Genome-wide		
2002	Free linalool	2	VMC3B10	19.3	5.8	2.7	4.7	31.6	-
	Free linalool	5	VrZAG47	73.7/68.7	10.0	3.0	4.7	63.6	*******
	Free nerol	5	VrZAG47	73.7/68.7	17.7	5.6	8.2	84.1	*******
	Free geraniol	5	VrZAG47	73.7/68.7	25.3	11.4	14.4	90.4	*******
2004	Free linalool	5	VrZAG47	78.7/68.7	10.2	3.2	5.0	66.8	*******
	Free nerol	5	VrZAG47	78.7/68.7	22.3	7.9	11.2	93.0	*******
	Free geraniol	5	VrZAG47	73.7/68.7	18.0	5.4	7.9	84.3	*******

2002	Bound linalool	5	VrZAG47	78.7/68.7	14.7	3.5	4.9	72.4	*******
	Bound nerol	5	VrZAG47	73.7/68.7	27.3	14.3	15.7	91.0	*******
	Bound geraniol	5	VrZAG47	73.7/68.7	24.6	12.2	12.8	89.0	*******
2004	Bound linalool	5	VrZAG47	78.7/68.7	12.2	3.3	4.7	72.2	*******
	Bound nerol	5	VrZAG47	78.7/68.7	26.3	13.0	14.5	92.2	*******
	Bound geraniol	5	VrZAG47	78.7/68.7	17.5	5.4	6.8	82.6	*******

Abbreviations: LG = linkage group; Marker = marker nearest to the QTL position; Position = QTL position (two values were reported when there was no coincidence between the LOD peak and the marker; in this case the first value refers to the LOD peak and the second one to the marker); LOD peak = LOD (log of odds) value at QTL position; LOD threshold = chromosome-wide and genome-wide LOD threshold (P = 0.05); % var expl = proportion of the total phenotypic variance explained by the QTL; KW = Kruskal–Wallis significance level, given by the P value (* = 0.1, ** = 0.05, *** = 0.01; **** = 0.005; ***** = 0.001; ****** = 0.0005; ******* = 0.0001)

In the aromatic parent of Pop1 (Table 4A) a major QTL for the amount of linalool, nerol and geraniol was detected on LG 5 in three years. It explained 26–36% of the total variance of linalool, 69–83% of nerol and 69–84% of geraniol content. One additional QTL for linalool content (11–36% of explained variance) was found on LG 10 in three years. Because ratios of compound concentrations are more robust than individual metabolite levels (Morreel et al. 2006), we also calculated the linalool/nerol, linalool/geraniol and nerol/geraniol ratios. QTLs explaining a high percentage of the total variance for linalool/nerol (44–57%) and linalool/geraniol (23–52%) ratios were located on LG 10 in three years in the same position where the QTL for linalool content was identified (Table 5A). A QTL for nerol/geraniol ratio was detected on LG 7 in two years, which explained 8–20% of the total variance (Table 5A). QTLs on LGs 5 (Table 4A) and 10 (Tables 4A and 5A) were unambiguously confirmed by Kruskal–Wallis analysis and were recognized also in Big Perlon, the non-aromatic parent of Pop1 (data not shown).

In the aromatic parent of Pop2 (Table 4B) a major QTL for the content of the three monoterpenes, in their free and bound forms, was detected in both years on LG 5, as in Pop1. It explained 64–72% of the total variance of linalool, 84–93% of nerol and 83–90% of geraniol content. It was confirmed by KW analysis and was found also in *V. riparia*, the non-aromatic parent of Pop2 (data not shown). One additional QTL for the content of free linalool (32% of explained variance) was identified on LG 2 of Moscato Bianco map in 2002. It was not supported by KW analysis (Table 4B). The ratio between free linalool and

nerol or geraniol and that between free nerol and geraniol turned out to be regulated in both years respectively by the major QTL on LG 5 (35-55% of explained variance) and by a QTL on LG 6 (28-53% of explained variance). Both QTLs were confirmed by KW analysis (Table 5B). Finally, a QTL controlling the ratio between free linalool and nerol (35% of explained variance) was detected on LG 10 in 2002 (Table 5B).

Table 5 QTLs identified in Italia (A) and Moscato Bianco (B) for the ratio between free linalool, nerol and geraniol

A)

Year	Compound	LG	Marker	Position (cM)	LOD peak	LOD threshold 0.95		% var expl	KW
						Chromosome-wide	Genome-wide		
2002	Linalool/Nerol	2	VMC7G3	8.7/3.7	6.1	2.7	4.6	15.6	**
	Linalool/Nerol	2	VVIB01	44.5/46.8	4.8	2.7	4.6	11.2	-
	Linalool/Nerol	10	cnd41	79.4/81.1	16.4	3.2	4.6	43.8	*******
	Linalool/Geraniol	10	cnd41	79.4/81.1	15.4	3.0	4.4	47.0	*******
	Nerol/Geraniol	1	VVIS21	49.7/44.7	4.6	2.9	4.4	11.6	-
	Nerol/Geraniol	6	VMC4H5	19.6	6.0	2.6	4.4	15.8	******
	Nerol/Geraniol	7	VMC1A12	61.3/63.3	6.8	2.7	4.4	20.2	*
2003	Linalool/Nerol	10	cnd41	79.4/81.1	18.1	3.6	5.5	56.9	*******
	Linalool/Geraniol	10	cnd41	79.4/81.1	16.9	5.2	7.2	52.4	*******
2004	Linalool/Nerol	2	mCTCeATG3	0.0	5.2	2.7	4.3	12.0	**
	Linalool/Nerol	10	cnd41	79.4/81.1	17.6	3.0	4.3	46.9	*******
	Linalool/Geraniol	10	cnd41	81.1	16.5	3.1	4.5	23.4	*******
	Nerol/Geraniol	2	VMC7G3	13.7/3.7	6.3	2.6	4.5	15.4	******
	Nerol/Geraniol	7	VMC1A12	63.3	6.1	3.0	4.5	8.0	***
	Nerol/Geraniol	10	mCTCeATG2	0.0	5.2	3.0	4.5	48.7	-

B)

Year	Compound	LG	Marker	Position (cM)	LOD peak	LOD threshold 0.95		% var expl	KW
						Chromosome-wide	Genome-wide		
2002	Linalool/Nerol	5	VrZAG47	73.7/68.7	5.5	3.3	3.7	35.2	****
	Linalool/Nerol	10	VrZAG67	28.1/32.9	4.7	2.5	3.7	35.4	-
	Linalool/Geraniol	5	VrZAG47	68.7	6.3	3.2	4.5	50.0	*******
	Linalool/Geraniol	12	VMC8G6	40.3/47.5	5.5	2.8	4.5	34.1	****
	Nerol/Geraniol	6	VMC5C5	30.6	6.5	2.6	4.1	27.8	******
	Nerol/Geraniol	15	4H04	51.5	5.5	2.5	4.1	33.4	-
2004	Linalool/Nerol	5	VrZAG47	68.7	8.5	3.2	5.2	55.1	*******
	Linalool/Geraniol	5	VrZAG47	68.7	7.9	3.0	4.4	50.6	*******
	Nerol/Geraniol	6	VMC5C5	28.2/30.6	7.0	2.6	4.0	52.7	*******

Abbreviations: LG = linkage group; Marker = marker nearest to the QTL position; Position = QTL position (two values were reported when there was no coincidence between the LOD peak and the marker; in this case the first value refers to the LOD peak and the second one to the marker); LOD peak = LOD (log of odds) value at QTL position; LOD threshold = chromosome-wide and genome-wide LOD threshold (P = 0.05); % var expl = proportion of the total phenotypic variance explained by the QTL; KW = Kruskal–Wallis significance level, given by the P value (* = 0.1, ** = 0.05, *** = 0.01; **** = 0.005; ***** = 0.001; ****** = 0.0005; ******* = 0.0001)

Figure 4

A)

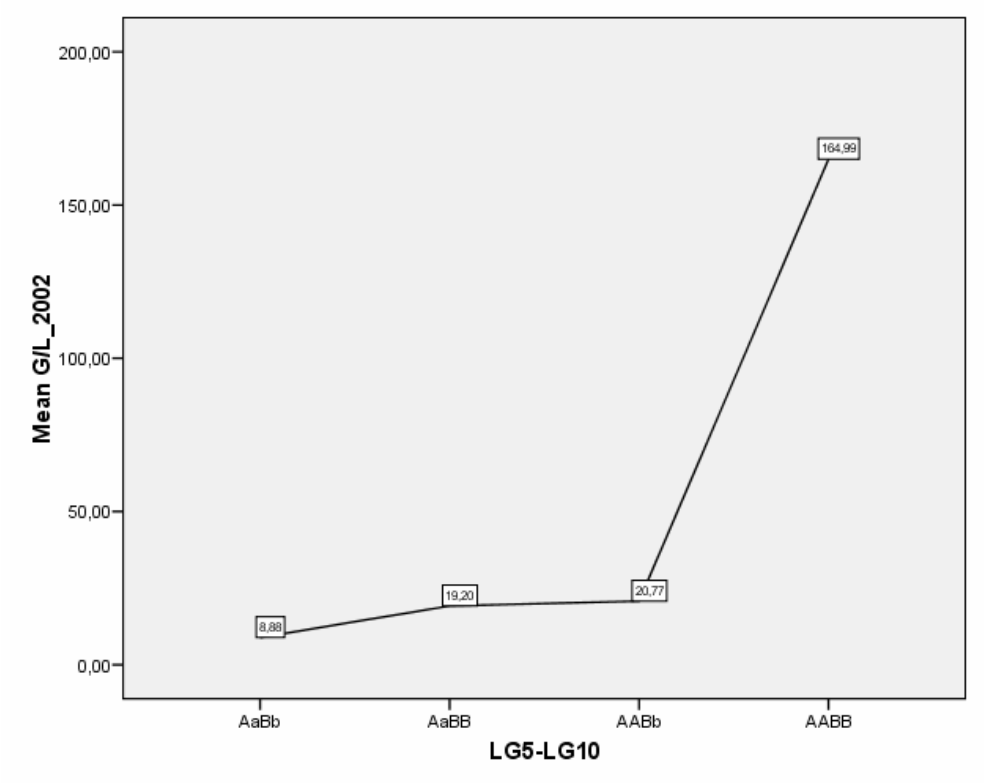

B)

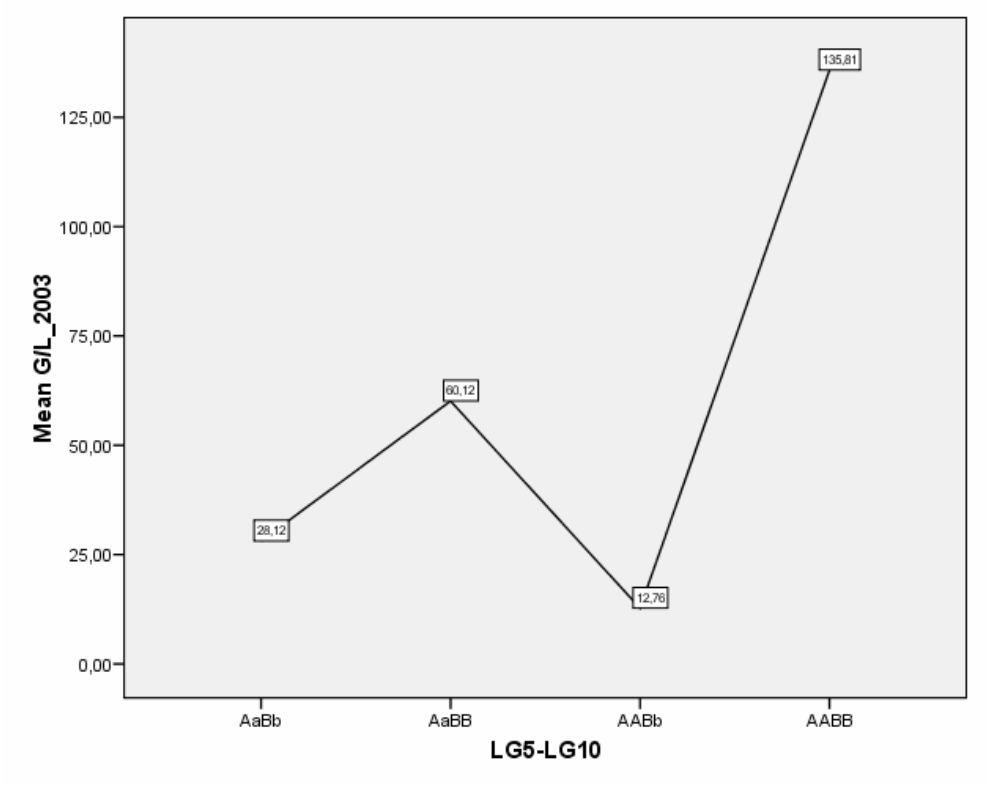
Mean G/L_2003
125,00
100,00
75,00
50,00
25,00
0,00
135,81
60,12
28,12
12,76
AaBb
AaBB
AABb
AABB
LG5-LG10

C)

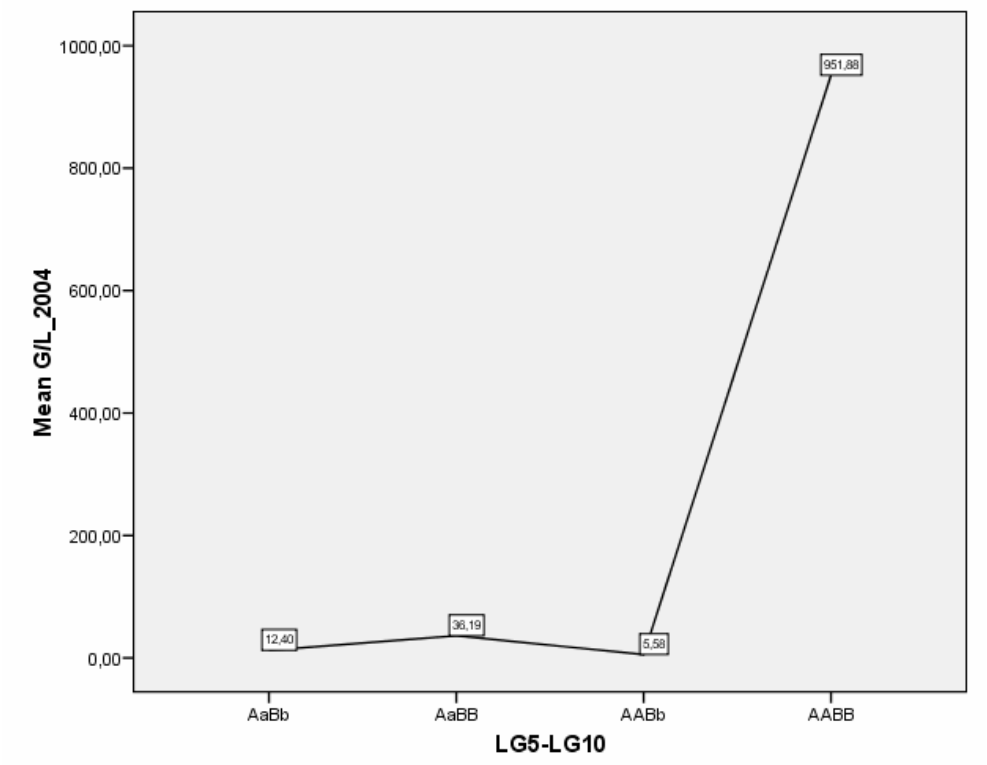
Mean G/L_2004
1000,00
800,00
600,00
400,00
200,00
0,00
951,88
36,19
12,40
5,58
AaBb
AaBB
AABb
AABB
LG5-LG10

Mean of geraniol/linalool ratio in Pop1 in 2002 (A), 2003 (B) and 2004 (C). F1 individuals were classified into four groups based on their genotype at locus DXS (A in the figure) on LG 5 and locus cnd41 (B in the figure) on LG 10; the corresponding mean values for geraniol/linalool (G/L) ratio were calculated. The univariate analysis of variance showed a significant ($P < 0.0001$) difference in the means of at least two groups ($F = 10.1$ in 2002, $F = 18.5$ in 2003; $F = 18.9$ in 2004). The post hoc LSD test indicated that group AABB was significantly ($P < 0.005$) different from the others in the three years

Figure 5

A)

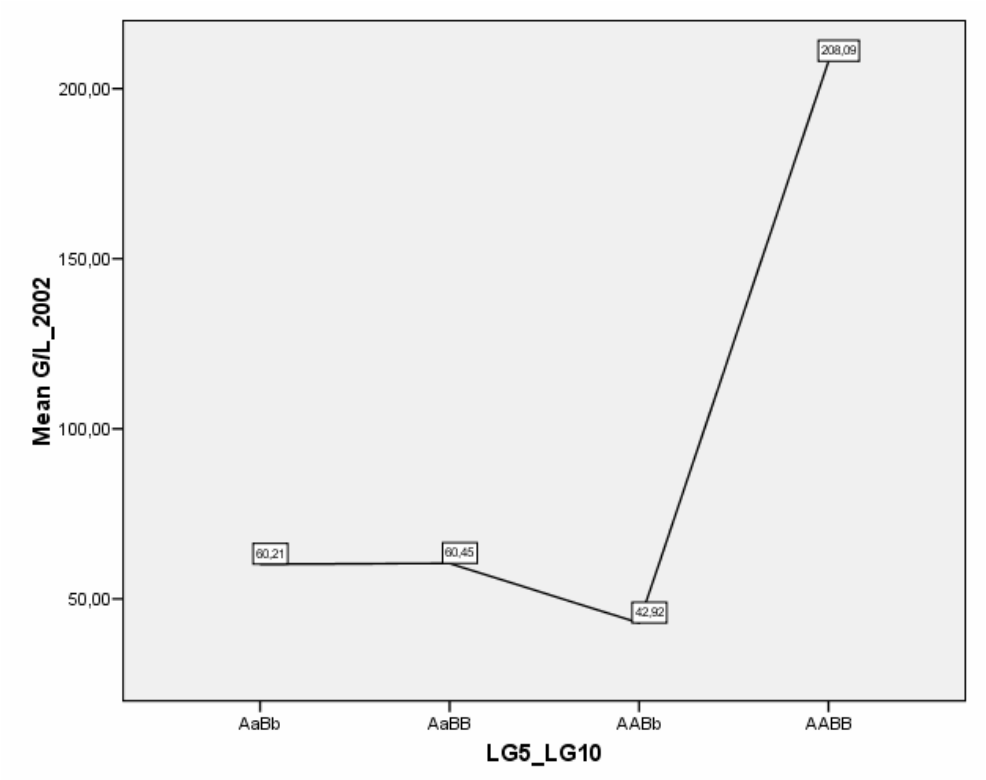

B)

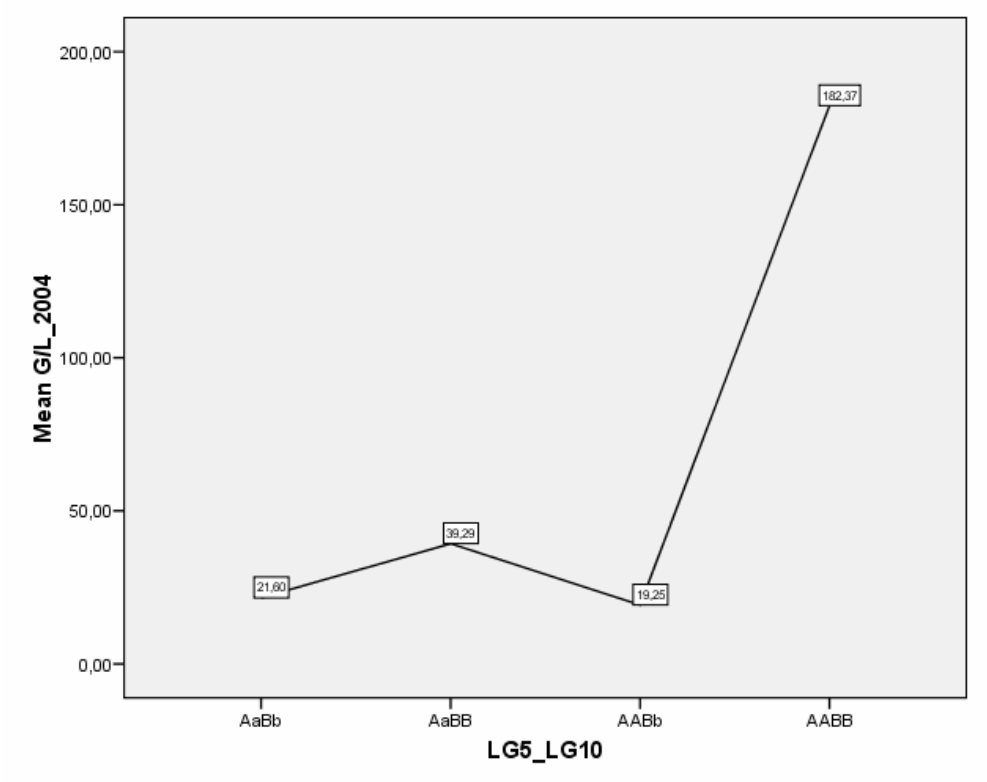

Mean of geraniol/linalool ratio in Pop2 in 2002 (A) and 2004 (B). F1 individuals were classified into four groups based on their genotype at locus DXS (A in the figure) on LG 5 and locus VVIH01 (B in the figure) on LG 10; the corresponding mean values for geraniol/linalool (G/L) ratio were calculated. The univariate analysis of variance showed a significant ($P < 0.05$) difference in the means of at least two groups ($F = 3.7$ in 2002, $F = 3.4$ in 2004). The post hoc LSD test indicated that group AABB was significantly ($P < 0.05$) different from the others in both years

1.3.5. CG markers co-localizing with QTLs

In Pop1 interval mapping and Kruskal–Wallis analysis revealed a significant association between three CG markers and QTLs for monoterpene concentration (Table 4A and Fig 2A). *DXS* marker (at 12.8 cM on LG 5 of Italia) was found to be linked to the content of linalool, nerol and geraniol. Another relevant association emerged between the markers cnd41/FAH1 (respectively at 81.1 and 88.2 cM on LG 10 of Italia) and linalool content. The cnd41 marker was also related to linalool/nerol and linalool/geraniol ratios (Table 5A). In Pop2 the *DXS* marker could be mapped only in the non-aromatic parent *V. riparia*, because of polymorphism lack in Moscato Bianco (Fig 2B). Nevertheless, QTL analysis

revealed a significant association between monoterpene content and *DXS* in *V. riparia* (data not shown) and between monoterpene content and VrZAG47 in Moscato Bianco (Tables 4B and 5B). In this last case the LOD peak of the QTL for free and bound compounds did not coincide with VrZAG47, but it was found at a position where *DXS* could be expected based on the Moscato Bianco x *V. riparia* and Italia x Big Perlon consensus maps (Fig 2B).

1.3.6. In silico analysis

The in silico analysis of Pinot Noir genomic sequence (Velasco et al. 2007) allowed us to estimate the physical length of the QTL intervals on LGs 5 and 10 of the Italia map and to predict the number of genes that are in these regions (Table 6). On LG 5 the average 1.3 cM-long 1-LOD interval corresponded to 267 kb, which were predicted to contain 27 genes. On LG 10 the average 8.7 cM-long 1-LOD interval was estimated to correspond to ca. 1540 kb spanning two distinct metacontigs. Around 200 genes might exist in this region.

Table 6 Genetical and physical distances of QTL intervals, number of predicted genes underlying QTLs found in Pop1

	Molecular markers	**Total length of metacontig (kb)**	**Total length of metacontig under study (kb)**	**Gene predictions**
Chromosome 5	DXS1 VMC3B9	5200	1087	120
	QTL interval	**Interval above genome wide LOD threshold (cM/kb)**	2.2/413	37
		1-LOD interval (cM/kb)	1.3/267	27
	Molecular markers	**Total length of metacontig (kb)**	**Total length of metacontig under study (kb)**	**Gene predictions**
Chromosome 10	VVIH01 FAH1 cnd41	3020	3020	388
	VrZAG67	3311	970	98
	QTL interval	**Interval above genome wide LOD threshold (cM/kb)**	11/2000	250
		1-LOD interval (cM/kb)	8.7/1540	200

Molecular markers represent the closest loci to the QTLs detected on LGs 5 and 10. They include the 3 CGs underlying the LOD peak and one microsatellite on each side of the LOD peak (only one side of the QTL on LG 5 is covered by microsatellites). Total length of metacontig corresponds to the entire metacontig containing these loci (on LG 10 two distinct metacontigs house the four indicated markers), whereas total length of metacontig under study refers to the region encompassed by the two microsatellites surrounding the QTL (on LG 5 this region is comprised between the locus VMC3B9 and the end of the metacontig, due to the lack of a second microsatellite). Additional analyzed regions are the QTL interval where the LOD values are above the 0.95 genome-wide LOD threshold and the 1-LOD interval. On LG 5 the physical distance reported for these QTL intervals is real, whereas on LG 10 it is an estimation made from the genetic distance according to Velasco et al. (2007), due to the presence of a gap between the two metacontigs containing VVIH01 and VrZAG67. Analogous considerations hold for the number of predicted genes

The expressed sequence on which the *DXS* marker was developed (TC56417) was blasted against the Nucleotide collection of the NCBI database (http://www.ncbi.nlm.nih.gov/BLAST/Blast.cgi). It aligned completely with locus AM447068 and partially with nine additional loci (AM431242, AM431698, AM441419, AM449097, AM461604, AM471792, AM480310, AM487977, AM488379). Contig AM447068 was 60967 bp long. The software FGENESH predicted the existence of a gene containing 10 exons. The deduced grape protein consisted of 669 amino acids and showed high identity with the 1-deoxy-D-xylulose 5-phosphate synthase of other plant species (the highest identity was 86% with *Pueraria montana*). By consulting the conserved domain database it emerged that proteins of the *DXS* family contain three functional domains: a thiamine pyrophosphate (TPP)-binding module, a transketolase, pyridine binding domain and the C-terminal domain of transketolase, which has been proposed as a regulatory molecule binding site.

The nine contigs that partially aligned to TC58417 strongly matched to bases 2705–2825 and 3290–4569 of the *DXS* sequence. In four cases (AM431242, AM441419, AM461604 and AM488379) the protein encoded by the predicted gene showed high identity with only two of the three *DXS* functional domains. These contigs were no longer considered as part of our study because they did not contain a putative *DXS* sequence. The *DXS* sequence from contig AM447068 proved to be similar to 1-deoxy-D-xylulose 5-phosphate synthase class 1 (*DXS*1), while putative *DXS* proteins from contigs AM449097, AM471792, AM480310 and AM487977 were highly similar to *DXS* class 2. Finally, the *DXS* sequence

obtained from contig AM431698 aligned to At5*DXS* of *Arabidopsis thaliana* (NP196699) and *DXS* of *Medicago truncatula* (ABE78977), which belong to class 3 (Table 7). A plastid targeting sequence is suggested for *DXS*1, *DXS*2 B, *DXS*2 C and *DXS*2 D.

Table 7 Description of *DXS* gene family in *Vitis*

Locus name[a]		Gene	LG
Velasco et al. (2007)	Jaillon et al. (2007)		
AM447068	CAAP02001192	*DXS1*	5
AM471792	CAAP02003958	*DXS2 A*	7
AM487977	CAAP02003415	*DXS2 B*	15
AM480310	CAAP02001170	*DXS2 C*	11
AM449097	CAAP02004722	*DXS2 D*	15
AM431698	CAAP02001517	*DXS3*	4

[a] from the Whole-Genome Shotgun reads (WGS) database (http://www.ncbi.nlm.nih.gov)

Abbreviations: LG = linkage group; ND = not detected

1.3.7. Phylogenetic analysis

DXS sequences from plants, algae and bacteria were considered in this study. Protein alignment with ClustalW showed that a number of regions were highly conserved among the majority of them (data not shown). The rooted phylogenetic tree inferred with the minimum evolution method is shown in Figure 6, and as well as the trees generated by UPGMA and neighbour-joining methods are inferred. Three groupings were identified: one for higher plants, one for algae and one for bacteria. The plant group was further classified into three clusters (*DXS* class 1, 2 and 3). Vv*DXS*1 grouped with class 1, Vv*DXS*2 A, B, C and D with class 2 and Vv*DXS*3 with class 3 *DXS* sequences. V. vinifera *DXS* class 2 was split in two subgroups with the putative *DXS*2 A separated from the other *DXS*2 proteins, as supported by a bootstrap value of 100% (Figure 6).

Figura 6

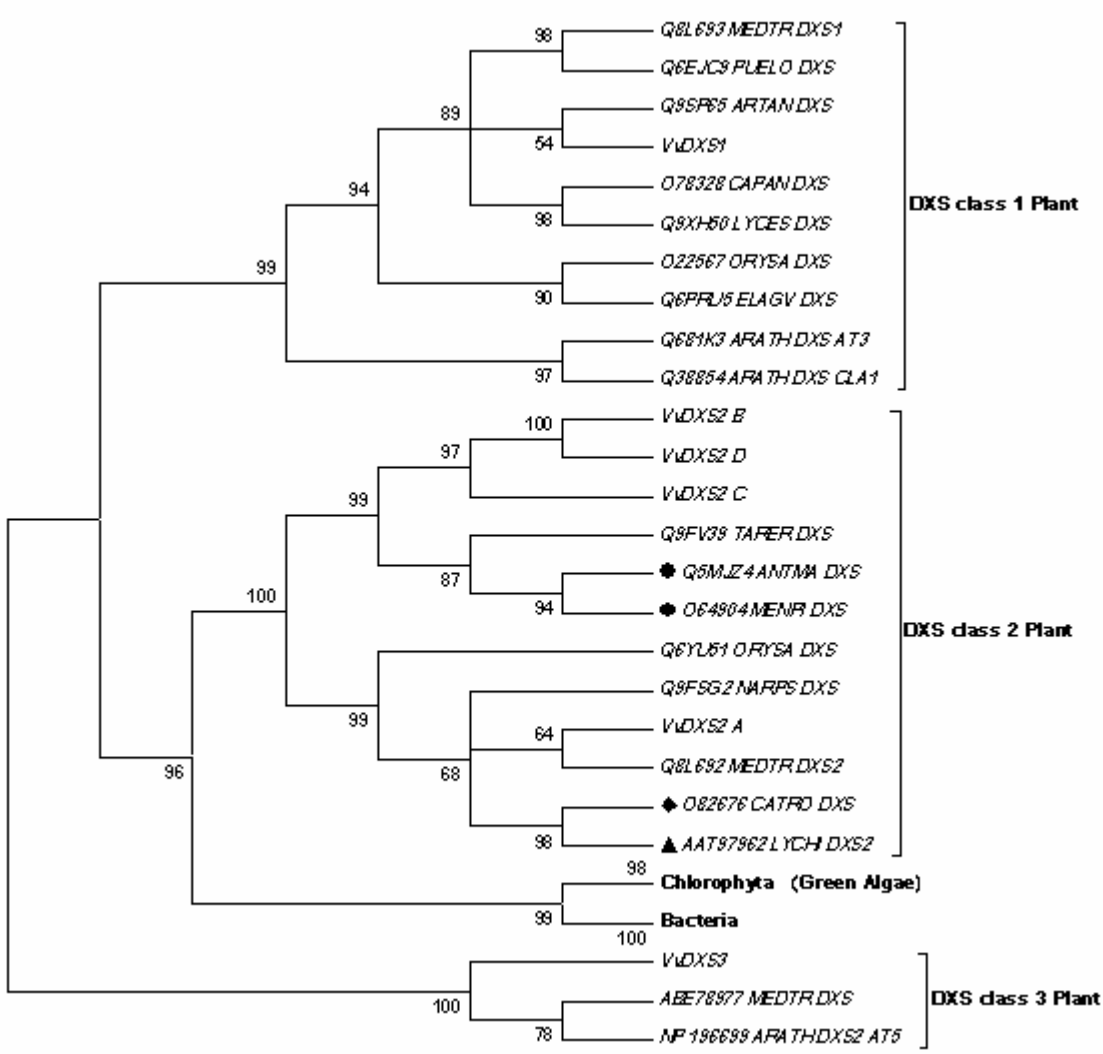

Phylogenetic rooted tree inferred from the functional region of the DXS protein sequences by UPGMA method. Numbers indicate bootstrap support for individual nodes. The scale on the bottom refers to the number of substitutions per amino acid site. GenBank accession numbers and full species names are as follows: Plants - AAT97962 *Lycopersicon hirsutum*, ABE78977 *Medicago truncatula*, NP_196699 *Arabidopsis thaliana* AT5, O22567 *Oryza sativa*, O64904 *Mentha x piperita*, O78328 *Capsicum annuum*, O82676 *Catharanthus roseus*, Q38854 *Arabidopsis thaliana CLA1*, Q5MJZ4 *Antirrhinum majus*, Q6EJC9 *Pueraria montana var. lobata*, Q6PRU5 *Elaeis guineensis chloroplast*, Q6YU51 *Oryza sativa*, Q681K3 *Arabidopsis thaliana AT3*, Q8L692 *Medicago truncatula*, Q8L693 *Medicago truncatula*, Q9FSG2 *Narcissus pseudonarcissus*, Q9FV39 *Tagetes erecta*, Q9SP65 *Artemisia annua,* Q9XH50 *Lycopersicon esculentum*; Bacteria - Q2YMF0 *Brucella melitensis biovar Abortus*, Q21A74 *Rhodopseudomonas palustris*, Q57ET1 *Brucella melitensis biovar Abortus*, Q89RW1 *Bradyrhizobium japonicum*; Chlorophyta (green algae) - ABO94483 *Ostreococcus lucimarinus*, CAL52263 *Ostreococcus tauri* and O81954 *Chlamydomonas reinhardtii*. Members of Asterids are marked: *Antirrhinum majus* and Mentha x piperita by solid circles, *Catharanthus roseus* by a solid rhombus and *Lycopersicum hirsutum* by a solid triangle.

1.4. Discussion

In this chapter we applied the candidate gene method, combined with QTL analysis, to the identification of gene sequences putatively involved in the regulation of Muscat flavor in grapevine.

Candidate gene mapping: The choice of ESTs for candidate genes was based on keywords and gene ontology terms related to Muscat aroma. This strategy, followed by EST quality checking, functional characterization and clustering, proved to be suitable for selecting a manageable number of gene sequences. The 53 candidate genes selected are involved in a few biological processes: 26 in the metabolism of terpenoids, 20 in the metabolism of aromatic amino acids and 7 in stress or regulation of chloroplast gene expression. Eighty-seven per cent (46/53) of these sequences were fruitfully amplified. CG marker development was based on the detection of molecular polymorphisms through SSCP and minisequencing methods. Both techniques were successful, but the second one turned out to be more powerful in terms of yield and reproducibility.

QTL analysis: The availability of two linkage mapping experiments allowed us to identify QTLs with effects either in diverse or in specific genetic backgrounds. Moreover, QTL analysis for the content of single monoterpenes rather than based on taste scoring provided interesting information about branch points playing an essential role in monoterpene biosynthesis.

Co-localization of significant ($\alpha = 0.05$) QTLs was observed at two levels: between pedigrees and between monoterpene compounds. A major QTL was identified in all years on LG 5 of Italia x Big Perlon and Moscato Bianco x *V. riparia* maps for the ln-transformed content of linalool, nerol and geraniol (Table 4) and on the same chromosome of Moscato Bianco x *V. riparia* map for the content of several other aromatic compounds analyzed only in Pop2 (data not shown). In some cases, MapQTL located the peaks for individual monoterpenes at slightly different positions within the same or adjacent intervals. These results suggest that a large part of the genetic variability of Muscat aroma might be due to a few genes with pleiotropic effects, but it is also possible that there are linked genes influencing the content of different aromatic compounds. In accordance with our findings, Doligez et al. (2006) detected a major QTL for linalool, nerol and geraniol

content on LG 5 in the interval VrZAG79-VVC6, which exhibited smaller effects for linalool than for nerol and geraniol.

Additional QTLs were identified for linalool content on LG 2 of Moscato Bianco map and on LG 10 of Italia x Big Perlon map (Table 4). The QTL on LG 2 of Moscato Bianco map was detected in both years but in 2004 it was significant only at the chromosome-wide level (not reported in Table 4B). It was not sustained by Kruskal–Wallis analysis and its position should be made more precise by mapping new markers; however, its reliability is supported by the identification of a QTL for linalool content on the same chromosome of the non-muscat parent utilized by Doligez et al. (2006). These findings suggest that, in spite of the close genetic relationship existing among many muscat cultivars (Crespan and Milani 2001), different regulation points or allelic forms could be present and explain their aroma tipicity (total terpene content and ratio between specific compounds, i.e. linalool and geraniol).

Our results also indicate that the observed phenotypic correlations between the three monoterpenes are, in large part, of genetic origin. The existence of common (on LG 5) and linalool-specific (on LG 10) QTLs is in agreement with the significant correlation existing between these compounds (stronger between nerol and geraniol than between linalool and nerol or geraniol), which was also reported by Versini et al. (1993) and Doligez et al. (2006). The major QTL on LG 5 exhibited smaller effects for linalool than for nerol and geraniol in both populations analyzed in this study. In contrast with the hypothesis formulated by Doligez et al. (2006) to justify the secondary role played by linalool QTL, our work shows that the lower variance explained for the linalool content QTL on LG 5 is not linked with the geraniol/linalool ratio in the aromatic parent, which is high in Moscato Bianco (Versini et al. 1993), but low in Italia. QTL analysis of linalool/geraniol and linalool/nerol ratios revealed the existence of a genetic determinant on LG 10 in Pop1. In order to confirm this result and to test the possibility that the same locus plays a regulatory role also in Pop2, even though it could not be highlighted by QTL analysis, we investigated the association between geraniol/linalool ratio and the genotypes of the markers closest to the QTLs on LGs 5 (DXS) and 10 (cnd41 in Pop1 and VVIH01 in Pop2) by general linear models (GLM). This analysis suggested the existence of a locus regulating linalool accumulation on LG 10 in both populations, in addition to the locus controlling the level of

all three monoterpenes on LG 5 (Figure 4 and 5). From a chemical point of view, nerol and geraniol share a common precursor, geranyl-pyrophosphate (GPP), which produces also (S)-linalool in a one-step reaction catalyzed by (S)-linalool synthase (Ebang-Oke et al. 2003). However, additional distinct mechanisms for linalool synthesis could exist and nerol could be derived from the transformation of geraniol (Guardiola et al. 1996; Luan et al. 2005).

Co-localization of CG markers with QTLs: *DXS* acts upstream in monoterpene biosynthesis: it encodes 1-deoxy-D-xylulose 5-phosphate synthase, which is the first enzyme implicated in the non-mevalonate pathway of IPP biosynthesis. The correlated high concentration of linalool, nerol, geraniol and additional monoterpenes analyzed only in Pop2 (data not shown) is probably the consequence of an excess of a common skeleton, i.e. IPP, which, in turn, is expected to derive from a favorable allele at locus *DXS*.

The locus CND41 in the nuclear genome encodes a protein, which non-specifically binds chloroplast DNA. Characterization of antisense transgenic tobacco cells indicated that decreases in the CND41 protein increased the chloroplastic gene transcripts (Nakano et al. 1997). This suggests that CND41 is involved in the negative regulation of gene expression in chloroplasts, although the actual mechanism is not clear. CND41 also has a protease activity, by which it may degrade transcriptional factors or RNA polymerase and decrease the level of chloroplast transcripts. CND41 might be implicated not only in the regulation of gene expression, but also in the biogenesis of the functional apparatus of chloroplasts and in the degradation of denatured proteins. It may function under stress conditions, which lower the cytosolic pH to its optimal value (Murakami et al. 2000). Nakano et al. (2003) reported a role for CND41 in the control of chloroplast development and GA biosynthesis in an antisense tobacco transformant. A direct regulation effect of CND41 on the expression of the genes involved in the MEP pathway should be excluded since they are encoded by the nuclear genome and then translocated to the plastids. Nevertheless, we think that the locus CND41 is worth further investigation in order to unravel other potential mechanisms explaining its co-mapping with the QTL on LG 10 for linalool content. Also this gene (TC57402) was found to be differentially expressed during berry ripening (C. Moser, personal communication).

FAH1 corresponds to the gene encoding fumarylacetoacetase, an enzyme of the hydrolase class that catalyses the cleavage of fumarylacetoacetate to form acetoacetate and fumarate. This reaction is a step in the tyrosine catabolic pathway. Further investigation, i.e. analysis of the genomic region comprised between VrZAG67 and VVIH01 and mapping of additional markers to increase QTL power detection, is required to confirm CND41 and FAH1 as the loci underlying the QTL on LG 10 or to identify other genes with a role in the control of linalool content.

No genes underlying the QTL for linalool content on LG 2 of Moscato Bianco map could be identified since in Pop2 we mapped only the four CG markers, which turned out to be monomorphic in Pop1. Good candidate loci for this QTL could be genes acting downstream in the biosynthetic pathway of linalool, such as the (S)-linalool synthase (Ebang-Oke et al. 2003) or loci regulating it.

In silico analysis of *DXS* genomic sequence: Multi-copy gene families encode *DXS* and a number of genes involved in isoprenoid biosynthesis in plants, which may facilitate the tightly regulated expression of isoenzymes with roles specific to certain tissues, developmental stages and/or environmental challenges (Lange and Ghassemian 2003). The existence of a small *DXS* gene family has been suggested for Arabidopsis (Estévez et al. 2000; Rodríguez-Concepción and Boronat 2002), *Ginko biloba* (Kim et al. 2006), *Medicago truncatula* (Walter et al. 2002), *Morinda citrifolia* (Han et al. 2003), Norway spruce (Phillips et al. 2007), oil palm (Khemvong and Suvakitannont 2005), rice (Kim et al. 2005) and even for the purple non-sulphur bacterium *Rhodobacter capsulatus* (Hahn et al. 2001).

By using TC56417 as query to mine the grapevine whole genome sequence, we identified six contigs encoding orthologue *DXS* sequences. To our knowledge this is the first evidence of the existence of *DXS* genes class 1, 2 and 3 in grape. *DXS*2 B and D, which were both located on LG 15, could represent allelic variants of the same gene. A high level of similarity at the nucleotide level was observed among the coding regions of all the identified *DXS* sequences, as revealed by the presence of seven exons with the same length, whereas the level of similarity among intron regions was very low even within the same gene class.

Phylogenetic analysis: The three methods adopted to infer phylogenetic trees from *DXS* sequences produced similar results. Clustering of *DXS* sequences reported in this work does not correspond to the plant taxonomy established previously by other research groups using, for instance, 18S rRNA, rbcL and atpB genes (Soltis et al. 2000). One example of disagreement concerns the members of the Asterids clade: *Antirrhinum majus* and Mentha x piperita (Lamiales) were mis-separated from *Lycopersicum hirsutum* (Solanales) with a bootstrap value of 100%. Similar misclustering was observed by Walter et al. (2002) and Krushkal et al. (2003). These authors provided a number of potential explanations, the most obvious being the existence of two or more copies of the *DXS* gene. An additional explanation could be the lower number of sequences used in this work, as well as in the works by Walter et al. (2002) and Krushkal et al. (2003), with respect to the analysis performed by Soltis et al. (2000).

II

Capitolo II

Transcriptomic and metabolite analysis during ripening in aromatic and non-aromatic varieties of *Vitis vinifera* L.

2.1. Introduction

Plants produce a large number of secondary metabolites, some of them are known to function as mediators necessary for the interaction with other organisms, and being allelopathic substances or insect attractants to facilitate pollination (Hoballah et al., 2005). To achieve those functions, accumulation or secretion of compounds has to be highly regulated, for instance, flavonoids acting as UV protectant are specifically accumulated in epidermal cells (Schmitz-Hoerner et al., 2003), and insect attractants are emitted from flower petals (Kolosova et al., 2001).

Flavour and aroma compounds are involved in seed dispersion in which they serve as important attractants to dispersal agents when fruits are ripe and ready to consume, but are more susceptible to pathogen attack (Slaughter, 1999). Aromas arise from volatile compounds, such as terpenes, norisoprenoids, and thiols stored as sugar or amino acid conjugates in the vacuoles of exocarp cells (Lund & Bohlmann 2006). The biochemical and regulatory pathways involved in flavor and aroma development in grapes are still not well understood. There are clear sensory differences in the aromas of most grape varieties and the interactions among the different monoterpenes increase the total aroma, moreover both free and bound forms of these terpenols are involved in aroma determination (Ribérau-Gayon et al., 1975; Gunata et al., 1985; Strauss et al., 1986). Furthermore the overall volatile composition of most varieties is similar, with the varietal aroma deriving largely from differences in relative ratios of many volatile compounds.

Wine "character" depends on different combinations and concentrations of the diverse varietal aroma compounds present in grape berries. It has emerged from many studies that the characteristic aroma of Muscat grape varieties is tightly related to the presence of some monoterpene compounds. Considering their high concentration in Muscat grape varieties, geraniol, linalool, nerol and α-terpineol are often described as the major contributors to the typical muscat aroma in spite of their low olfactory perception thresholds (Mateo and Jiménez, 2000).

Aroma compounds have been previously evaluated (from 2002 to 2004) in the segregating progeny in of Italia x Big Perlon and Moscato Bianco x *V. riparia* and these studies underlined a co-localization of *DXS1* (1-deoxyxylulose-5-phosphate synthase class 1)

marker in both linkage maps (linkage group 5) and through the years of analysis with a major quantitative trait loci (QTL) explaining a high percentage of the total variance.

Many investigations support a regulatory role of *DXS* in terpene biosynthesis at the transcriptional level. Estévez et al. (2001) observed a positive correlation between the accumulation of several plastidic isoprenoids and the content of 1-deoxy-D-xylulose-5-phosphate synthase in transgenic *Arabidopsis* plants. They concluded that this enzyme catalyses a limiting step in the MEP pathway in plants. Moreover, a positive correlation between the level of *DXS* transcript and the production of specific isoprenoids has been observed in several other plant systems (Bouvier et al. 1998; Lange et al. 1998; Chahed et al. 2000; Lois et al. 2000; Veau et al. 2000; Walter et al. 2000; Han et al. 2003; Khemvong and Suvachittanont 2005; Gong et al. 2006). Luan and Wüst (2002) suggested that 1-deoxy-D-xylulose-5-phosphate synthase is a limiting enzyme for plastidic isoprenoid biosynthesis also in grapevine.

In this study the role of this candidate gene in the expression of aroma trait was indagated by evaluating the gene expression in berry skins during grape development from three *V. vinifera* L. cultivars (aromatic and non-aromatic varieties). Moscato Bianco, Chardonnay clone 130 and Chardonnay clone 809 were sampled approximately from pre-veraison to over-ripening. Candidate gene transcript profiling showed that a particular trend of expression, rather than the level of expression ratio, seems to be more important for monoterpenoids accumulation during grape maturation.

Microarray experiments were performed for comparing cDNA pools from different ripening stage of the two Chardonnay clones, which differ for their metabolic profile (year 2006). Functional categorization of the genes differentially expressed underlined that in the aromatic clone much more genes involved in different pathways are present than in the non-aromatic clone. In particular, genes involved in RNA regulation of transcript, transport, secondary metabolism (phenylpropanoids and lignin biosynthesis), cell wall and stress signalling pathways that can overlap or converge at specific points during grape development and aroma biosynthesis were found, as also reported by other studies (Grimplet et al. 2007).

This study aims to increase our knowledge about the genetic determinism of aroma in grape by evaluating the correlation of the level of metabolic compounds during grape maturation

with candidate genes transcription profiling. The results presented here allow us to plan further functional genomics studies in order to clarify the gene networks that can be involved in this important and complex quality trait.

2.2. Materials and methods

2.2.1. Plant materials and sampling method

V. vinifera L., cv. Moscato Bianco, Chardonnay clone 130 and Chardonnay clone 809 are maintained in experimental fields by Fondazione Edmund Mach in San Michele all'Adige (Italy). Grape clusters were picked randomly from 10 plants located in 10 different rows for about 250 plants per variety. The clusters were sampled from different positions and then pooled together in order to minimize ambient effects (soil, light and temperature). Berries were selected based on the same diameter and the development stage was characterized by monitoring total soluble solids and titratable acidity. Berries of cultivars Moscato Bianco, Chardonnay clone 130 and Chardonnay clone 809 have been sampled approximately each 1-2 weeks from pre-veraison to over-ripening during 2005, 2006 and 2007 years for a total of 13-14 sampling date each year.. Samples corresponding to stages 30 to 41 of the modified E-L system (Dry and Coombe, 2004) were measured by FTIR (Fourier Transform Infrared), FOSS instrument from 80 mL of juice crushed from harvested berries, in order to define the standard maturity analysis. Total soluble solids (°Brix), titratable acidity, pH, malic and tartaric acid concentration (g/L) were assayed.

For each sample, 200 g were stored at -20 °C for monoterpenoids analysis while skins and pulps of 40 berries were seperatly freezed in liquid nitrogen and then stored at -80°C for RNA extraction.

2.2.2. Monoterpenoids analysis

Free and bound aroma-active components were obtained from the whole berries stored at -20 °C by crushing those (2005, 2006 and 2007 seasons). Aroma forms (both free and bound) were fractionated on SPE (Solid Phase Extraction) by selective retention in a hydrophobic cross-linked polystyrene copolymer (XAD-2 resin) with particle size: 0.2-0.25

mm. According to the procedure described by Gunata et al. (1989) and Versini et al. (1989), the free fraction was eluted with pentane-dichloromethane (2:1, 100 mL) and the eluate was dried over anhydrous sodium sulphate and concentrated to 0.5 mL, by evaporation, then it was stored at -20 °C until high-resolution gas chromatogram-mass spectrometetry (HRGC-MS) analysis. The bound fraction was eluted with 100 mL of methanol-ethyl acetate (9:1) and concentrated to dryness in Rotavapor evaporator, before dissolution in citrate-phosphate buffer (pH 5.0, 5mL). AR-2000 (Gist Brocades, France) was added and the mixture was incubated at 40 °C for 18 h, to accomplish enzymatic hydrolysis. Glycosidically hydrolysates were added with internal standard and extracted three times with pentane-dichloromethane (2:1, 10 mL). After addition of 1-heptanol (internal standard) the extract was concentrated at 31°C to ~500 µL by distillation through a Vigreux before HRGC-MS analysis.

HRGC-MS was performed using a PerkinElmer gas chromatograph with a TurbomassGold Mass Spectrometer equipped with a DBWax fused silica column (60 m x 0.32 mm I.D., 0.5 µm film thickness, J and W Scientific, CA, USA). Helium with a constant flow of 1.2 ml min-1 was used as carrier gas. The oven program was as follows: 50 °C for 10 min, 60 °C at 10 °C min-1, 60 °C for 30 sec., than 200 °C at 2.5 °C min-1, 200 °C for 10 min, finally 250 °C at 10 °C min-1 and holding for 4 min; injector temperature, 250 °C; detector temperature was set to 220 °C and MS detector was employed and it was set as solvent delay for 5 min. Mass spectra were scanned in the range *m/e* 30-300 amu; *total ion chromatograms* (TIC) profiles were obtained. All monoterpenols and benzoyl derivatives like benzylic and 2-phenylethylic alcohols were quantified referring to the internal standard 1-heptano.

Repeatability tests: In order to calculate the percentage of variance that the methods could imply in monoterpenoids analysis, a pool of 1.2 kg berries was collected from cultivar Moscato Bianco (18 °Brix). To evaluate the variance due to the random sub sampling of berries, six samples were prepared by collecting 100 g of berries from the homogeneous pool and then analysed following the method previously described. The remaining 600 g of berries were crushed on N_2 air condition, and maintained on ice to avoid terpenoids oxidation. The resulting grape juice was quickly distribuited in 20 Falcon (about 30 g each)

and stored at -20 °C. This set of reference samples was used to assess the repeatability of the method during samples preparation.

2.2.3. Characterization of DXS class 1 sequence

Eight specific pairs of primer for *DXS1* genomic sequences of *V. vinifera* L. cv Chardonnay clone 130, Chardonnay clone 809 and Moscato Bianco were designed at locus AM447068 (nucleotide database) to cover the gene region from ATG to 3'-UTR (Table 8). As a result, 8 partially overlapping amplicons were produced and then sequenced in both directions.

Table 8 List of primers used for genome sequencing

Primer name	Sequence (5'-3')
DXSpolyAfw	GAACAACATGGCTTACGAATAAC
DXSpolyArw	TCCTATCATGGCATCCTTTC
DXS6f_Af	ATGGCTCTCTGTACGCTCTCA
DXS6r_a'r	GTGTGGGTAAGACTTCAGAAACA
DXS7f_b'f	GGTTACAATCTCACCTTCTCTG
DXS7r_Ar	CATCACCTATGACAGCAATGAC
DXS8f_Bf	CAACAACGTCATTGCTGTCATAG
DXS8rb'r	GCTAGACAGAACAGGTAAGATTTC
DXS9f_c'f	CCAAACAGATTGGCGGACCG
DXS9r_Br	CATAGCATTTGATTAAGAAGATATGGT
DXS10fw	CAGAAGCAGAGGTGGACAA
DXS10rw	CGGACACTAAGGTCATAGGCT
DXS11fw	CAGCCACTTGTCTCATTGTG
DXS11rw	CTCCAACCAGCCCAGC
DXS12fw	ATAGCGTTAGTTGGAAAACCG
DXS12rw	ATTGACCCTTCTTCTACTGTAATCA

PCR products were purified with ExoSapIT (Amersham Pharmacia Biotech, Uppsala, Sweden) and sequenced with the Big Dye ® Terminator v 3.1 Cycle Sequencing Kit (Applied Biosystems) in a GeneAmp PCR System 9700. After precipitation, the sequencing products were mixed with 15 µl of HiDiTM formamide and subjected to capillary electrophoresis in an ABI PRISM 3130xl Genetic Analyzer (Applied Biosystems). The resulting data were analyzed with the softwares Sequencing analysis v 3.7 (Applied Biosystems) and ChromasPro v 1.3 (http://www.technelysium.com.au) (for more details see materials and methods on chapter I).

2.2.4. Semi-quantitative RT-PCR

Total RNA was extracted from pericarp tissue for each sample by using SIGMA Spectrum™ Plant Total RNA Kit. RNA concentration and 260/280 nm ratios were determined before and after DNase I digestion (Invitrogen) with a spectrophotometer and RNA integrity was confirmed by electrophoresis on 1.5% agarose gels. cDNA first strand was synthesized on the triplicated mRNA by using SuperScript™ III Reverse Transcriptase (Invitrogen) according to the manufacturer's instructions.

Primers for genes assayed by real-time PCR were selected using Primer Express™ software v 2.0 (Applied Biosystems) and primers properties like melting temperature (Tm), percentage of G-C (GC%), primer loops, primer dimers and primer-primer compatibility was checked by using Oligo Analyzer software.

Real-Time PCR conditions: LightCycler® 480 SYBR Green I Master Mix (Roche) in 20 µl reactions containing cDNA and 0.5 µM of each primer. Reaction plates included a non-template negative control and reference and target genes, PCR cycling conditions were: Pre-incubation at 95 °C for 5 min for activation of FastStart Taq DNA polymerase and denaturation of the cDNA, Amplification step, 40 cycles at: 95 °C for 10 sec., 60 °C for 30 sec. and 72 °C for 10 second. Finally, it was included a post-PCR melt curve analysis, to detect non-specific amplification in cDNA samples.

Table 9 List of primers used for semi-quantitative Real-Time RT-PCR analysis.

Gene name	Primer name	Primer sequence (5'-3')
1-deoxi-D-xilulose 5-phosphate synthase 1	RT-DXS1F	CCAAGGGCGTTACCAAACAG
	RTDXS1R	TCAACTTTTGCAGCCAATTCA
1-deoxi-D-xilulose 5-phosphate synthase 2	RT-DXS2_CF	CTGATGAAGCAGAGCTTATGC
	RT-DXS2_CR	GAACAGCTCCAATTCCATTTCC
	RT-DXS2_AF	GAAAATTTCAGCAGCTCCATCA
	RT-DXS2_AR	CATGGGCCTGGCCTCCAACT
	RT-DXS2_BF	GCTGAACTAACCATTGCACTTCA
	RT-DXS2_BR	CCCCACGTCCCAAATTATCTT
1-deoxi-D-xilulose 5-phosphate synthase 3	RT-DXS3F	GCTCGAGGATGGTCAGGCTA
	RT-DXS3R	GGATTTACTTGACTGGAGCTTGGT
Actin 7 (ACT7)/actin 2	RT-ACT_F	CTTGCATCCCTCAGCACCTT
	RT-ACT_R	TCCTGTGGACAATGGATGGA
Elongation factor 1-alpha	RT-EF1a_F	GAACTGGGTGCTTGATAGGC
	RT-EF1a_R	AACCAAAATATCCGGAGTAAAAGA
Glyceraldehyde 3-phosphate dehydrogenase	RT-GAPDH_F	TTCTCGTTGAGGGCTATTCCA
	RT-GAPDH_R	CCACAGACTTCATCGGTGACA

Real-time RT-PCR efficiencies were calculated (Pfaffl, 2001) from the slope given by LightCycler software (Roche). Expression was determined for triplicate biological replicates and using serial dilution cDNA standard curves per gene. First we used the '*fit point method*' implemented by LightCycler (Roche) that measure the crossing-point (C_P) at a constant fluorescence level. This method is extremely robust because uninformative background points are discarded and plateau values are excluded by entering the number of log-linear points. Second, C_p and background level were defined correctly by using the *second derivative maximum method* that avoids the problem in a multiple sample analysis.
A combination of several housekeeping genes: Glyceraldehyde 3-phosphate dehydrogenase (GADPH), Actin (ACT) and Elongation factor 1-alfa (EF1-α) (Reid et al., 2006) was used for determining a normalization factor. *GeNorm* (Vandesompele et al., 2002) was used to confirm these genes in our experiments. This Visual Basic applet for Microsoft Excel® allows the relative quantification for an accurate normalization of real-time RT-PCR data by geometric averaging of multiple internal controls. *GeNorm* determines the most stable reference genes from a set of genes in a given cDNA sample panel, and calculates a gene expression normalization factor for each tissue sample based on the geometric mean of defined number of reference genes.
Relative expression software tool (REST) was used to compare several gene expressions on C_P level referred on the first sampling data of each variety. The major advantage of REST is the statistical test of the analyzed C_P values by a *Pair-Wise Fixed Reallocation Randomization Test* (Pfafll et al., 2002). A good estimate of significant differences were obtained through 2000 permutations and expression ratios were reported (standard error <0.005 at $P = 0.05$).

2.2.5. Microarray experiments

Total RNA extraction from berries skin was performed as described by Bais A.J. et al. (2000) and DNAseI (Invitrogen) was used in order to obtain pure RNA without DNA contamination. The absence of DNA was checked by PCR using primers for DXS11F (intronic) and DXS11R (exon) (Table 8). cDNA first strand was synthesized on the triplicated mRNA by using SuperScript™ Indirect cDNA Labeling System (Invitrogen) according to the manufacturer's instructions. Microarray experiments were performed by

using two cDNA pools from different ripening stage for each Chardonnay clone (year 2006). In this way the ripening steps in which the amount of total monoterpenoids of aromatic clone increased about twofold (from *véraison* to 1-2 week post-*véraison*) were compared.

For microarray experiments the Array-Ready Oligo Set™ for the Grape (*V. vinifera*) Genome Version 1.0 was used, containing 14,562 70mer probes in two replicates, representing 14,562 transcripts from The Institute for Genomic Research (TIGR) Grape Gene Index (VvGI), release 3. Oligonucleotides were re-annotated with the most recent release of gene predictions of the Pinot Noir Genome (IASMA Research Center) by BLASTN. Thus, annotated functions corresponding to the *Arabidopsis* homologues according to gene ontology annotations in TAIR and chromosome position were assigned to genes represented on microarray. Plant materials used in our experiment were labelled in twice, both with Cy3 and Cy5 (GE Helthcare, Amersham), a total of two independent labelling reactions each sample were used to compare four microarray slides.

After hybridisation, slides were subsequently washed in a solution 1X SSC/0.2% SDS, a solution 0.1X SSC/0.2% SDS, a solution 0.2X SSC, and a solution 0.1X SSC for 5 min each. Slides were scanned using Perkin Elmer ScanArray LITE Scanner at 532 nm (Cy3 green laser) and 660 nm (Cy5 red laser) at 10 μm resolution using an array scanner. Image analysis was performed using TIGR SpotFinder software. Grids were predefined and manually positioned over the image to ensure optimal spot recognition. Spots with high intensity due to dust particles or other artefacts were manually flagged. Each slide data from both Cy3- and Cy5-labelled and dye swap probes were normalized using the Locfit (LOWESS) normalization in TIGR Microarray Data Analysis System (MIDAS). Multiexperiment Viewer from TIGR (MeV) was used to calculate the Significance Analysis of Microarrays (SAM). SAM allowed estimation at the False Discovery Rate (FDR) by selecting a δ-value corresponding to none false significant genes. The significance was calculated at $\alpha = 0.01$ by theoretical t-distribution from t-test.

2.2.6. Statistical analysis.

SPSS software (version 15.0; SPSS, Chicago, IL) was used for the statistical analysis. Parametric and non-parametric tests were used when necessary to establish the presence or absence of significant differences (P-value < 0.05).

2.3. Results

2.3.1. Grape berries development during ripening

The phenology status of all varieties was characterized by the analysis of pH, total acidity, sugar, malic and tartaric acid content of the berries. From these data and field observations, *véraison*, the onset of ripening, was determinated. Therefore all samples could be precisely assigned to stages 30 - 42 based on the modified E-L system (Coombe 1995).

The °Brix concentration and titratable acidity of the grape analized are reported in figure 7A, 7B and 7C. Ripening time was similar but not equal in 2005 and 2006. On the contrary, in the warm 2007 season berries development was 10 to 20 days ahead of time, depending of the variety.

Figure 7

A)

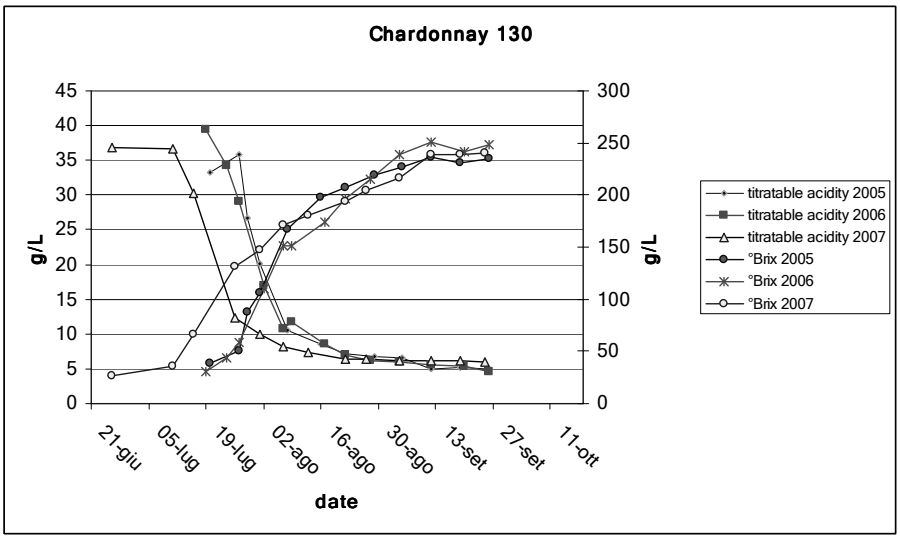

B)

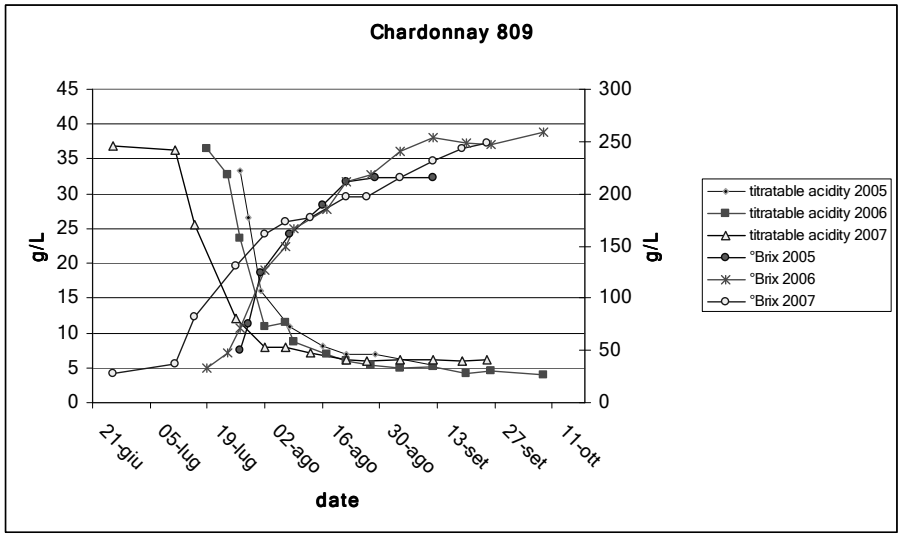

C)

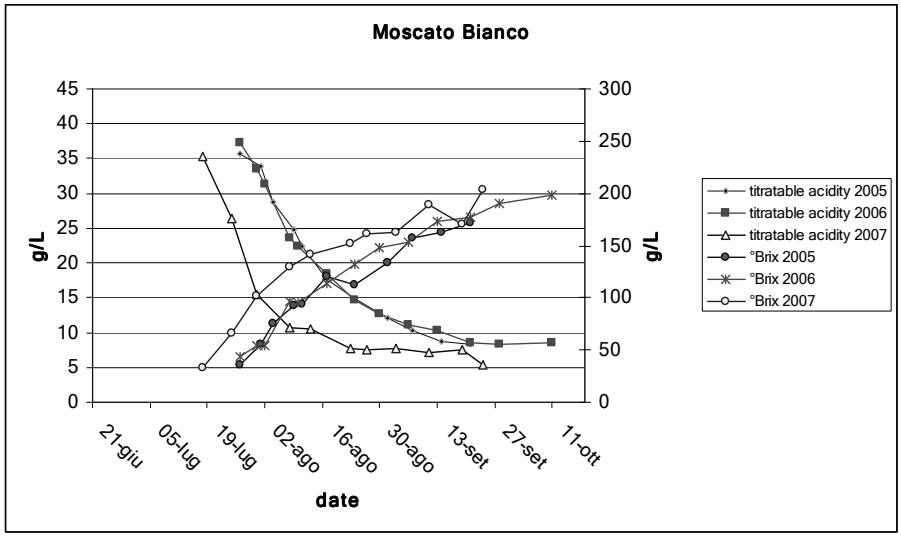

°Brix concentration and titratable acidity of grapes sampled from berry onset to over-ripening stages. Secondary Y-axes correponde to concentration of sugar (°Brix) measured in grams per liter of must.

2.3.2. Evolution of aroma compounds through berries development

The evolution of the total concentrations of aroma compounds was different for all the cultivars analyzed. About 33 aroma compounds were detected for all extrats of Moscato Bianco, Chardonnay clone 130 and clone 809. From these, the list of compounds shown in table 10 was finally considered because of their concentration and interest. Among

them some compounds i.e. C6 compounds, α-terpineol, citronellol and 7-hydroxygeraniol did not show any significative variation of concentration during the sampling period.

Table 10 Concentrations, (micrograms per Kg of berries, 1-heptanol) of free and bound aroma compounds from Moscato Bianco, year 2006. Mean of six repetitions and percentage of Standard Deviation (%SD).

Aroma compounds	**Free forms**		**Bound forms**	
Monoterpenoids	Average content	% SD	Average content	% SD
trans furan linalool oxide (OxA)	16.4	6.5	47.8	8.6
cis furan linalool oxide (OxB)	16.2	6.9	18.7	6.1
linalool	385.8	7.3	135.5	8.5
trans pyran linalool oxide (OxC)	223.8	8.4	36.4	3.9
cis pyran linalool oxide (OxD)	45.6	8.3	3.2	10.1
α-terpineol	4.4	12.8	22.4	13.8
citronellol	8.6	8.9	18.9	11.7
nerol	42.4	9.3	264.3	10.7
geraniol	108.8	7.8	236.4	11.8
HO-diendiol (I) + HO-trienol	636.0	23.6	120.0	14.3
HO-diendiol (II)	119.5	16	8.4	21.3
trans 8-hydroxylinalool	32.9	26.3	99.5	14.3
cis 8-hydroxylinalool	27.1	45.4	59.9	8.2
7-hydroxygeraniol	20.2	35.6	17.9	11.3
trans geranic acid	100.1	19.9	513.3	13.9
Benzenoids				
Benzyl alcohol	32.7	5.3	55.0	7.9
2-Phenylethanol	40.6	6.3	84.3	3.4
C_{13}-norisoprenoids				
3-hydroxy-β-damascone	0.5	25.6	15.3	16.8
3-oxo-α-ionol	1.0	24.6	23.8	14.2
C_6 compounds				
hexanol	126.2	5.2	16.2	7.2
trans 3-hexen-1-ol	1.4	9.2	0.5	36.4
cis 3-hexen-1-ol	100.2	2.1	10.4	9.8

Ritention time and mass spectrometry were used as selection methods.

2.3.2.1. Free Monoterpenoids

Chardonnay clone 809

Linalool was the most concentrated monoterpenoid in Chardonnay clone 809. It was present after *véraison* at a level of 150 µg/Kg. Other free compounds were found in the fruit starting from *véraison*: HO-diendiol I and HO-diendiol II, furan and pyran linalool oxides. Except for the *véraison* stage in 2005 and 2006 nerol and geraniol showed a similar accumulation trend independently of the year, as shown in Figure 8.

Figure 8

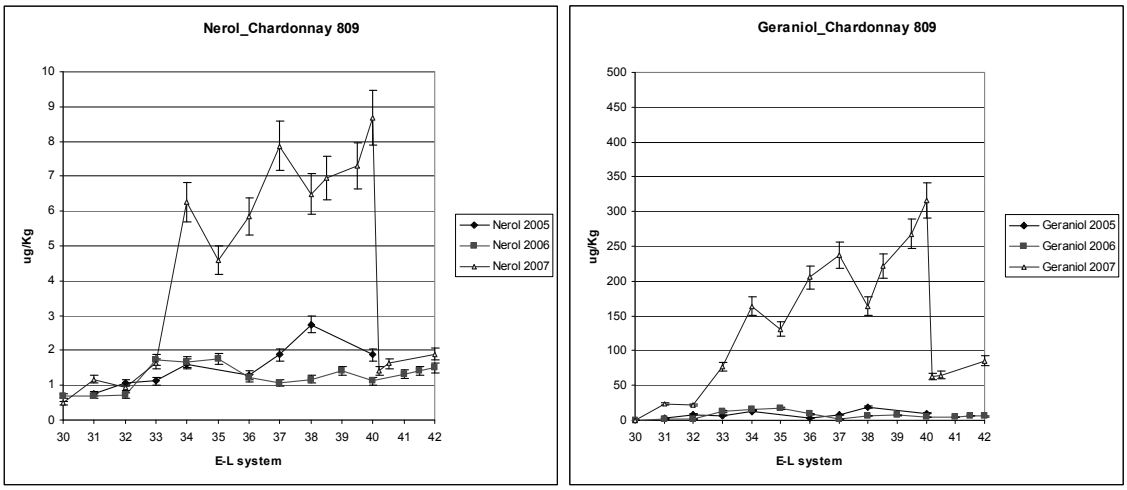

Free nerol and geraniol content of Chardonnay clone 809 grapes. Dots corresponde to concentrations (micrograms per Kg of berries) measured during 2005 and 2006 ripening seasons. Triangles correspond to the 2007 season. Phenological stages are reported on X-axes following the E-L system.

At the *véraison* stage, geraniol concentration was 7 µg/Kg in 2005 and 11 µg/Kg in 2006, then at stage 38 (2005), it showed an increased content of 19.1 µg/Kg. Nerol trend was similar to the geraniol one and was present at stage 35 at a very low level of concentration: 1.74 µg/Kg in 2005. In 2006, nerol accumulation showed a second peak as well (2.74 µg/Kg). Finally, in 2007 both nerol and geraniol showed a different trend of accumulation and the peaks were at higher level than in 2005 and 2006. Nerol reached a concentration of 8.67 µg/Kg, while geraniol was many times higher concentrated: 316 µg/Kg at stage 40.

After *véraison*, only three monoterpenes, linalool, *cis* and *trans* pyran linalool oxides, began to accumulate to a significant extent in the berries.

Figure 9

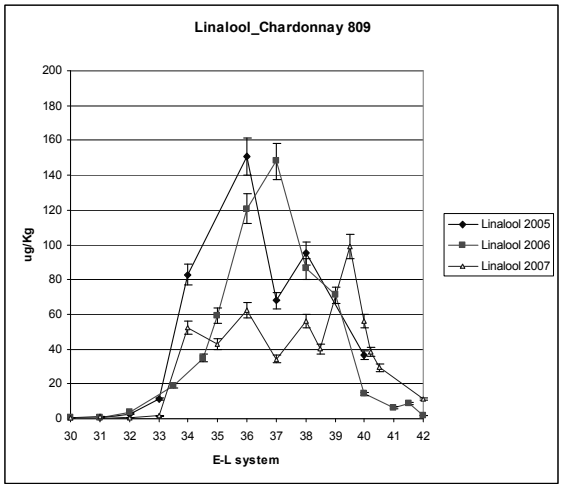

Free linalool content of Chardonnay clone 809 grapes. Dots corresponde to concentrations (micrograms per Kg of berries) measured during 2005 and 2006 ripening seasons. Triangles correspond to the 2007 season. Phenological stages are reported on X-axes following the E-L system.

Linalool content quickly increased just before the *véraison* stage. At stage 34 the concentration of this compound was more than 20 µg/Kg. In 2005 and 2006 seasons, the accumulation kinetic of linalool was similar in terms of shape but the trend was shifted of one stage of E-L system (Figure 9). In 2007, linalool content achived the 100 µg/Kg at over-ripening only (stage 40).

The *cis* pyran linalool oxide (OxD) was always present at high levels (about 100 µg/Kg) just before the peak of linalool concentration. Therefore its presence seems to be not affected by different environmental conditions. In fact, throught the three years, we could only see a simply shift of the accumulation curve without detecting any change of trend (Figure 10). In 2005 and 2006, *trans* pyran linalool oxide (OxC) reached the peak of accumulation a couple of weeks after the *véraison* stage: 89.9 µg/Kg and 100.98 µg/Kg rispectively. The accumulation trend of this compound was similar for 2005 and 2006. In 2007, it reached a concentration of 63 µg/Kg of berries one week post *véraison* and then decreased until the stage 38. Finally, in the overipening period OxC showed a second preak of 50 µg/Kg and then decresed (Figure 10).

Figure 10

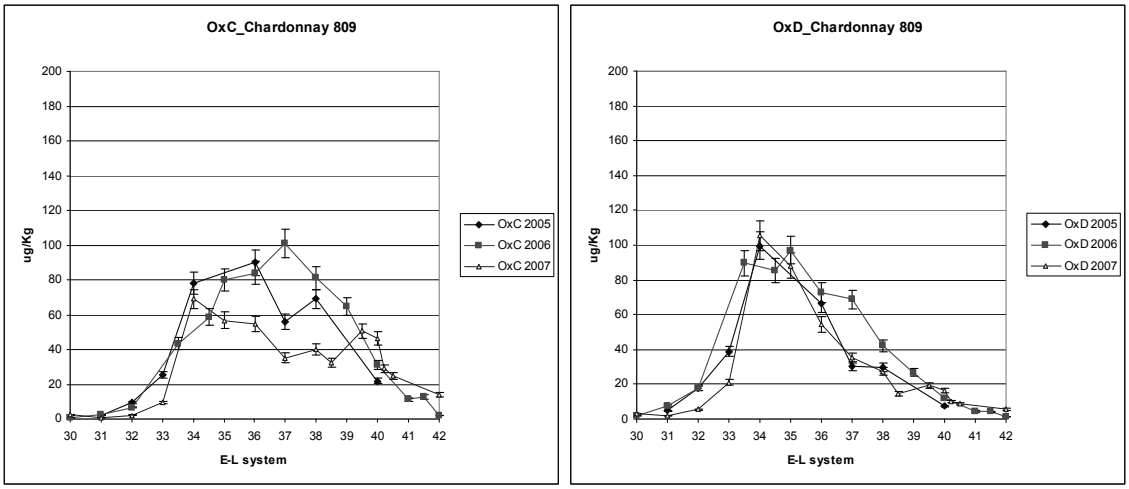

Free pyranoids linalool oxide (*cis* and *trans* forms) content of Chardonnay clone 809 grapes. Dots corresponde to concentrations (micrograms per Kg of berries) measured during 2005 and 2006 ripening seasons. Triangles correspond to the 2007 season. Phenological stages of growth are reported on X-axes following the E-L system.

The accumulation trend of the *cis* furan linalool oxide (OxB) was shifted depending on different conditions through the three years. In addiction, concentration levels were low for this compound and in 2005 the peak was 6.76 µg/Kg. *Trans* furan linalool oxide (OxA) and linalool concentration trends were very similar for all the analyzed years but showed a different shape of accumulation curve.

HO-diendiol II was present at significant levels from *véraison* onward in all the three years observed. The peak of concentration was at stage 38 in 2005 (62.6 µg/Kg), at stage 39 in 2006 (130.2 µg/Kg) and at stage 40 in 2007 (56.1 µg/Kg). Accumulation trends for the three years were anyway similar until stage 36. HO-diendiol I + HO trienol achieved the accumulation peak between stages 38 and 40 for the three years analysed, in particular: in 2005 the concentration was 22.9 µg/Kg, in 2006 was 66.4 µg/Kg and in 2007 was 35.3 µg/Kg (Figure 11).

Figure 11

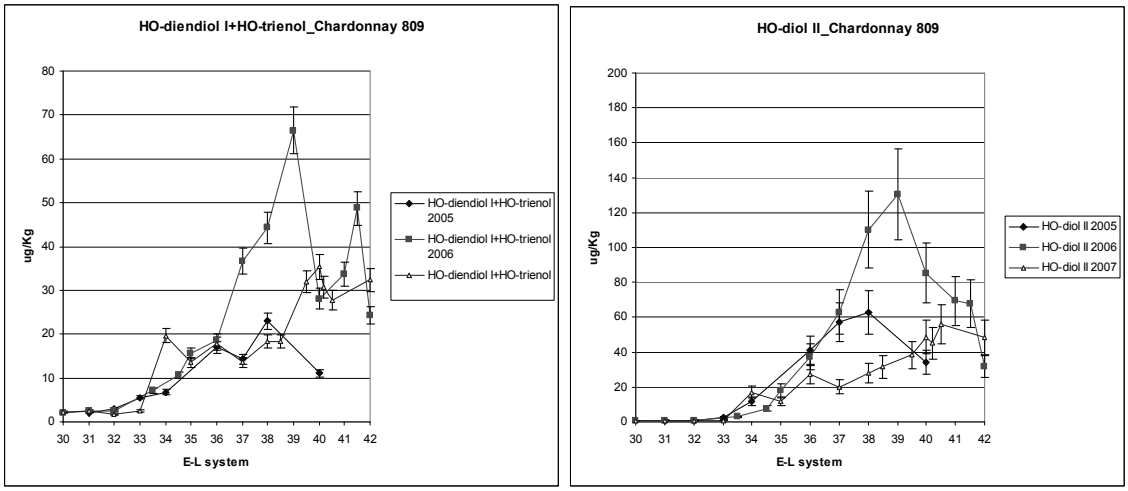

Free diendiols content of Chardonnay clone 809 grapes. Dots corresponde to concentrations (micrograms per Kg of berries) measured during 2005 and 2006 ripening seasons. Triangles correspond to the 2007 season. Phenological stages are reported on X-axes following the E-L system.

Figure 12

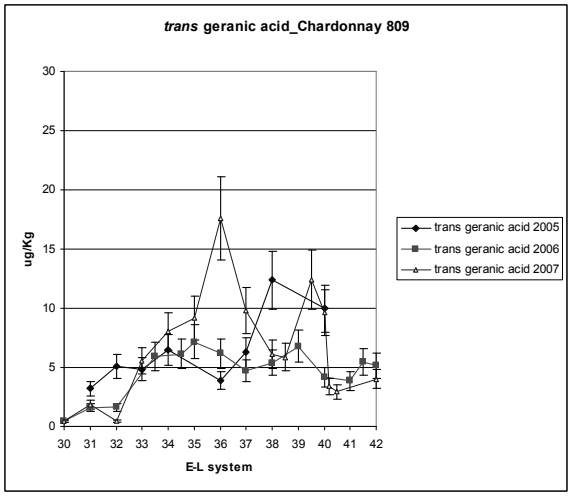

Free t*rans* geraniol acid content of Chardonnay clone 809 grapes. Dots corresponde to concentrations (micrograms per Kg of berries) measured during 2005 and 2006 ripening seasons. Triangles correspond to the 2007 season. Phenological stages are reported on X-axes following the E-L system.

In figure 12 levels of *trans* geranic acid detected during ripening time in 2005, 2006 and 2007 are reported. Different trends of accumulation can be observed. *Trans* geranic acid did not show the similar trend of accumulation: the first peak was present in 2005 and 2006 at stage 35 (6.5 µg/Kg, 7 µg/Kg), while in 2007 reached the 17 µg/Kg at stage 36.

Between the 38 and 40 stage a second accumulation peak of 12.4 μg/Kg, 6.7 μg/Kg and 12.4 μg/Kg was present respectively in 2005, 2006 and 2007.

Chardonnay clone 130

In the non-aromatic clone (Chardonnay 130) most free monoterpenoids were found at very low concentration. Only *trans* pyran linalool oxide (OxC) in 2006 and geraniol in 2007 reached a significant level, respectively at stage 36 (15.6 μg/Kg) and at stage 38 (61.8 μg/Kg). With regard to other monoterpenols, hotrienol, α-terpineol, *trans*-linalool oxide (furanoid), *cis*-linalool oxide (furanoid and pyranoid), citronellol, nerol, 7-hydroxygeraniol, *trans*-geranic acid, and linalool were identified, all in low concentrations as expected for a neutral variety.

Moscato Bianco

Moscato Bianco berries are known to be rich in monoterpenoids. In fact, also in this study monoterpens were found abundant, nearly 10 times higher concentrated than in the Chardonnay clone 809.

Free monoterpenoids were present before *véraison* at elevated levels of concentration, in particolar: HO-diendiol I + HO-trienol, OxC, linalool, geraniol, 7-hydroxygeraniol and *trans* geranic acid. From *véraison* onward all the other compounds were accumulated and showed different pattern of behaviour as well. The *trans* furan linalool oxide (OxA) was present at berries onset at significant levels only for 2005 and 2006 and decreased until stage 33. Starting from *véraison*, OxA was accumulated depending on the season and it achieved a peak at stage 38: 14.7 μg/Kg in 2005 and 18.2 μg/Kg in 2006. In 2007, OxA increased quickly than in the other seasons and reached 29.1 μg/Kg at stage 36, as reported in figure 13.

Figure 13

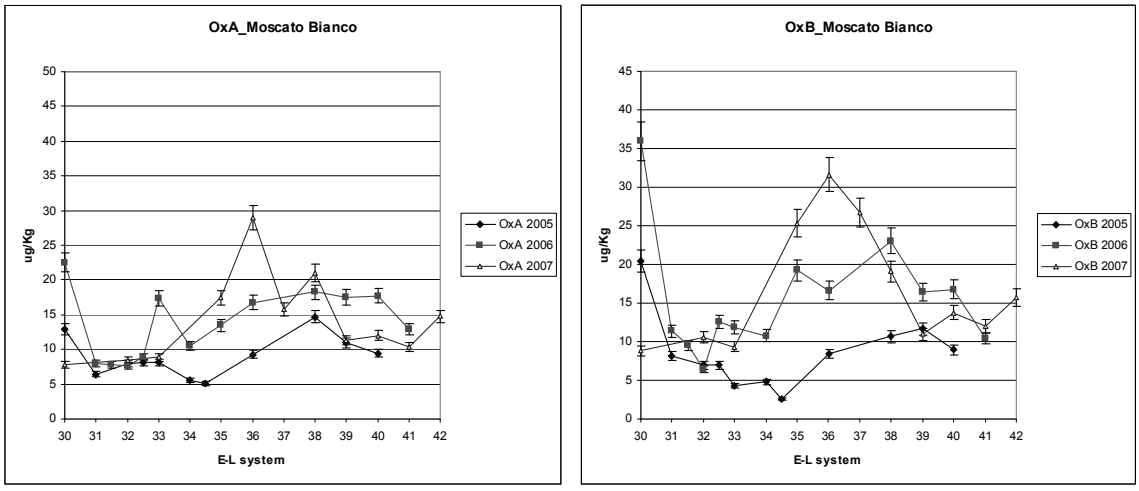

Free furanoids linalool oxide (*cis* and *trans* forms) content of Moscato Bianco. Dots corresponde to concentrations (micrograms per Kg of berries) measured during 2005 and 2006 ripening seasons. Triangles correspond to the 2007 season. Phenological stages of growth are reported on X-axes following the E-L system.

The *cis* furan linalool oxide (OxB) trend was similar to the OxA accumulation curve but the level of concentrations was different. After *véraison*, OxB decreased to 6.5 µg/Kg and from stage 32 it increased to: 11.6 µg/Kg at 39 stage of 2005 season; 23.1 µg/Kg at stage 38 in 2006 and 31.6 µg/Kg at stage 36 in 2007.

Before *véraison* stage, linalool content was present at high levels of concentration through three years of analysis. At stage 32 the concentration was more than 20 µg/Kg. In 2006 and 2007 the kinetics of accumulation of linalool were similar until stage 35, and for both curves the peak reached 800 µg/Kg at stage 36 in 2007, and stage 38 in 2006 (Figure 14A). In 2005, linalool reached the limit of 583.7 µg/Kg at stage 39.

Figure 14

A)

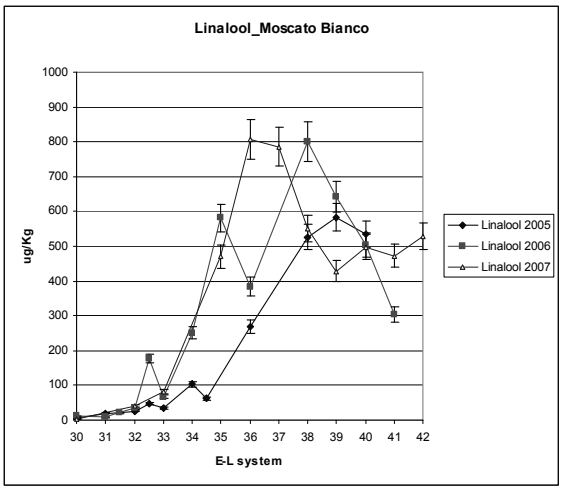

B)

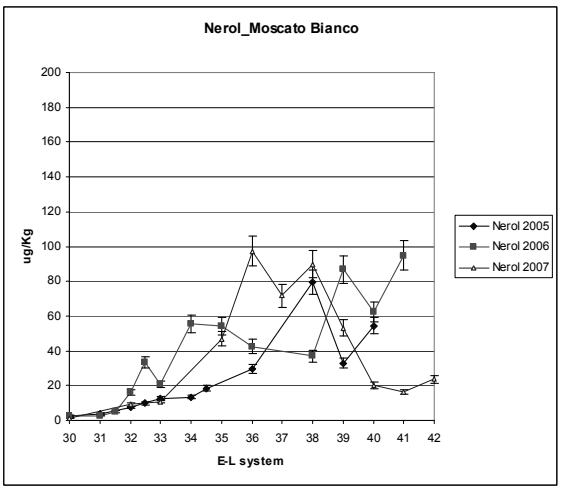

C)

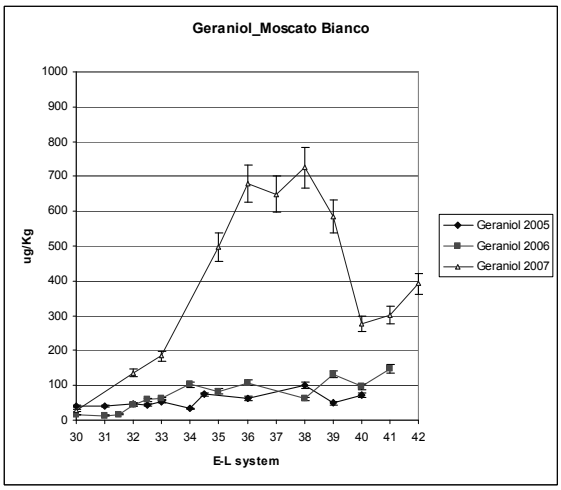

Free linalool, nerol and geraniol content of Moscato Bianco. Dots corresponde to concentrations (micrograms per Kg of berries) measured during 2005 and 2006 ripening seasons. Triangles correspond to the 2007 season. Phenological stages of growth are reported on X-axes following the E-L system.

By comparing the seasonal trends, nerol and geraniol accumulation curves resulted similar in terms of kinetic, but with different levels of concentration. Nerol content was 79.5 µg/Kg at stage 38 in 2005, 94.7 µg/Kg at stage 40 in 2006 and 97.4 µg/Kg at stage 36 in 2007. Geraniol content was 100.5 µg/Kg at 38 stage and 147.7 µg/Kg at 41 stage in 2005, and was 678.8 µg/Kg at stage 36 and 725.6 µg/Kg at stage 38 in 2007 (Figure 12B and 12C).

In Moscato Bianco the kinetics of HO-diendiol I + HO-trienol and HO-diendiol II seem to be inverted in the accumulation trend (Figure 15A and 15B). HO diendiol I + HO-trienol was present at very high level from the first stage of maturation (from 1.33 mg/Kg to 2.1 mg/Kg) and decreased during ripening, while HO-diendiol II was accumulated from *véraison* onward and reached peaks of 130 µg/Kg, 292 µg/Kg and 252 µg/Kg in the three years.

Figure 15

A) B)

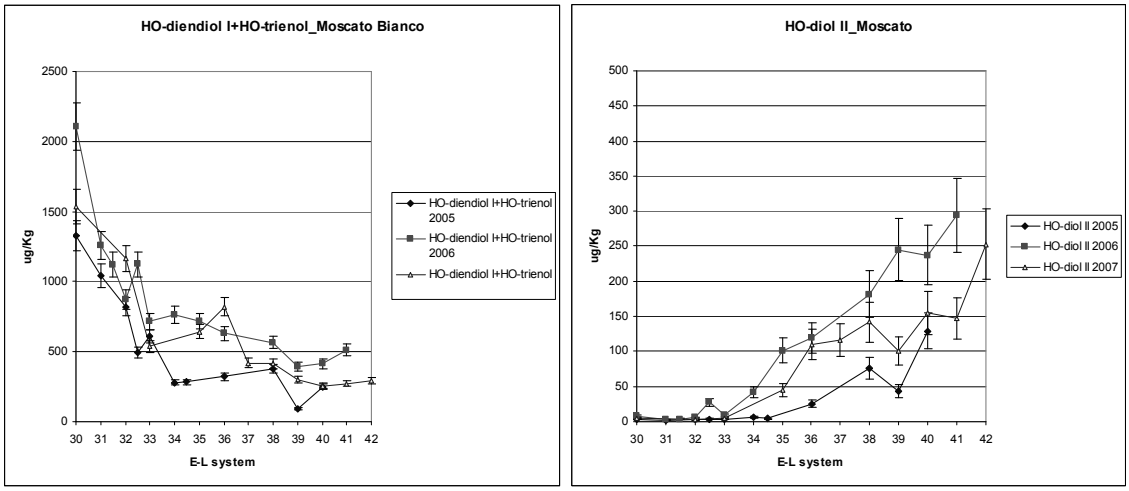

Free diendiols content of Moscato Bianco. Dots corresponde to concentrations (micrograms per Kg of berries) measured during 2005 and 2006 ripening seasons. Triangles correspond to the 2007 season. Phenological stages of growth are reported on X-axes following the E-L system.

Finally, only in Moscato Bianco, free α-terpineol and free citronellol were detected, even at low levels of concentration (less than 8 µg/Kg)

2.3.2.2. Bound monoterpenoids

During berry development, the relative abundance of the free and bound monoterpenes for the most part was shifted. Enzymatic hydrolysis determined the releasing of aglycons from glycosilated terpenoids. Monoterpenoids were found at very high levels of concentration for all the aromatic grapes, and also the kintetic of accumulation seemed to be similar in Chardonnay aromatic clone and Moscato Bianco. Most bound monoterpene

forms increased during berries development. *Trans* furan linalool oxide (OxA), *trans* pyran linalool oxide (OxC) and linalool accumulation through three years are reported in figure 16A, 16B and 16C.

Figure 16

A)

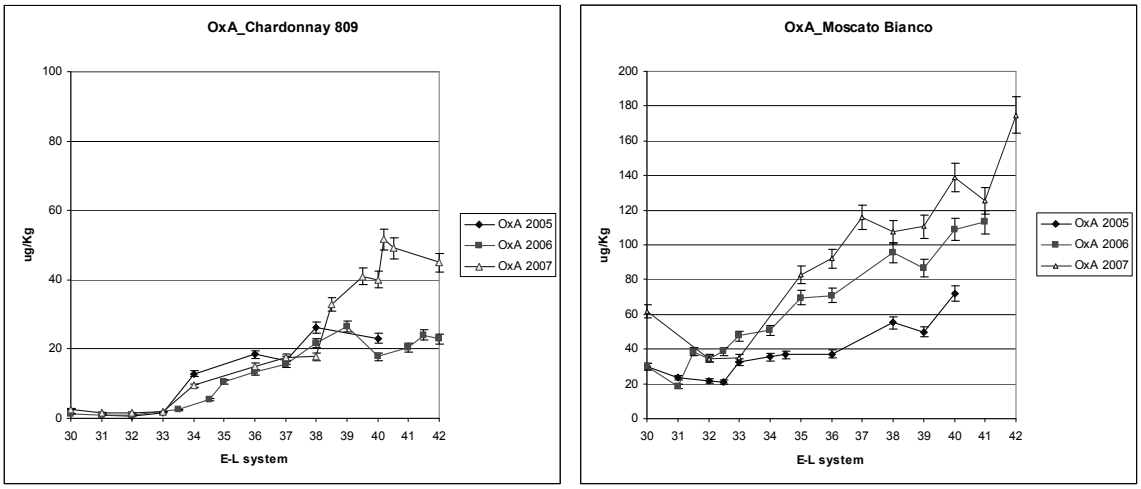

B)

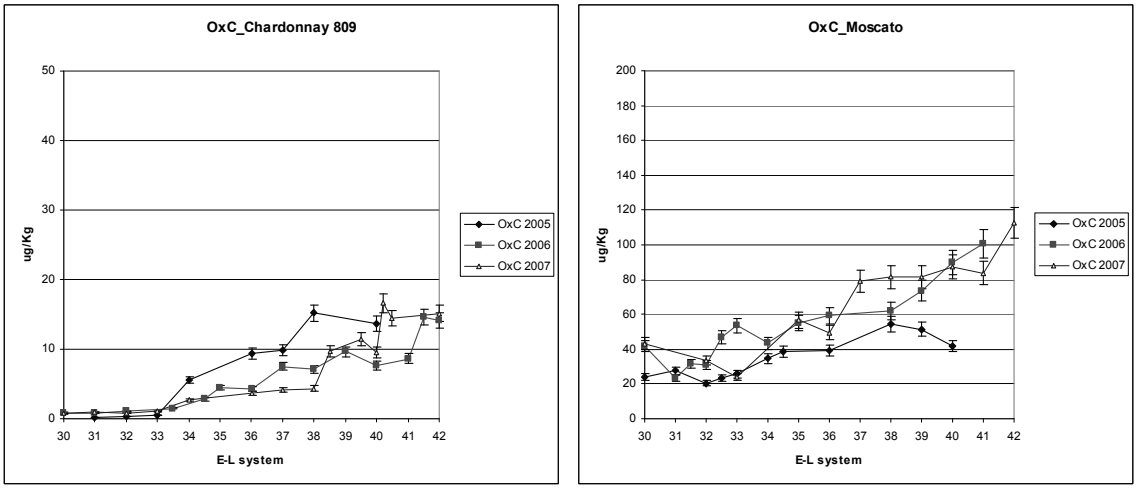

C)

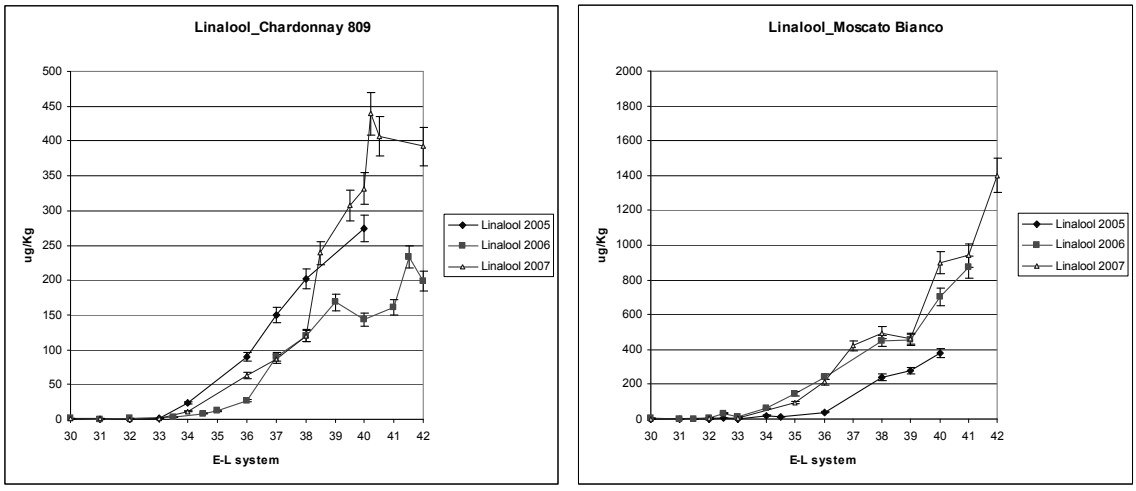

A) and **B)** Bound furanoid linalool oxide (*trans* forms) content of Chardonnay clone 809 and Moscato Bianco. Dots corresponde to concentrations (micrograms per Kg of berries) measured during 2005 and 2006 ripening seasons. Triangles correspond to the 2007 season. Phenological stages of growth are reported on X-axes following the E-L system. **C)** linalool content of Chardonnay clone 809 and Moscato Bianco.

The *cis* furan linalool oxide (OxB) and *cis* pyran linalool oxide (OxD) were detected at very low levels (less than 10 µg/Kg) through berries development both in Chardonnay 809 and in Moscato Bianco.

As soon as the berries matured, bound linalool, nerol, and geraniol became more equally distributed, indicating dynamic changes in distribution and concentration. Geraniol and its geometrical isomer nerol showed a correlated accumulation trend when comparing the same year of sampling. In 2007 both nerol and geraniol were accumulated at very high level: they reached respectively 250 µg/Kg and 2.4 mg/Kg in Chardonnay 809 after harverst time; and 1 mg/Kg and 7 mg/Kg in Moscato Bianco at stage 42. In figure 17A and 17B their kinetic curves of accumulation are reported.

Figura 17

A)

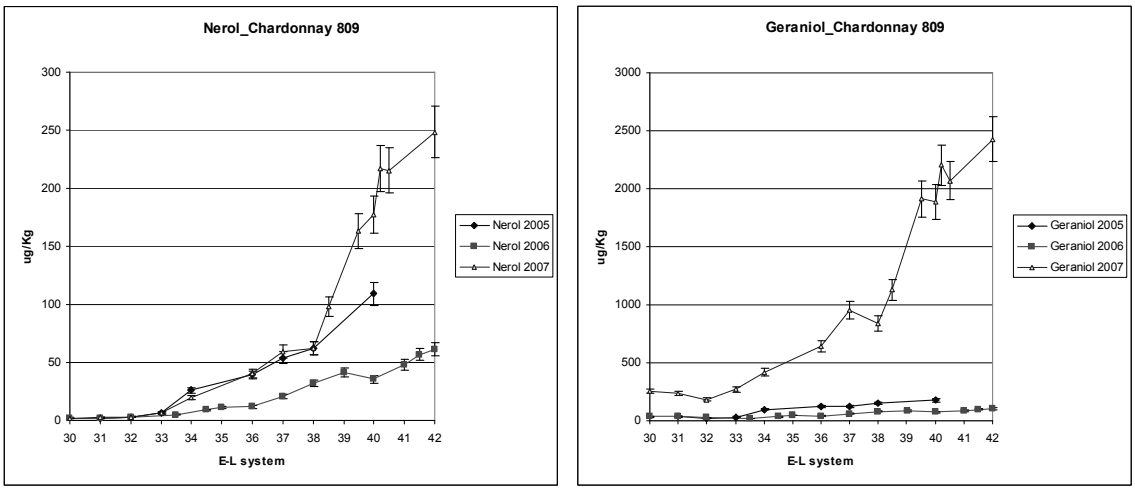

B)

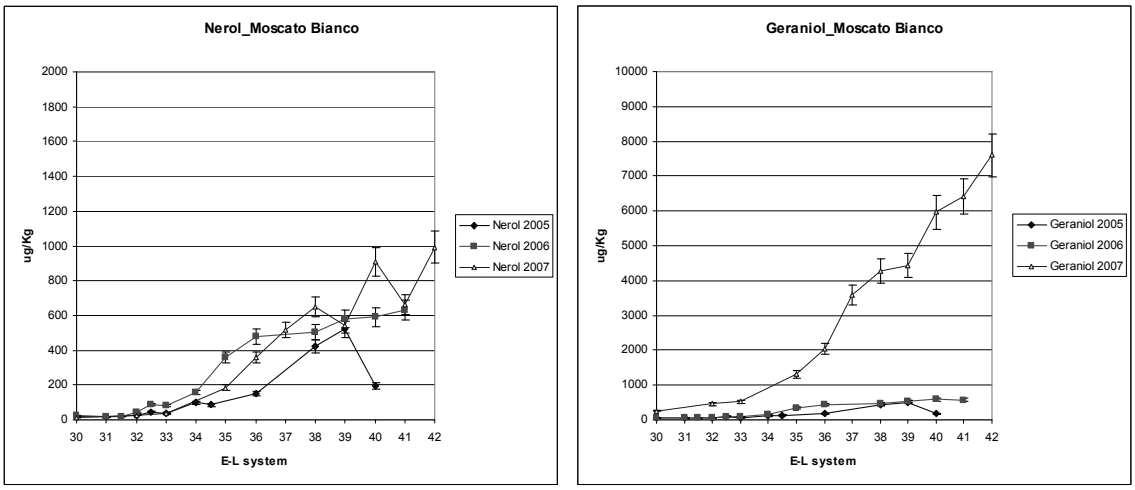

A) Bound nerol and geraniol content of Chardonnay clone 809. **B)** Nerol and geraniol content of Moscato Bianco. Dots corresponde to concentrations (micrograms per Kg of berries) measured during 2005 and 2006 ripening seasons. Triangles correspond to the 2007 season. Phenological stages of growth are reported on X-axes following the E-L system.

In 2007 the bound form of geraniol was accumulated also for Chardonnay clone 130 reaching 210.9 µg/Kg at stage 37, as shown in figure18.

Figure 18

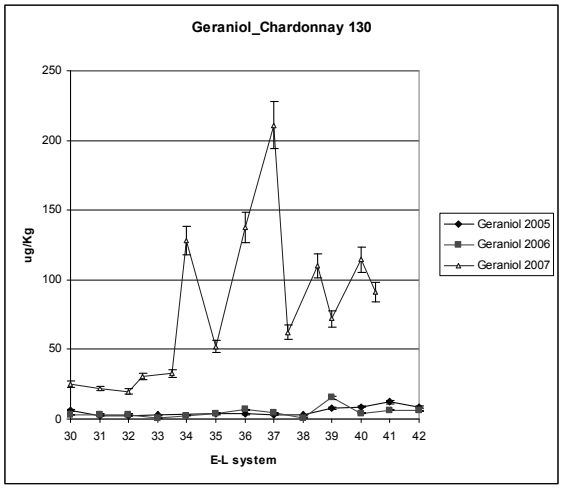

Bound geraniol content of Chardonnay clone 130. Dots corresponde to concentrations (micrograms per Kg of berries) measured during 2005 and 2006 ripening seasons. Triangles correspond to the 2007 season. Phenological stages of growth are reported on X-axes following the E-L system.

Compositional differences are clearly observed between Chardonnay clones, but Chardonnay clone 130 was able to accumulate some glycosilated monoterpens.

Figure 19

A)

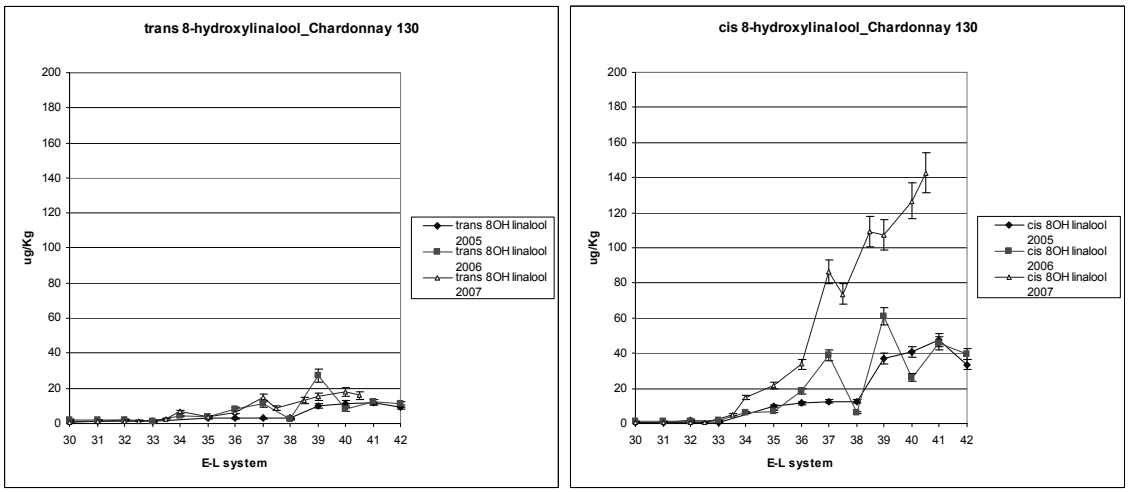

B)

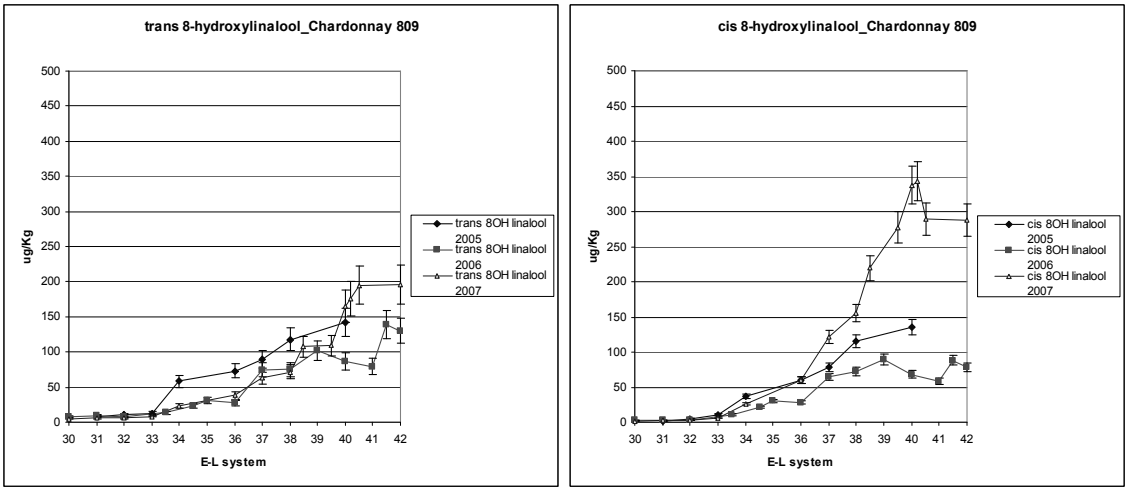

C)

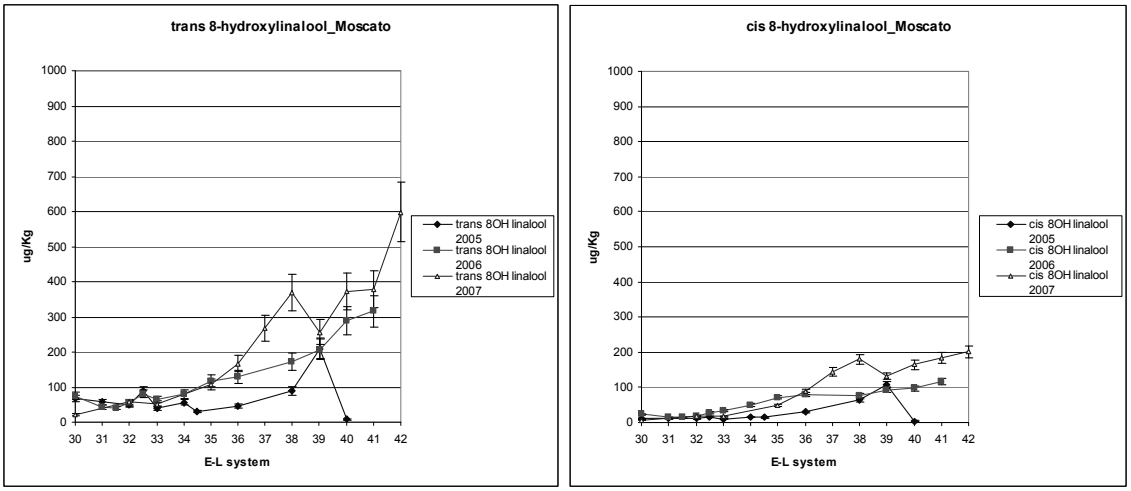

Bound t*rans* 8-hydroxy linalool and *cis* 8-hydroxy linalool content of Chardonnay clone 130 (A), Chardonnay clone 809 (B) and Moscato Bianco (C). Dots corresponde to concentrations (micrograms per Kg of berries) measured during 2005 and 2006 ripening seasons. Triangles correspond to the 2007 season. Phenological stages of growth are reported on X-axes following the E-L system.

In figure 19A, 19B and 19C both *trans* 8-hydroxy linalool and *cis* 8-hydroxy linalool concentration curves for Moscato Bianco, Chardonnay 809 and Chardonnay clone 130 are reported. Moscato Bianco showed an inverted ratio of these compounds with respect to the other varieties.

Figure 20

A)

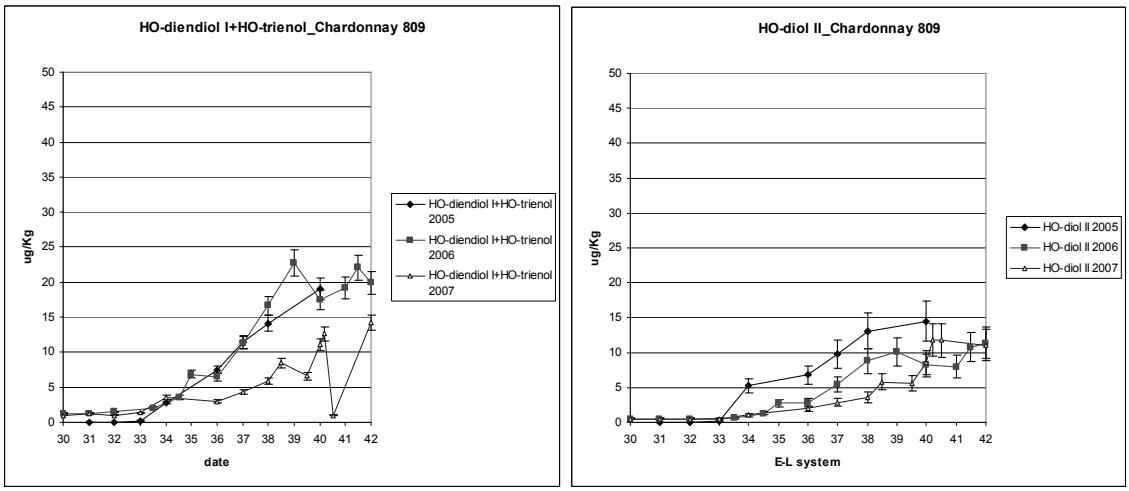

B)

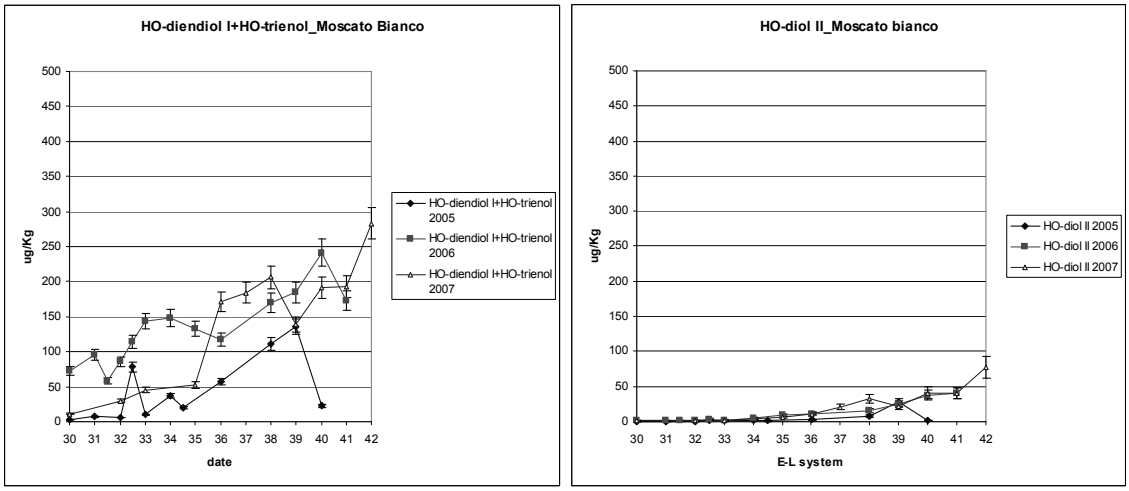

Bound diendiols content of Chardonnay clone 809 (A) and Moscato Bianco (B). Dots corresponde to concentrations (micrograms per Kg of berries) measured during 2005 and 2006 ripening seasons. Triangles correspond to the 2007 season. Phenological stages of growth are reported on X-axes following the E-L system.

The amounts of HO diendiol I + HO-trienol and HO diendiol II were correlated in Chardonnay clone 809, while in Moscato Bianco they differed, as shown in Figure 20. In Moscato Bianco (2007), HO diendiol I + HO-trienol reached a first peak of accumulation (206.2 µg/Kg) at stage 38, while HO diendiol II just reached the 77.1 µg/Kg at over-ripe stage.

2.3.3. Transcription profiling of DXS in berries development

The temporal patterns of *DXS1* expression from pre-veraison to post-veraison development stages were similar in the aromatic clone of Chardonnay and Moscato Bianco. *DXS1* was found significantly up regulated at P-value < 0.05 just before the accumulation peak of linalool, nerol and geraniol compounds. Trends of *DXS1* expression ratio referred to the first sampling date and sum of monoterpens accumulation in both Moscato Bianco and Chardonnay clone 809 were quite similar (Figure 21 and 22). Kolmogorov-Smirnov tests, used to determine if the two datasets differed significantly, revealed a difference in the *DXS1* expression trend at $p<0.05$ between Chardonnay 809 and Moscato Bianco. However as a result of statistic test, a positive correlation of both *DXS1* expression profiles and the monoterpenoids accumulation were detected.

Figure 21

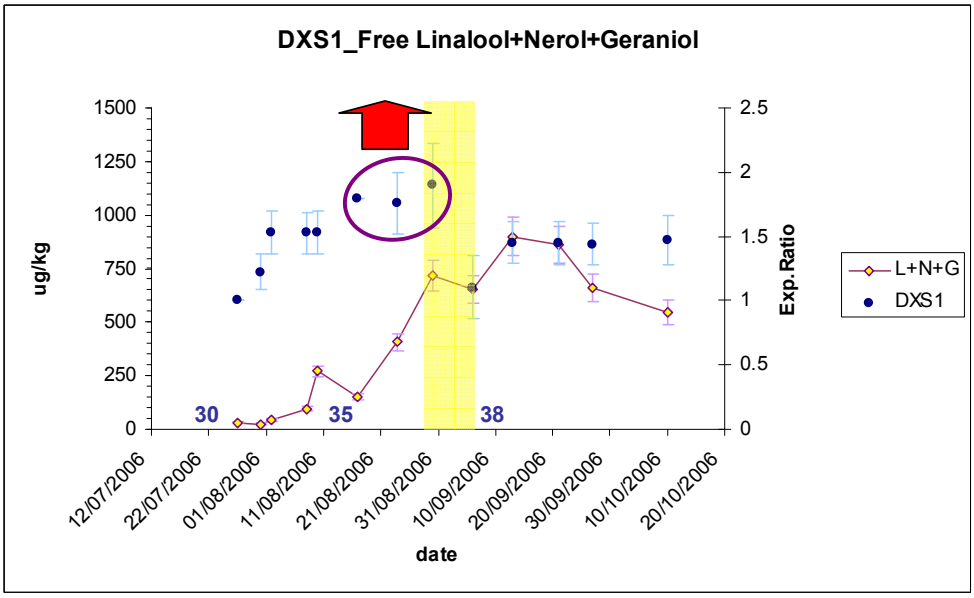

DXS1 expression ratio referred to the first sampling date (blue dots) in Moscato Bianco was significantly up-regulated starting from 2-3 weeks post *véraison* until stage 38. Purple line indicates the sum of concentrations (µg/Kg of berries) of free linalool, nerol and geraniol, while the yellow bar indicates the harvest time.

Figure 22

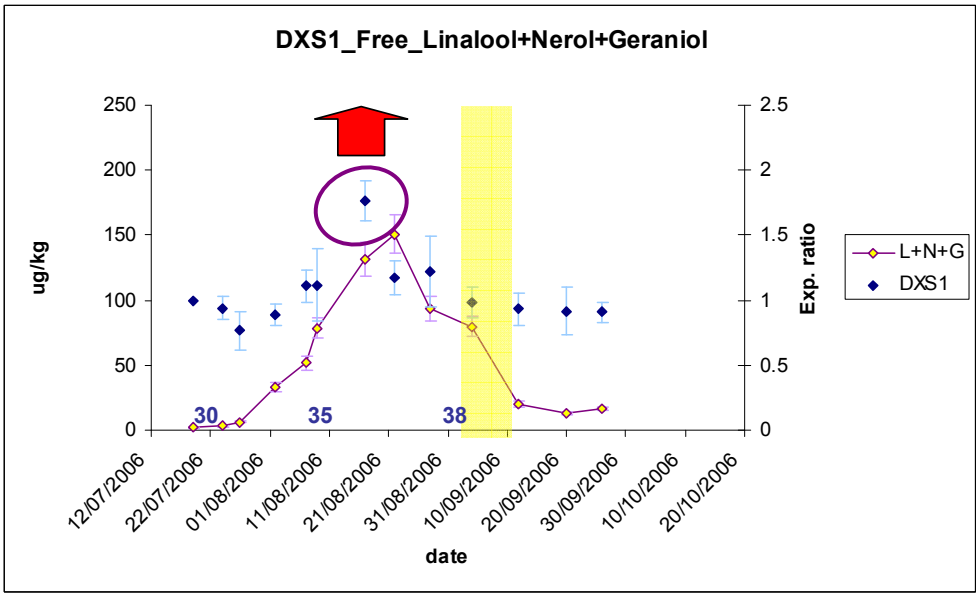

DXS1 expression ratio referred to the first sampling date (blue dots) in Chardonnay clone 809 was significantly up-regulated at 1 week post *véraison*. Purple line indicates the sum of the concentrations (µg/Kg of berries) of free linalool, nerol and geraniol, while the yellow bar indicates the harvest time.

Figure 23

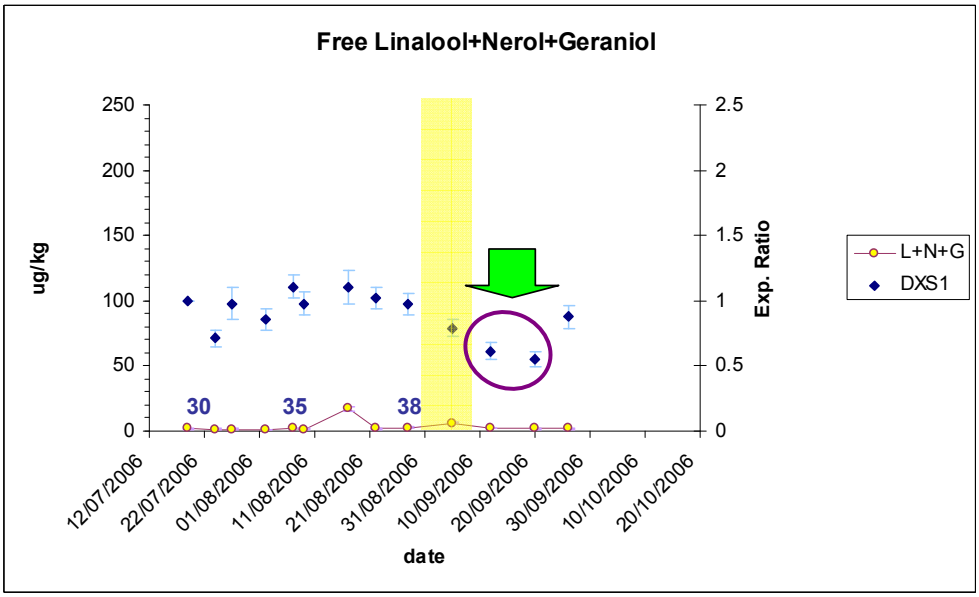

DXS1 expression ratio referred to the first sampling date (blue dots) in non aromatic, Chardonnay clone 130. *DXS1* was significantly down-regulated at stage 39 (E-L system). Purple line indicates the sum of the concentrations (µg/Kg of berries) of free linalool, nerol and geraniol, while the yellow bar indicates the harvest time.

The expression profile of *DXS1* in the non-aromatic Chardonnay clone is shown in figure 23. A down-regulation of *DXS1* during latest stages of berry development of Chardonnay clone 130 was found a couple of weeks post-harvesting, when the organic acid levels were stabilized and the rate of soluble solids accumulation was high.

Calculation of a cumulative sum (CUSUM) procedure was used to detect changes during time in the geometrical means of ratios C_p (target)/C_p (housekeeping genes). This method combined with Kolmogorov-Smirnov test and Jonckheere-Terpstra test allowed the identification of a trend change of *DXS1* expression in Moscato Bianco at the stage 37 (30 august 2006) as underlined by *Pair-Wise Fixed Reallocation Randomization Test. DXS1* expression profile of the Chardonnay clone 809 showed a significative trend change with P-value < 0.05 at stages 36 and 37, corresponding to 17 August 2006 and 22 August 2006. In Chardonnay clone 130 a change in expression trend was also found at stage 37 (22 August 2006) as the aromatic clone. But differently to Chardonnay clone 809, Jonckheere-Terpstra test revealed a change of the *DXS1* expression trend from stage 37 to over-ripening.

Finally, the expression pattern of other *DXS* forms was investigated. *DXS2A* and *DXS2B* do not seem to be expressed during berries development, while *DXS3* and *DXS2C* were expressed at berry development but not significant differences were found.

2.3.4. Sequencing of DXS1

Eight pairs of primers were used to sequence the *DXS1* cDNA and the genomic *DXS1* of the grapevine cultivars considered in this study. The amino acid sequences were predicted for 2151 bp of the Moscato Bianco cDNA and 5039 bp of genomic *DXS1* of Moscato Bianco, Chardonnay clone 130 and Chardonnay clone 809. In Figure 24 the *DXS1* protein sequence is reported and the conserved domains of *DXS* protein of plants are depicted. Chardonnay clones and Pinot Noir have the same DXS1 prediction protein sequence, while Moscato Bianco DXS1 protein shows three amino acids substitution: K284N, V560I, and S717L.

Figure 24

DXS1_Pinot protein sequence of Pinot Noir. DXS1_CH130 correspondes to DXS1 sequence of Chardonnay clone 130 and DXS1_CH809 correspondes to DXS1 sequence of Chardonnay clone 809. Nexus (PAUP 3.0/MacClade) format was exported by MEGA 4 software, and amino acids position are shown as numbers between brackets ([ ]).

2.3.5. Microarray experiments

The peak of monoterpenoids concentration showed a significant accumulation between stage 35 and 37 of grape berry development. In order to identify transcriptomic differences among Chardonnay clones, pools of these two time points were compared. In figure 25 and 26 are reported values of physiological parameters measured in correspondence of the main phases of berry development and ripening of Chardonnay clones and those of some free monoterpenoids.

Figure 25

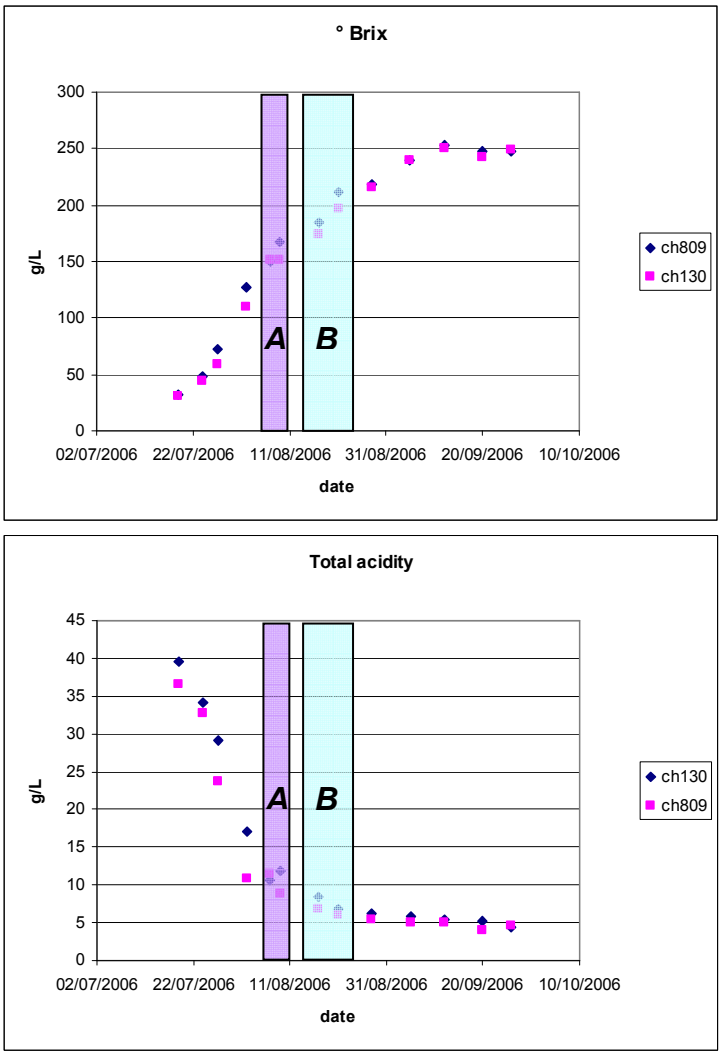

Sugar content and titratable acidity of Chardonnay clone 130 and clone 809. Changes in the physiological parameters measured in correspondence of the main phases of berry development and ripening of the Chardonnay clones. *A* and *B* correspond to the pools used for the transcriptome profiling: "*A*" full veraison on 7/08/2006 and 9/8/2006 (stage 35), and the next closed step "*B*" on 17/08/2006 and 22/08/2006 (stages 36 and 37).

Figure 26

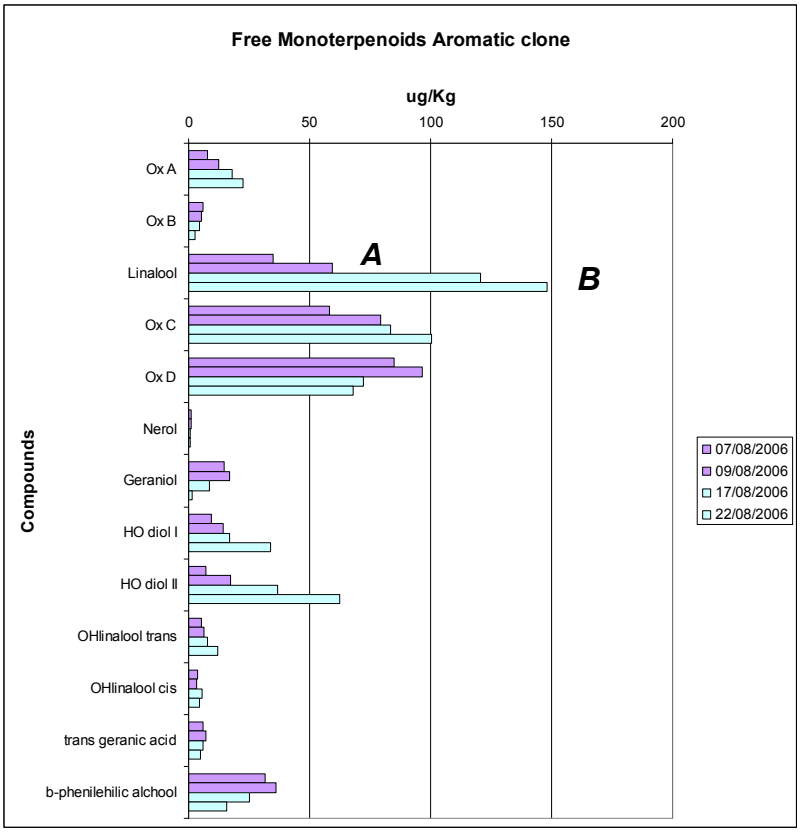
Free Monoterpenoids Aromatic clone
ug/Kg
0
50
100
150
200
Ox A
Ox B
Linalool
Ox C
Ox D
Nerol
Geraniol
HO diol I
HO diol II
OHlinalool trans
OHlinalool cis
trans geranic acid
b-phenilehilic alchool
Compounds
A
B
07/08/2006
09/08/2006
17/08/2006
22/08/2006

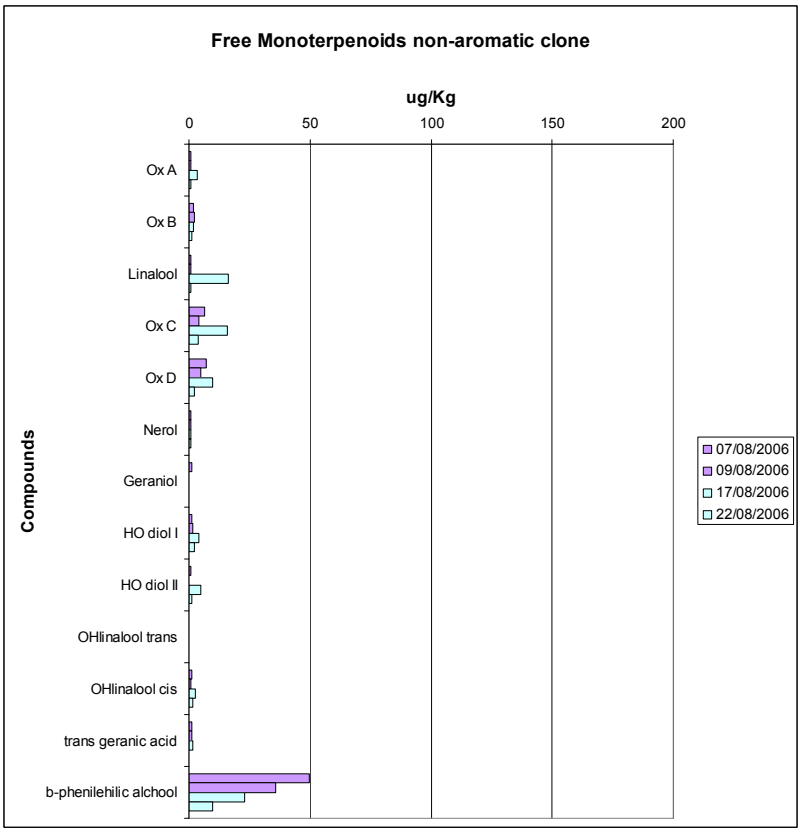
Free Monoterpenoids non-aromatic clone
ug/Kg
0
50
100
150
200
Ox A
Ox B
Linalool
Ox C
Ox D
Nerol
Geraniol
HO diol I
HO diol II
OHlinalool trans
OHlinalool cis
trans geranic acid
b-phenilehilic alchool
Compounds
07/08/2006
09/08/2006
17/08/2006
22/08/2006

Concentration of free monoterpenoid compounds in aromatic and non-aromatic clones composition measured from stage 35 to 37. Histograms represent level of free monoterpenoids and benzenoids compound measured (2006) in aromatic and non-aromatic clone berries. Legend shows the sampling date and the same colour represents the mixed samples.

Microarrays based on the Array-Ready Oligo Set™ for the Grape (*V. vinifera*) Genome Version 1.0 were hybridized with fluorescent targets derived from mRNA extracted from skin of berries *véraison* (pool A) and next close stage (pool B) of aromatic and non-aromatic clones.

For annotation purpose The 14,532 sequences, representing the whole set of sequences of the Ready Oligo Set™ for the Grape (*V. vinifera*) Genome Version 1.0, were re-blasted to the genome sequence of *Vitis* and 77% of them showed significant matches with the gene prediction made by IASMA (http://genomics.research.iasma.it/). Among these, 3524 were annotated as genes encoding proteins with unknown functions.

Differential gene expression in the berries of Chardonnay clone 130

By comparing transcritome of berry from stage 35 and 37 of the Chardonnay clone 130 10,648 out of 14,562 *Vitis* genes spotted on the array (73.1%), showed an hybridization signal. Among these, 143 genes (1.15%) were significant to the SAM analysis and applying an δ-values giving a False Discovery Rate (FDR) equal to zero.

After performing re-annotation genes and t-test (P-value < 0.01) we found 7 unigenes that were more expressed in the pool "A" and 93 unigenes more expressed in the pool "B". In order to elucidate the pathways activated in correspondence of significant changes involved in aroma formation, we applied the MapMan software that allowed assigning functional classes and biological function to the genes that showed significant differences in the expression profile (Figure 27).

Figure 27

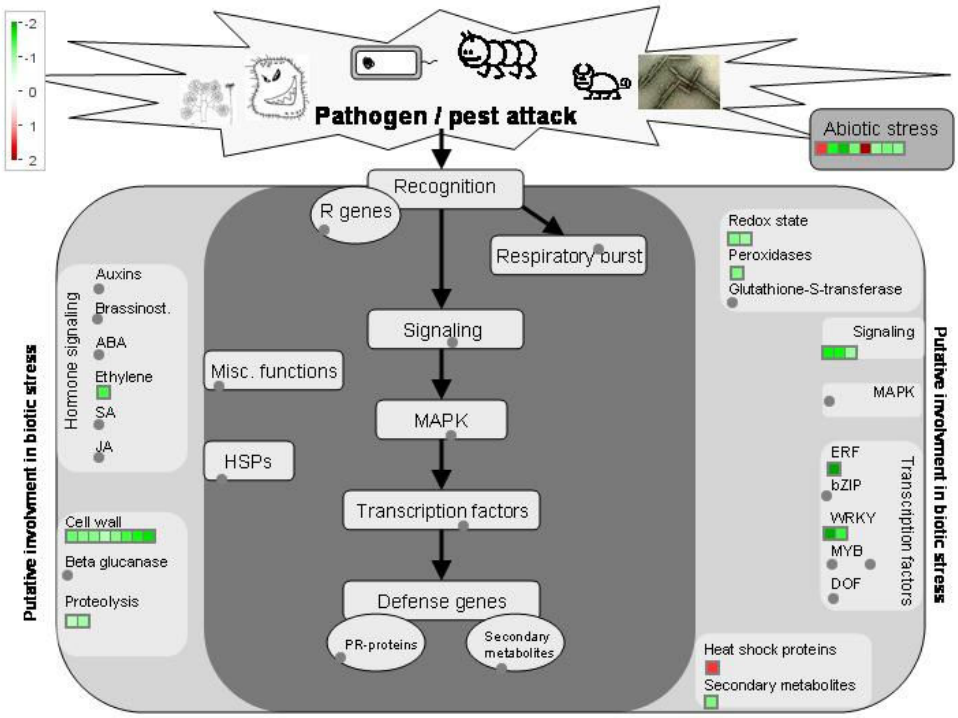

Mapman biotic stress overview of genes differentially expressed in Chardonnay clone 130 (p-value < 0.01). Changes in the transcript levels: Genes are classified by functional categories putatively involved in biotic and abiotic stress in Chardonnay clone 130 experiments. Red points represent the genes with positive ratio between A/B stages in mRNA abundance, while green points represent the negative ratio between A/B stages in mRNA abundance.

Among the 100 unigenes highly represented in the Chardonnay clone 130 experiment, several are involved in Photosystem (4.9%), Cell wall (9.9%), S-assimilation (1.2%), Secondary metabolism (1.2%), Hormone metabolism (1.2%), major CHO metabolism (1.2%), Stress (14.8%), Redox regulation (2.5%), Miscellaneous enzyme family (4.9%), RNA processing and regulation of transcription (13.6%), DNA synthesis/chromatin structure (1.2), Protein (6.2%), Signalling (3.7%), Cell (2.5%), Development (8.6%), Transport (9.9%) and not assigned function (12.3%).

Differential gene expression in the aromatic clone of Chardonnay

The mRNA expression profiles of Chardonnay clone 809 stages were compared and 10,809 (74.8%) targets showed a hybridization signal. By applying Significant analysis microarray (SAM) (with a δ-value giving a FDR = 0) 528 genes (3.98%) have been

selected: 410 genes were more expressed in the pool “A” and 118 were more expressed in the pool “B”. After performing t-test (P-value < 0.01), 413 genes were found to have significant difference in expression among ripening steps of aromatic clone.

For 360 of the genes was possible to perform a re-annotation, as described before, and among these 204 showed differential expressions with a 1.75-fold change or greater in mRNA abundance. In figure 28 the genes classified by functional category putatively involved in biotic and abiotic stress are shown.

Figure 28

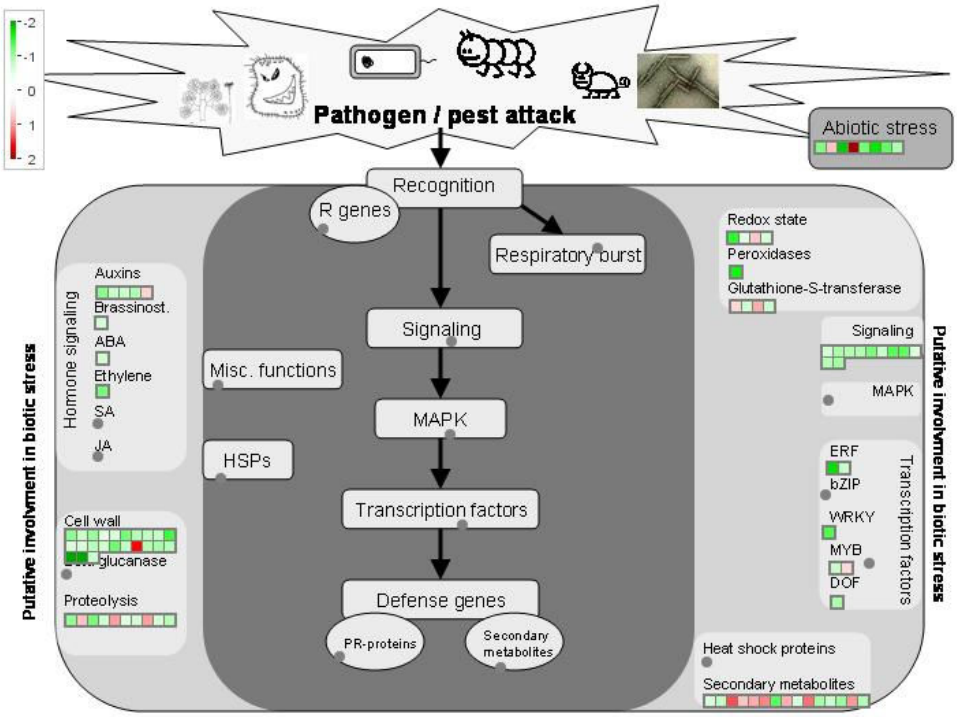

Mapman biotic stress overview of genes differentially expressed in Chardonnay clone 809 (p-value < 0.01). Changes in transcript levels: Genes are classified by functional category putatively involved in biotic and abiotic stress in Chardonnay clone 809 experiments. Red points represent the genes with positive ratio between A/B stages in mRNA abundance, while green points represent the negative ratio between A/B stages in mRNA abundance.

Among the 204 unigenes highly represented in the experiment with Chardonnay clone 809, several are involved in Photosystem (3.7%), Cell wall (8.9%), S-assimilation (0.5%), Secondary metabolism (4.2%), Hormone metabolism (2.1%), major CHO metabolism

(1.0%), Stress (10.5%), Redox regulation (1.6%), Miscellaneous enzyme family (8.4%), RNA processing and regulation of transcription (8.9%), DNA synthesis/chromatin structure (1.6%), Protein (6.8%), Signalling (5.2%), Cell (3.1%), Development (6.3%), Transport (11.0%), C1-metabolism (1.0%), minor CHO metabolism (1.6%), mitochondrial electron transport (0.5%) and 13.1% have not assigned function.

Looking at the transcripts common between the Chardonnay clones, it has been possible to identify 73 unigenes, validated with t-test statistic (Table 11).

Table 11 List of common genes between the experiments validated with t-test statistic and a P-value < 0.01

Gene_ID	New_TC	Chr	Description	CH130	Ch809
fgenesh.VV78X032908.3_1	TC56479	16	Chlorophyll a/b-binding protein	-1.17	-1.08
fgenesh.VV78X190210.17_3	TC61693	5	Photosystem I reaction center subunit II-2, chloroplast precursor	-0.87	-0.91
fgenesh.VV78X263622.19_2	TC61603	12	Putative caltractin	-1.65	-1.93
glimmer.VV78X207172.29_3	TC52297	10	Subtilisin-like serine protease, partial (4%)	-1.05	-0.84
glimmer.VV78X073696.19_1	TC68949	5	unknown	-1.39	-1.22
sim4.VV78X168225.9_1	TC60619	15	Aquaporin PIP1-2	-0.95	-0.96
glimmer.VV78X075663.22_7	TC58885	5	GDP-mannose 3,5-epimerase	-1.14	-1.11
glimmer.VV78X273964.41_2	TC51824	7	Probable xyloglucan endotransglucosylase/hydrolase protein 6 precursor	-0.84	-1.05
glimmer.VV78X215150.12_2	TC53227	19	Putative uncharacterized protein	-1.88	-1.47
fgenesh.VV78X106753.9_2	TC54968	7	Similarity to endo-1	-0.97	-1.17
glimmer.VV78X077500.11_2	TC56399	16	Ethylene-responsive transcription factor 6	-1.29	-1.32
glimmer.VV78X131860.31_5	TC55048	3	NADPH oxidoreductase, putative	-1.62	-2.03
glimmer.VV78X266542.9_1	TC52467	10	Peroxidase 41 precursor	-0.92	-1.01
glimmer.VV78X056050.8_1	TC62636	3	Subtilisin proteinase-like	-1.12	-1.17
glimmer.VV78X087740.6_3	TC61828	16	Serine/threonine protein kinase-like protein, partial (18%)	1.45	1.20
fgenesh.VV78X166400.20_4	TC59118	19	RING-H2 finger protein ATL4K	-1.35	-1.96
glimmer.VV78X239794.6_5	TC56317	7	Pectinesterase-2 precursor	-1.30	-1.05
twinscan.VV78X193469.7_2	TC51886	5	Sulfate transporter 1.3	-1.69	-1.34
fgenesh.VV78X249214.9_1	TC58159	13	Putative tropinone reductase	-1.60	-1.04
glimmer.VV78X050535.4_8	TC55531	12	5'-adenylylsulfate reductase 2, chloroplast precursor	-0.86	-1.81
glimmer.VV78X085330.6_2	TC63963	2	Arabinogalactan peptide 20 precursor	-1.29	-1.34
fgenesh.VV78X067174.8_1	TC62514	16	Tubulin beta-2/beta-3 chain	-1.46	-1.11
twinscan.VV78X072672.8_6	TC63565	14	Hydroxyproline-rich glycoprotein GAS28 precursor, partial (6%)	-1.40	-1.78
glimmer.VV78X201714.14_4	TC71022	3	Ethylene-responsive transcription factor ERF112	-1.13	-1.07
glimmer.VV78X076308.25_1	TC69009	11	Transcription factor ICE1	-1.76	-1.38
glimmer.VV78X086565.4_1	TC63431	10	Amino acid/polyamine transporter II, partial (81%)	1.45	1.24
twinscan.VV78X085037.7_4	TC59788	10	Tonoplast dicarboxylate transporter	-0.91	-0.90
sim4.VV78X038611.7_3	TC65080	15	Similar to late embryogenesis abundant proteins	1.36	1.23
fgenesh.VV78X014102.6_3	TC54010	1	probable pectinerase protein	-0.90	-0.96

fgenesh.VV78X066558.24_3	TC66009	8	Aquaporin TIP1-3	-1.31	-1.58
sim4.VV78X203135.19_5	TC65556	13	Chlorophyll a-b binding protein CP29.1, chloroplast precursor	-1.70	-1.20
glimmer.VV78X151728.5_2	TC60693	12	Beta-fruct: Beta-fructofuranosidase (Fragment)	-0.87	-1.11
glimmer.VV78X016914.14_1	TC54052	none	Calmodulin-7	-1.41	-1.11
glimmer.VV78X112440.8_4	TC51921	19	Ethylene-responsive transcription factor 5	-1.19	-1.39
sim4.VV78X247308.5_1	TC54167	13	At4g29190: Putative uncharacterized protein AT4g29190	-1.76	-0.95
glimmer.VV78X075364.12_2	TC55261	6	CCR4-associated factor 1-like protein	-2.06	-1.77
sim4.VV78X180461.16_1	TC58115	11	ribonuclease/ transcriptional repressor	-1.14	-1.19
glimmer.VV78X203731.3_2	TC63907	11	Similarity to cell wall-plasma membrane linker protein	-1.84	-1.23
glimmer.VV78X013848.15_1	TC58585	12	Probable wound-induced protein	-1.84	-1.86
glimmer.VV78X152177.6_4	TC58912	16	Tubulin beta-2/beta-3 chain	-1.07	-2.17
sim4.VV78X049585.19_1	TC56835	1	unknown	-0.99	-1.10
fgenesh.VV78X035074.7_5	TC68052	1	Probable UDP-glucose 6-dehydrogenase 1	-0.91	-1.26
glimmer.VV78X259070.11_5	TC59548	15	Probable WRKY transcription factor 25	-2.70	-1.88
glimmer.VV78X153233.10_2	TC67407	6	AT5g17860/MVA3_210	-1.44	-1.10
glimmer.VV78X170195.9_1	TC59424	11	unknown	-1.51	-1.54
fgenesh.VV78X035546.6_6	TC59629	15	Homeobox-leucine zipper protein HAT5	-1.01	-0.98
glimmer.VV78X250222.4_2	BM438092	7	Disease resistance protein (Fragment)	-1.42	-1.09
fgenesh.VV78X277701.9_5	TC69160	1	unknown	-1.28	-1.02
fgenesh.VV78X268558.4_3	TC54946	1	Nudix hydrolase 4	-1.74	-2.09
glimmer.VV78X031878.8_2	CB921312	6	ATFP2 (Fragment)	-2.31	-1.84
sim4.VV78X160356.7_1	TC71116	4	CBL-interacting protein kinase 16	-1.34	-1.75
glimmer.VV78X031461.9_1	CD005432	17	Arm repeat containing protein	1.31	1.28
glimmer.VV78X127727.49_1	TC55407	7	NAC domain-containing protein 2	-2.24	-1.32
fgenesh.VV78X023879.7_1	CF209376	18	Plasma membrane aquaporin	-1.12	-0.95
fgenesh.VV78X216174.29_3	TC53968	7	Sulfate transporter 3.2	-2.27	-1.97
fgenesh.VV78X124178.14_1	TC66195	6	Pathogenesis-related protein 10.3	2.86	2.21
fgenesh.VV78X220362.21_3	TC63622	6	SCARECROW gene regulator	-1.41	-1.62
glimmer.VV78X153392.6_4	TC58513	2	CELL WALL-PLASMA MEMBRANE LINKER PROTEIN	-2.75	-2.23
glimmer.VV78X139444.15_16	TC53971	13	Aquaporin TIP1-3	-1.51	-0.93
fgenesh.VV78X085993.13_2	TC55604	6	SNF1-related protein kinase regulatory subunit beta-1	-1.14	-1.53
glimmer.VV78X225495.6_2	TC52279	8	Peroxidase precursor	-1.59	-1.14
twinscan.VV78X211539.4_9	TC70740	10	Scarecrow-like 1	-1.13	-0.86
glimmer.VV78X055060.34_3	TC64102	11	Harpin inducing protein (Hin1), partial (86%)	-0.89	-1.66
glimmer.VV78X125768.3_1	TC58023	19	Putative caltractin	-0.91	-0.87
glimmer.VV78X227342.7_1	TC56756	5	Pollen-specific protein	-1.28	-1.08
glimmer.VV78X227342.7_2	TC62717	5	unknown	-0.88	-1.19
glimmer.VV78X185772.13_2	CF212592	11	Probable xyloglucan endotransglucosylase/hydrolase protein 25 precursor	-1.49	-1.14
fgenesh.VV78X081148.26_1	TC65275	7	unknown	-1.43	-1.84
glimmer.VV78X269695.4_1	BM436925	16	Copia-type reverse transcriptase-like protein	-1.07	-0.99
glimmer.VV78X108629.8_1	CB346454	11	Probable xyloglucan endotransglucosylase/hydrolase protein 17 precursor	-0.81	-0.99
glimmer.VV78X045459.8_4	TC58991	11	Probable xyloglucan endotransglucosylase/hydrolase protein 25 precursor	-1.02	-1.23
sim4.VV78X002846.67_1	TC61870	15	Alpha-tubulin, partial (13%)	-1.26	-1.04
twinscan.VV78X180406.5_7	TC63468	3	unknown	-1.00	-1.15

Gene_ID indicates the gene index of Gene Predictions (http://genomics.research.iasma.it/); New_TC represents the Tentative Consensus, oligonucleotides were re-annotated with the most recent release of the DFCI Grape Gene Index Version 5.0, June 2006. Description has been obtained by BLASTX of gene predictions sequences from the whole genome sequencing project to *Arabidopsis thaliana* homologues. CH130 and CH809 represent the experiments of Chardonnay 130 and Chardonnay 809, respectively. Positive numbers (red) correspond to genes that are more expressed in pool "A". Negative numbers (green) correspond to genes that are more expressed in pool "B".

Among these unigenes, independently by the clone, 68 were more expressed in the pool "B", when level of total monoterpenoids peaked, while 5 unigenes were more expressed in pool "A". By considering the clone, 12 genes were more expressed (plus 30%) in Chardonnay 130 than Chardonnay 809, vice versa 12 genes were more expressed in Chardonnay 809 rather than Chardonnay 130 at stage "B". Finally one gene was down regulated during ripening development in Chardonnay clone 809 more than neutral clone (Table 12).

Table 12

Annotation	Ratio	Involved in
xyloglucan endotransglycosylase 17	1.4	cell wall modification
xyloglucan endotransglycosylase 3	1.7	cell wall modification
xyloglucan endotransglycosylase	1.5	cell wall modification
Late embryogenesis abundant protein Lea14-A	2.1	development.late embryogenesis abundant
NAC domain-containing protein 2	1.4	development.unspecified
yellow-leaf-specific gene 9	1.9	development.unspecified
gag-pol polyprotein	1.3	DNA.synthesis/chromatin structure
Peroxidase 41 precursor	1.4	miscellaneous enzyme family.peroxidases
unknown	1.7	not assigned
RING-H2 finger protein	1.5	protein.degradation.ubiquitin.E3.RING
Photosystem I reaction center subunit II-2	1.3	PS.lightreaction.photosystem I
chlorophyll a/b binding protein 3	1.4	PS.lightreaction.photosystem II
Photosystem II subunit X	1.5	PS.lightreaction.photosystem II
GDP-D-mannose 3',5'-epimerase	1.3	redox.ascorbate and glutathione.ascorbate
WRKY25	1.5	RNA.regulation of transcription
Homeobox-leucine zipper protein	1.4	RNA.regulation of transcription
zinc finger (CCCH-type)	1.3	RNA.regulation of transcription
isoflavone reductase	1.3	secondary metabolism.flavonoids.isoflavonols
similar to nodulin-related	1.3	stress.abiotic.drought/salt
MLP-like protein 423	1.4	stress.abiotic.unspecified
MLP-like protein 34	1.4	stress.abiotic.unspecified
ubiquitin-protein ligase	1.3	stress.biotic
Sodium/calcium exchanger membrane	1.5	transport.calcium
Aquaporin TIP1-3	1.5	transport.Major Intrinsic Proteins
tonoplast dicarboxylate transporter	1.7	transport.unspecified cations

Blue ratio corresponds to genes that are more expressed (plus 30%) in Chardonnay clone 130 than Chardonnay clone 809 in the pool "B". Violet ratio corresponds to genes that are more expressed in Chardonnay clone 809 rather than Chardonnay clone 130 in the pool "B".

In tables 12A and 12B: 27 unigenes found only in Chardonnay clone 130 experiment, and 131 unigenes found only in Chardonnay clone 809 experiment with 1.75 or greater fold change.

Table 13:

A) Genes differentially expressed in Chardonnay clone 130 only.

Gene_ID	New_TC	Chr	Gene_Annotation	Ratio
glimmer.VV79X004837.6_1	TC53165	none	unknown	-1.30
fgenesh.VV78X000894.6_1	TC57973	none	unknown	-1.67
glimmer.VV79X006832.4_2	CB919220	1	Phosphate/triose-phosphate translocator	-1.07
glimmer.VV78X150626.14_6	TC59428	1	Probable zinc transporter 10 precursor	-1.35
fgenesh.VV78X030876.17_1	TC63786	2	transcription factor, Similarity to NAM	-0.95
glimmer.VV78X178537.24_8	TC52500	2	Beta-fructosidase	-1.10
fgenesh.VV78X054954.15_3	CB345765	3	sulA, plastid-targeted protein	-0.98
glimmer.VV78X238526.9_6	TC69265	5	unknown	-0.98
fgenesh.VV78X208633.16_2	TC61483	5	Retroelement pol polyprotein-like	-1.12
fgenesh.VV78X029747.10_2	CA816502	7	Senescence-associated gene 101	-1.34
sim4.VV78X260730.42_11	TC58032	9	Probable aquaporin TIP2-2	-0.89
glimmer.VV78X033748.3_1	TC63623	10	Monothiol glutaredoxin-S7	-1.00
fgenesh.VV78X009646.12_6	TC57989	10	Arm repeat containing protein	-1.09
glimmer.VV78X185772.13_2	TC58991	11	Probable xyloglucan endotransglucosylase/hydrolase protein 25 precursor	-0.95
glimmer.VV78X172274.5_1	TC57528	12	heat shock protein	1.44
fgenesh.VV78X263061.11_8	TC51953	12	Fasciclin-like arabinogalactan protein 13 precursor	-0.86
sim4.VV78X015037.17_5	TC57849	12	Monothiol glutaredoxin-S7	-0.96
glimmer.VV78X013848.15_1	TC56430	12	unknown	-2.23
sim4.VV78X154954.28_5	TC63994	13	unknown	-1.34
glimmer.VV78X139444.15_8	TC66761	13	60S ribosomal protein L23a-1	-1.41
fgenesh.VV78X240429.8_5	TC58747	14	Similarity to nodulin	-1.05
twinscan.VV78X075610.16_1	TC55552	15	Putative uncharacterized protein	1.32
fgenesh.VV78X077986.6_1	TC64282	15	Probable WRKY transcription factor 30	-1.44
glimmer.VV78X087740.6_3	TC61828	16	Putative uncharacterized protein	-0.99
glimmer.VV78X024929.13_4	TC64370	18	Putative calmodulin	-1.12
glimmer.VV78X079753.10_1	TC62621	18	Dehydrin COR47	-1.20
glimmer.VV78X028377.30_7	TC53421	18	EXO phosphate-responsive protein	-1.62

B) Genes differential expressed in Chardonnay clone 809 only.

Gene_ID	New_TC	Chr	Gene_Annotation	Median
fgenesh.VV78X125421.34_5	TC58892	none	Glutathione transferase	-1.01
glimmer.VV78X110616.9_2	TC67019	none	Glutathione transferase 8	-1.74
sim4.VV78X271510.6_2	TC53886	1	senescence-associated family protein	1.54
glimmer.VV78X231955.55_1	TC63258	1	alliinase family protein / carbon-sulfur lyase	1.21
glimmer.VV78X202561.5_4	CD715744	1	PHOT2 Phototropin-2	0.80
glimmer.VV78X029806.3_3	TC67064	1	Putative glycosyl transferase	-0.85
sim4.VV78X273463.16_1	TC56669	1	Xyloglucan endotransglucosylase/hydrolase protein 4 precursor	-0.87
twinscan.VV78X226055.5_2	CB921642	1	Receptor-protein kinase-like protein	-0.89
twinscan.VV78X037166.10_1	TC66322	1	MLP34, At1g70850, F15H11.10: MLP-like protein 34	-1.17
fgenesh.VV78X088960.11_1	TC68781	1	unknown	-1.43
glimmer.VV78X211641.9_1	TC61612	2	transferase family protein	1.40
sim4.VV78X030347.25_1	TC65907	2	AOX3, Alternative oxidase 3, mitochondrial precursor	1.32
sim4.VV78X106690.3_1	TC59789	2	invertase/pectin methylesterase inhibitor family protein	0.84
fgenesh.VV78X115352.4_1	TC51780	2	Putative uncharacterized protein	0.83
glimmer.VV78X020928.13_1	TC55780	2	Aquaporin PIP1-2	-0.85
glimmer.VV78X072496.9_2	TC53798	2	Putative uncharacterized protein	-1.12
glimmer.VV78X041959.4_8	TC56582	2	plastocyanin-like domain-containing protein	-1.21
fgenesh.VV78X064711.9_2	TC61028	3	Putative phytosulfokines 4 precursor	-0.87
glimmer.VV78X011652.21_5	TC52780	3	Peptidyl-prolyl cis-trans isomerase CYP18-4	-0.99
twinscan.VV78X180406.5_7	TC63468	3	Putative uncharacterized protein	-1.22
fgenesh.VV78X139537.28_1	TC55227	4	C2H2 SET	1.04
twinscan.VV78X097167.8_1	TC69716	4	ATPase 2, plasma membrane-type	0.90
fgenesh.VV78X256089.26_1	TC55820	4	Expansin-A3 precursor	-0.95
fgenesh.VV78X272109.31_6	TC68878	4	unknown	-1.10
sim4.VV78X227342.7_2	TC55986	5	Pathogenesis-related protein 10	3.06
glimmer.VV78X253398.2_1	TC56222	5	disease resistance response	2.31
sim4.VV78X088810.7_1	TC65214	5	Class IV endochitinase	1.15
fgenesh.VV78X170540.2_1	TC59101	5	Putative ubiquitin-conjugating enzyme	1.01
glimmer.VV78X093984.21_18	TC63589	5	Putative uncharacterized protein	-0.86
sim4.VV78X104218.19_23	TC65158	5	Putative UPF0497 membrane protein	-1.07
glimmer.VV78X009806.10_4	TC65993	5	Probable pectate lyase 8 precursor	-1.22
glimmer.VV78X075663.22_7	TC58885	5	GDP-mannose 3,5-epimerase	-1.48
sim4.VV78X211789.9_1	TC70715	6	Trans-cinnamate 4-monooxygenase	0.92
fgenesh.VV78X194990.4_1	TC60503	6	WBC12, White-brown complex homolog protein 12	0.87
fgenesh.VV78X197454.15_6	CB923231	6	Receptor-like protein kinase precursor	-0.88
glimmer.VV78X197454.15_10	TC52488	6	Receptor-like protein kinase precursor	-0.97
fgenesh.VV78X012342.7_2	TC70833	6	Glucosyltransferase-like protein	-1.18
fgenesh.VV78X226545.10_1	TC58959	6	Glutathione S-transferase 103-1A	-1.30
sim4.VV78X085993.13_5	TC65948	6	CAM7, Calmodulin-7	-1.56
fgenesh.VV79X009893.3_9	TC56635	7	Putative uncharacterized protein	1.14
glimmer.VV79X002434.5_3	TC52643	7	glutathione S-transferase, putative	0.91
fgenesh.VV78X142034.3_1	TC58405	7	rubber elongation factor (REF) family protein	0.88
fgenesh.VV78X210042.3_1	TC62295	7	PP2C, Protein phosphatase 2C, putative	-0.81
fgenesh.VV78X026826.29_1	TC53829	7	3-ketoacyl-CoA thiolase 5, peroxisomal precursor	-1.07
fgenesh.VV78X108675.15_2	TC56821	7	Putative uncharacterized protein	-1.10
fgenesh.VV78X106753.9_2	TC54968	7	Similarity to endo-1	-1.59
glimmer.VV78X140156.6_1	TC66528	8	phenylalanine ammonia-lyase 1 (PAL1)	1.35

fgenesh.VV78X218418.10_2	CB923118	8	Cysteine synthase, mitochondrial precursor	1.09
fgenesh.VV78X066558.24_4	TC56449	8	Putative zinc-finger protein	0.89
fgenesh.VV78X218406.3_1	TC57642	8	Histone deacetylase HDT1	0.80
glimmer.VV78X104344.5_10	TC66168	8	Putative uncharacterized protein At1g19170	-0.81
fgenesh.VV78X211100.7_1	CF209366	8	CAX3, Vacuolar cation/proton exchanger 3	-0.86
glimmer.VV78X064570.20_2	TC58869	8	Putative uncharacterized protein	-0.89
glimmer.VV78X121987.7_4	TC69704	8	Cinnamyl alcohol dehydrogenase-like protein	-0.93
sim4.VV78X081162.7_3	TC61865	8	Putative uncharacterized protein (Fragment)	-0.94
glimmer.VV78X033427.2_2	TC54286	8	unknown	-0.96
glimmer.VV78X233982.51_1	TC59520	8	TUBB2, Tubulin beta-2/beta-3 chain	-1.27
glimmer.VV78X077123.10_5	CF373275	8	Putative uncharacterized protein	-1.35
glimmer.VV78X159776.2_1	CF207368	9	Phosphoglycerate dehydrogenase	-0.86
sim4.VV78X082636.6_1	TC58280	9	unknown	-0.97
glimmer.VV78X099104.8_2	TC52484	9	CBL-interacting protein kinase 15 (CIPK15)	-1.08
glimmer.VV78X251477.5_4	TC53549	10	Thiazole biosynthetic enzyme, chloroplast precursor	0.95
fgenesh.VV78X252289.7_3	TC60623	10	Sucrose-phosphate synthase-like protein	0.88
glimmer.VV78X128499.5_2	CF210547	10	Lipase/hydrolase, putative	-0.84
glimmer.VV78X053969.18_6	TC56952	10	F-box family protein	-0.85
fgenesh.VV78X107337.7_1	TC52528	10	Photosystem I reaction center subunit III family protein	-1.04
fgenesh.VV78X168936.5_1	CB921347	11	nodulin family protein	1.16
glimmer.VV78X247793.3_1	TC60943	11	4CL3, 4-coumarate-CoA ligase 3	1.11
sim4.VV78X047607.17_6	TC57113	11	zinc finger (ubiquitin-hydrolase) domain-containing protein	0.99
glimmer.VV78X013512.52_1	TC61460	11	unknown	0.90
sim4.VV78X166267.15_1	TC65421	11	GER3, Germin-like protein subfamily 3 member 3 precursor	-0.90
fgenesh.VV78X052536.6_1	TC51758	11	Pyrophosphate-energized vacuolar membrane proton pump 1	-0.91
glimmer.VV78X264312.11_2	TC52209	12	Legumin-like protein	1.29
sim4.VV78X221198.31_3	TC68430	12	unknown	1.27
fgenesh.VV78X221198.31_1	TC62635	12	RPS5 Disease resistance protein	1.10
glimmer.VV78X243798.37_16	TC63546	12	Putative uncharacterized protein	-0.88
glimmer.VV78X029500.7_2	TC52851	12	Peptide transporter PTR2	-0.91
twinscan.VV78X063867.5_5	TC52544	12	tetratricopeptide repeat (TPR)-containing protein	-2.07
fgenesh.VV78X071547.8_3	TC55039	13	PHD finger transcription factor, putative	0.97
sim4.VV78X081633.37_5	CB918260	13	Putative uncharacterized protein (Fragment)	-0.80
glimmer.VV78X010440.9_1	TC52177	13	leucine-rich repeat transmembrane protein kinase, putative	-0.93
twinscan.VV78X135834.21_3	TC52786	13	GDP-mannose pyrophosphorylase like protein	-1.08
twinscan.VV78X061535.9_2	TC66244	13	Wall-associated receptor kinase-like 17 precursor	-1.17
fgenesh.VV78X184233.28_1	TC54970	13	unknown	-1.22
fgenesh.VV78X173348.8_5	TC58665	14	unknown	1.06
glimmer.VV78X248264.14_6	TC58932	14	rapid alkalinization factor (RALF) family protein	-0.87
glimmer.VV78X250398.9_3	TC64478	14	MDR4, Multidrug resistance protein 4	-0.88
sim4.VV78X267733.89_2	TC53570	14	At1g67080: Putative uncharacterized protein	-0.89
glimmer.VV78X157796.9_4	TC60883	14	Calmodulin-binding family protein-like	-0.90
glimmer.VV78X082844.4_3	TC64460	14	proton-dependent oligopeptide transport (POT) family protein	-0.96
fgenesh.VV78X171075.10_2	TC57978	14	UDP-glucose glucosyltransferase	-1.02
glimmer.VV78X218333.6_1	TC62699	14	Nodulin-like protein protein	-1.03
glimmer.VV78X023027.2_1	TC54542	14	Photosystem II reaction center W protein, chloroplast precursor	-1.05
glimmer.VV78X180904.6_1	TC58750	15	Putative expansin-B2 precursor	1.60
glimmer.VV78X165013.22_2	TC63749	15	IQ domain-containing protein / BAG domain-containing protein	-1.84

glimmer.VV78X129424.15_1	TC54681	16	Putative uncharacterized protein	1.72
sim4.VV78X011687.6_1	TC66542	16	transferase family protein	1.02
glimmer.VV78X229312.6_1	TC52364	16	Quercetin 3-O-methyltransferase 1	-1.30
glimmer.VV78X269695.4_1	TC61800	16	Copia-type reverse transcriptase-like protein	-1.69
glimmer.VV78X077202.32_1	TC57520	17	cytochrome P450, putative	0.95
glimmer.VV78X094999.7_5	TC54851	17	Alpha-mannosidase	-0.80
fgenesh.VV78X211751.53_1	TC55912	17	unknown	-0.89
fgenesh.VV78X031549.6_7	TC67067	17	Nucleobase-ascorbate transporter 8	-0.89
glimmer.VV78X093217.9_2	TC63118	18	Na+/solute symporter	1.26
fgenesh.VV78X021565.13_3	TC58160	18	unknown	1.19
glimmer.VV78X110308.50_1	TC59043	18	FLS1 Flavonol synthase/flavanone 3-hydroxylase	1.02
fgenesh.VV78X166662.36_1	TC55124	18	Eukaryotic peptide chain release factor subunit 1-1	0.99
glimmer.VV78X095527.10_1	TC62666	18	GASA1 Gibberellin-regulated protein 1 precursor	0.92
twinscan.VV78X204471.10_3	TC54593	18	Cellulose synthase A catalytic subunit 6 [UDP-forming]	-0.80
glimmer.VV78X110378.12_1	TC53854	18	Putative uncharacterized protein	-0.83
fgenesh.VV78X228317.25_1	TC53468	18	Sugar transport protein 13	-0.84
sim4.VV78X191412.7_1	TC70238	18	Putative histidine decarboxylase	-0.86
fgenesh.VV78X173560.19_8	TC65400	18	Inositol transporter 4	-0.86
fgenesh.VV78X165735.5_1	TC68429	18	Dof zinc finger protein DOF5.3	-0.92
glimmer.VV78X210575.8_1	TC54405	18	Photoreceptor-interacting protein-like; non-phototropic hypocotyl-like protein	-0.98
glimmer.VV78X276728.26_1	CF213967	18	Tubulin alpha-2/alpha-4 chain	-1.07
glimmer.VV78X254995.6_1	TC64723	18	Cysteine proteinase inhibitor 5 precursor	-1.18
fgenesh.VV78X071618.5_2	TC68882	18	unknown	-1.32
glimmer.VV78X026862.5_3	TC61079	18	Tubulin beta-8 chain	-1.41
glimmer.VV78X113451.28_2	TC59949	19	unknown	0.86
fgenesh.VV78X140187.28_4	TC56961	19	Probable glycerophosphoryl diester phosphodiesterase 1 precursor	-0.80
twinscan.VV78X091561.7_4	TC57180	19	Receptor-protein kinase-like protein	-0.88
glimmer.VV78X058295.10_5	TC58996	19	Putative uncharacterized protein	-0.91
glimmer.VV78X252736.11_3	TC65249	19	unknown	-0.97

Gene_ID indicates the gene index of Gene Predictions (http://genomics.research.iasma.it/); New_TC represents the Tentative Consensus, oligonucleotides were re-annotated with the most recent release of the DFCI Grape Gene Index Version 5.0, June 2006. Ratio represents the median log2 values found, ±0.80 corresponding to ±1.75 fold change. Positive ratios correspond to genes that are more expressed in pool "A". Negative ratios correspond to genes that are more expressed in pool "B".

The functional categorization highlighted that in Chardonnay aromatic clone, before that the accumulation of major monoterpenoids (linalool, nerol and geraniol) peaked, there is an higher number of genes encoding proteins implicated in response to abiotic or biotic stimuli, transport, transcription factors, cell wall organization, secondary metabolites and other process in comparison to those identified in the Chardonnay clone 130 (Figures 24 and 25). Among the common functional categories, aromatic clone was represented by 104 elements that have not been found in non-aromatic clone, as reported in figure 29.

Figure 29

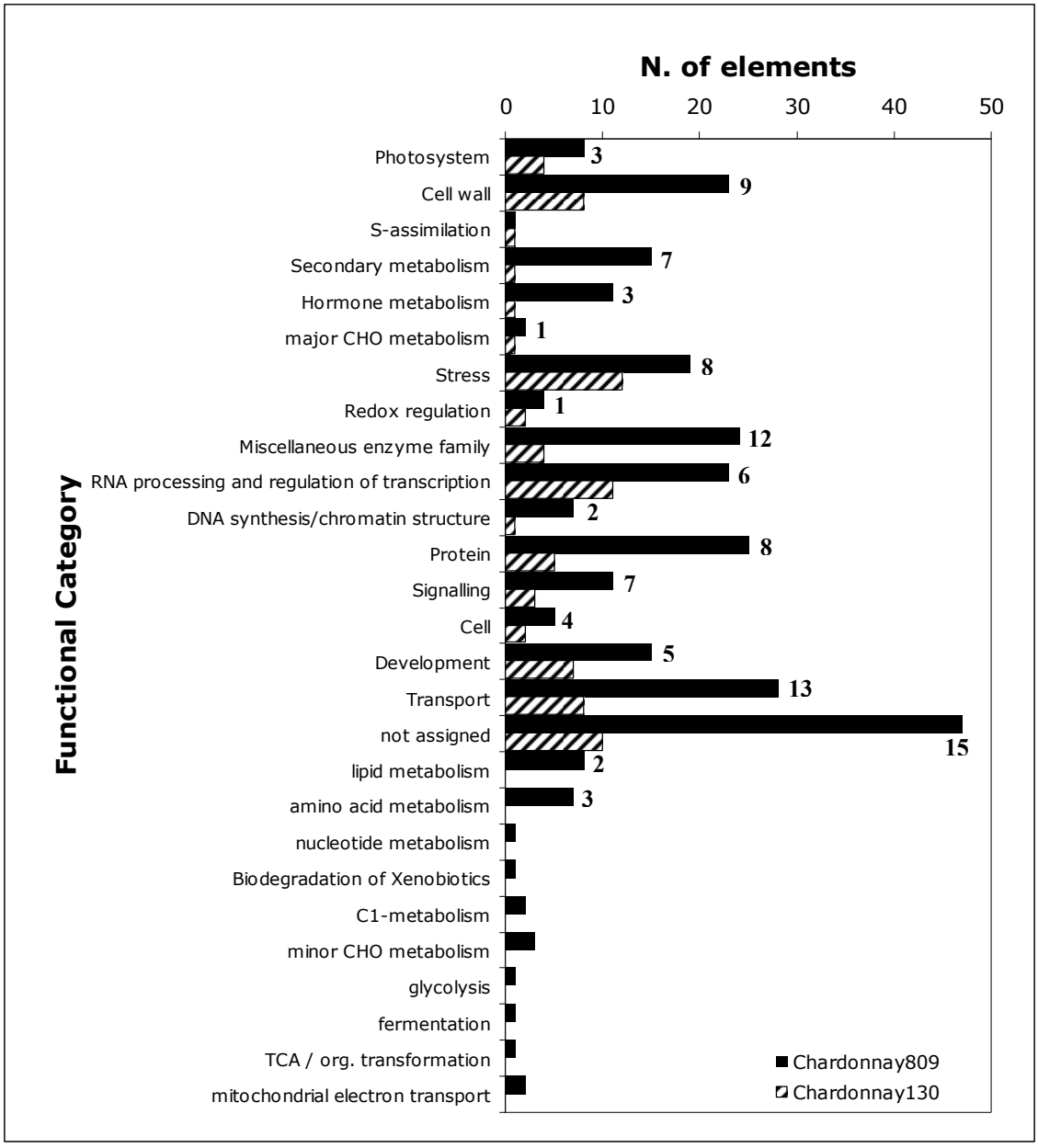

Functional analyses of transcripts differentially express over the course of berry development. Histogramm represent the number of significant genes differentially expressed (p-value<0.01at t-test) grouped by functional category according to their TAIR index annotation (Mapman 2.0). The numbers over the black bars represent the number of annotated unigenes that show two-fold or greater change in transcript abundance in the Chardonnay clone 809.

2.4. Discussion

Origin and development of aroma compounds

The procedures employed in this study allowed the isolation of free monoterpenes by direct extraction of juice from aromatic and non-aromatic grapevine cultivars. Like many fruits, mature grape berries contain numerous non-volatile and non-odorant glycoside compounds whose levels are higher than those of volatile compounds (Baumes et al., 2002). During wine-making, some of these compounds give rise to odorant compounds that play a role in affecting wine 'character'.

After enzymatic hydrolysis of the residual bound monoterpenes from their glycosides, the liberated aglycons can be recovered by a second extraction. In this way, both volatiles and non-volatiles of grape berries were monitored during ripening by analyzing the composition of the berry extracts at 13 different phenological stages for three years.

Berry development was considerably affected by the diverse climatic conditions occurred in the years. Ripening time was similar but not equal in 2005 and 2006. On the contrary, in the warm 2007 season berries development was 10 to 20 days ahead of time, depending on the variety.

Some authors suggested that light and temperature could strongly modify the accumulation of aroma compounds. Kasahara et al. (2002) suggested that the relative contribution of each isoprenoid pathway could vary when either pathway is up- or down-regulated during plant development or in response to environmental conditions.

Carotenoids decrease from the time of *véraison* together with the disappearance of chlorophyll. This is probably due to the modification of chloroplasts that are not transformed into chromoplasts. Bureau et al. (2000) showed that glycosylated C13-norisoprenoids are more abundant at maturity in berries exposed to sunshine for a certain period than in permanently shaded berries. The proportion of compounds that are derived from non-epoxy xanthophylls such as bound 3-hydroxy-7,8-dihydro-α-ionone, 3-oxo-α-ionol and 3-hydroxy-7,8-dihydro-α-ionol is increased by exposing bunches of grapes to sunlight during maturation (Baumes et al., 2002).

In our experiment, free forms of 3 oxo-α-ionol and 3 hydroxy β-damascone were identified and quantified at very low concentration only in Muscat flavoured varieties. However, glycosilated forms were detected in all varieties analysed: 3 oxo-α-ionol

accumulated during ripening and the peak was at stage 41 in Chardonnay clones and at stage 35 in Moscato Bianco, whereas 3 hydroxy β-damascone did not show a continuous pattern of accumulation.

Other major flavour compounds derive from the shikimic acid pathway (Croteau and Karp, 1991) that links carbohydrate metabolism to the synthesis of aromatic amino acids. This pathway can in turn act as precursor for various primary and secondary metabolites, such as benzenoids. Phenylacetaldehyde and phenylethylalcohol are synthesized from phenylalanine, whereas the other volatile benzenoids have *trans*-cinnamic acid (*t*-CA) as the precursor, which is formed from phenylalanine by the activity of phenylalanine ammonia lyase (PAL). The *t*-CA side chain is shortened through the action of the β-oxidative and non-β-oxidative pathways, with benzaldehyde and benzylbenzoate as key intermediates between phenylalanine and benzoic acid.

Accumulation trends of free 2-phenylehanol and benzyl alcohol seem to be identical in the neutral Chardonnay clone 130 and in the aromatic Chardonnay clone 809 as they are probably influenced by environmental conditions.

The variety-environment interaction was shown to affect the synthesis of aroma compounds in different Chardonnay clones (Scienza at al., 1989, Versini et al., 1989). These studies involved clones with high terpenoids content: Chardonnay clone 77 that exhibits considerable fluctuation of monoterpenoids content during berry development; Chardonnay Musquè that presents a certain anticipation of terpenic accumulation with respect to the optimal sugar content for harvest (similarly to our Chardonnay clone 809), and finally two non aromatic clones of Chardonnay (clone 116 and clone 130). These studies proved that in Chardonnay clone 130 free linalool is present at very low content and the peak of bound linalool appears at overripening, as also noted in our study (23 µg/Kg at stage 40).

Looking at the kinetics of monoterpenoids investigated, free *cis* linalool oxide content (furanoid and pyranoid) (OxB and OxD) in the aromatic Chardonnay clone, were only related to the growing stage but slightly. Indeed the trend of free *trans* linalool oxide (furanoid and pyranoid) (OxA and OxC) significantly depended by environmental conditions. Both free *cis*- linalool oxides are less abundant than the free *trans* linalool

oxides, and this difference are even more evident in their glycosides, as reported for Muscat of Alexandria (Wilson et al., 1984).

Chardonnay aromatic clone showed a different accumulation trend in the warm 2007 from stage 33 onward. In 2005 and 2006 seasons free linalool content was similar in terms of kinetic, with the peak of accumulation (150.6 μg/Kg and 147.9 μg/Kg respectively) shifted from stage 36 to stage 37. Instead, during the warm 2007 season free linalool was produced in a lower amount, reaching 99.3 μg/Kg at stage 40.

Accumulation trend of bound linalool was comparable through years, but in 2007 a higher amount was found (440 μg/Kg at stage 40). Free and bound forms of nerol and geraniol were accumulated at higher level in 2007 too.

These results show that bound forms of nerol and geraniol are more susceptible to climatic variation, supporting a different regulation in respect of their free forms and to free and bound linalool. This is also suggested by the fact that bound geraniol accumulated in Chardonnay clone 130 (61.8 μg/Kg at stage 37) only in 2007. The presence of neryl and geranyl glycosides in the fruit compositon and the absence of free nerol and geraniol in neutral varieties were also reported by Wilson et al. (1984). These authors affirmed that glycosides of primary alcohols are expected to be formed enzymatically more readily than those of secondary and tertiary alcohols.

Bound form of *trans* 8-hydroxy linalool of Chardonnay clones showed a positive correlation with bound linalool trend, while bound *cis* 8-hydroxy linalool increased and seemed subjected to a second regulation point independent of linalool content, as also reported by Versini et al. (1989).

The HO-diendiol II and HO-diendiol I + HO-trienol behaviour patterns depend on the variety. In the aromatic clone of Chardonnay both free and bound forms of these two polyols were positively correlated.

In Moscato Bianco the three major monoterpenes, geraniol, linalool and nerol contents continued to increase until a week after the grapes reached the normal technological maturity. Moreover, the rates of increasing observed in the last week were higher than those observed at any other developmental stage. The increasing concentration of the three major bound monoterpenes could be shown despite the plateau in sugar accumulation at berry technological maturity.

With regard to the free and bound linalool, no significant trend variation was seen throughout the season of analysis, however free and bound forms of geraniol showed a different accumulation trend in 2007 season, as seen for Chardonnay clones.

We found that *trans* 8-hydroxy linalool correlates to bound linalool also in Muscat cultivar, instead *cis* 8-hydroxy linalool increased in a different trend in respect of Chardonnay clones.

In Moscato Bianco, free HO-diendiol II and free HO-diendiol I + HO-trienol had interesting inverted accumulation trend, however glycosilic forms showed a positive correlation. Despite free HO-diendiol I + HO-trienol derives from free linalool, they are present at more than 1.5 mg/Kg at berry onset when linalool is not yet produced. This aspect may mean that mechanisms involved in diendiols accumulation are regulated in different ways and at different levels during berries development.

Candidate gene expression and nucleotide sequences

Rodríguez-Concepción et al. (2004) deduced that the activity of the MEP pathway was reduced in etiolated seedlings of Arabidopsis because of the observed low level of expression of genes that encode DXS and DXR, thought the rate-limiting enzymes (Mandel et al., 1996; Estévez et al., 2001; Carretero-Paulet et al., 2002). They also proposed that upon illumination, cryptochrome and phytochrome photoreceptors trigger specific signalling pathways that converge in lighthyposensitive5 (*HY5*) and probably other factors, eventually repressing HMGR gene expression. A distinct phytochrome-specific and *HY5*-independent pathway would transduce the light signal to repress the uptake of cytosolic prenyl diphosphates of developing chloroplasts. In addition, light up regulates the expression of MEP pathway genes (Mandel et al., 1996; Carretero-Paulet et al., 2002), resulting in activated synthesis of plastidial isoprenoids, many of which are key compounds for photosynthesis.

Positive correlation between the level of *DXS* transcript and the production of specific isoprenoids was observed in several other plant systems (Bouvier et al. 1998; Lange et al. 1998; Chahed et al. 2000; Lois et al. 2000; Veau et al. 2000; Walter et al. 2000; Han et al. 2003; Khemvong and Suvachittanont 2005; Gong et al. 2006). Luan and Wüst (2002) analyzed the incorporation of labelled 1-deoxy-D-xylulose into linalool and geraniol in

grape berries and suggested that 1-deoxy-D-xylulose-5-phosphate synthase is a limiting enzyme for plastidic isoprenoid biosynthesis also in grapevine. Furthermore, it is interesting to note that the gene *DXS1* was found differentially expressed during berry ripening, in distinct grape berry tissues and in experiment of grapevines under water-deficit conditions (Grimplet et al. 2007).

The relationship between transcription profile of *DXS1* and monoterpenoids accumulation in the grape berry was investigated in our study targeting the expression of *DXS1* over an extended time course of fruit development. Sampling was started at pre-*véraison* stage and ended at late ripening stage thus covering a period of three months from late July to early October 2006.

In Chardonnay 809, *DXS1* was significantly up-regulated just before the peak of monoterpenoids accumulation (stage 37) while in the non-aromatic Chardonnay clone it was significantly down-regulated only at over-ripening. In Moscato Bianco this gene was considerably up-regulated from 2-3 weeks post *véraison* until stage 38. Our results show that a particular trend of gene expression rather than the level of expression ratio can be more important for this trait. Therefore the comparison of the deduced amino acid sequences of DXS1 revealed that in Chardonnay clones and Pinot Noir no differences are present. Instead the DXS1 of Moscato Bianco shows three amino acid substitutions with respect to DXS1 of Pinot Noir. These non-synonymous polymorphisms may be non-neutral mutations that explain the different accumulation of monoterpenoids between Chardonnay clone 809 and Moscato Bianco..

Other experiments are ongoing in our laboratory on *DXS2* and *DXS3* genes aiming to understand the roles of the *DXS* family on berry development. Further studies are required to investigate the role of these enzymes evaluating the effect of different plant growing conditions such as light exposition and temperature.

Microarray analysis

For a better understanding of the molecular mechanisms responsible for the differences in the aroma profile of the two Chardonnay clones examined in this work, a large scale analysis of their transcriptome has been carried out to identify, in addition to *DXS* genes, several other candidate genes that may have roles in the production of aroma compounds.

Our results pointed out that ripening syndrome is accompained by significant changes in the transcription of large set of genes. These genes have been mainly assigned to functional categories regarding cell wall, protein and secondary metabolisms, and transport but, above all, that including genes associated to responses to biotic and abiotic stresses. For this latter category important changes in terms of transcription has been reported by Deluc et al. (2007) and Pilati et al. (2007); therefore its role in the ripening must be reconsidered. In particular, a sharp activation of transcription has been observed for genes, such as catalases and peroxidases, encoding enzymes responsible for detoxification from H_2O_2 and the other ROS species (Pilati et al., 2007), but also for genes involved in the phenylpropanoid and polyphenols biosynthetic pathway (Deluc et al., 2007) that are strictly related to several abitioc and biotic stresses (Dixon and Paiva, 1995). Our results appear to be consistent for both physiological processes: an increase of a peroxidase-precursor has been detected in both clones (Table 11), while genes involved in the phenylpropanoid and polyphenols biosynthesis (PAL, CAD, 4CL3, FLS, Quercetin 3-O-methyl transferase) were overrepresented in the specific gene set of aromatic clone (table 13B). Many compounds of the phenylpropanoid biosynthetic pathaway are essential for grape berry pigmentation, but some of them (especially phenolic acids) are also involved in the formation of aroma acting as non volatile aroma precursors together with unsaturated lipids, carotenoids, S-cysteine conjugates, glycoconjugates and S-methylmethionine (Baumes 2009). These non-volatile, odorless, constituents are susceptible to transformation into volatile varietal aroma compounds during the biotechnological sequence of wine, from the cellular disorganization of grape berries during harvest to the wine maturation. In this context, the increase of expression of PAL, CAD, 4CL3 indicated that the biosynthetic pathway is addressed to phenolic acid. Note of worthy is, also, the Quercetin 3-O-methyl transferase gene, a member of a methyltransferase gene family, which catalyze the formation of small-molecule methyl esters using S-adenosyl-L-Met (SAM) as a methyl donor and carboxylic acid-bearing substrates as methyl acceptors (Zubieta et al., 2003). In climacteric fruits, hormonal signals activating the transcription of genes involved in biosynthetic pathaways related to stresses are mainly represented by ethylene or jasmonates. In both clone gene sets more expressed are present three genes that showing homology to ethylene transcription factors

(ERFs, table 11). One of them (TC 56399) is similar to a carrot ERF that acts as an activator of PAL gene transcription (Kimura et al., 2007) suggesting that the first steps of phenylpropanoids/polyphenols biosynthetic pathway, as well as the steps regarding anthocyanins (El-Kereamy et al., 2003), is controlled by ethylene. A similar regulation has been suggested for apple in which often the aroma biosynthesis first step, and in all pathways the last steps, is performed by enzymes that are ethylene regulated (Schaffer et al., 2007). In addition to ERFs, an increase of other transcription factors involved in the controlling of transcription of genes related to stresses, as WRKY, have been observed (Table 11). In particular, one showing homology to WRKY 25 of *Arabidopsis*, is more expressed in the aromatic clone. The WRKY 25 factor appear to be induce in many vegetative organ by the exposure to UV light (Winter et al., 2007). As previously mentionated a significant relationship has been found that UV are able to modulate the biosynthesis of some carotenoids that are believed to be precursors of β-damascenone, vitispirane and other C_{13}-norisoprenoid. In the aromatic clone a higher concentration of C_{13}-norisoprenoid has been detected, if WRKY 25-like transcription factor is one of element regulating the biosynthesis of these metabolite, it will be investigated. The level of aromatic coumpunds, as well as other metabolites, is not only associated to their synthesis but, also, to their transport, conjugation and degradation. Among the genes showing a differential expression in the two pool samples considered in this work, those involved in the trasport are highly represent. Membres of Glutatione S-transpherases (GSTs) and ABC families appear to be those showing more significant changes. GSTs play a pivotal role in the detoxification processes and redox buffering. The analysis of different plant genomes indicate that there are 25 or more genes coding for GSTs, and some studies demonstrated that GSTs have a role to conjugate metabolites arising from oxidative damage products like cytotoxic alkenals derived from the peroxidation of natural products or exogenous compounds such as phytotoxins produced by competing plants and through of microbial pathogen activity. The latter is the case of some thiols that are produced during fermentation starting from a cysteine-conjugate of the final thiolated aroma compound. It has been hypothesised that the production of the final precursor involves the action of a class glutathione-S-transferases acting in the vacuolar compartiment (Winefield et al., 2006). These coumpund are typical of Cabernet

Sauvignon aroma, but is not possible to exclude that GSTs might play a similar role also for other aromatic substances. Also, the large number of ABC transporter genes in *Arabidopsis* and in other plants underlined the hypothesis that these transporters are involved in the compartmentalisation of secondary metabolism (Sánchez-Fernández et al., 2001). In grape, they have been involved in the traasportation of anthocyanins and carotenoids that can be acting as precursor of some important aromatic compounds (Grimplet et al., 2007).

In conclusion the application of this large scale analysis of transcriptome allowed to identify putative genes having a role in the formation of aroma that can be exploited for hypothesis testing by traditional functional assays to improve our understanding of this complex process and to ultimately utilize this information to improve quality traits of wine grapes.

References

Baumes, R.; Wirth, J.; Bureau, S.; Gunata, Y.; Razungles, A (2002) Biogeneration of C13-norisoprenoid compounds: experiments supportive for an apo-carotenoid pathway in grapevines. Anal. Chim. Acta 2002, 458, 3-14

Baumes R. (2009) Wine Aroma Precursors. In Wine Chemistry and Biochemistry. Eds Moreno-Arribas M.V. and Polo M.C. Springer New York Publisher. pp 251-274. 2009 DOI 10.1007/978-0-387-74118-5

Bendtsen JD, Nielsen H, von Heijne G, Brunak S (2004) Improved prediction of signal peptides: SignalP 3.0. J Mol Biol 340:783–795

Birney E, Clamp M, Durbin R (2004) GeneWise and genomewise. Genome Res 14:988–995

Bouvier F, d'Harlingue A, Suire C, Backhaus RA, Camara B (1998) Dedicated roles of plastid transketolases during the early onset of isoprenoid biogenesis in pepper fruits. Plant Physiol 117:1423–1431

Chahed K, Oudin A, Guivarc'h N, Hamdi S, Chénieux JC, Rideau M, Clastre M (2000) 1-deoxy-D-xylulose 5-phosphate synthase from periwinkle: cDNA identification and induced gene expression in terpenoid indole alkaloid-producing cells. Plant Physiol Biochem 38:559–566

Chervin C, El-Kereamy A, Roustan J-P, Latche A, Lamon J, Bouzayen M: Ethylene seems required for the berry development and ripening in grape, a non-climacteric fruit. Plant Science 2004, 167:1301-1305.

Churchill GA, Doerge RW (1994) Empirical threshold values for quantitative trait mapping. Genetics 138:963–971

Clastre M, Bantignies B, Feron G, Soler E, Ambid C (1993) Purification and characterization of geranyl diphosphate synthase from *Vitis vinifera* L. cv Muscat de Frontignan cell cultures. Plant Physiol 102:205–211

Coombe, B.G. (1995) Adoption of a system for identifying grapevine growth stages. Australian Journal of Grape and Wine Research 1, 100–110.

Coombe, B.G. and Iland, P.G. (2004) Grape berry development and winegrape quality. In: Viticulture. Volume 1 – Resources. Eds P.R. Dry and B.G. Coombe. (Winetitles: Adelaide) pp. 210–248.

Costantini L, Battilana J, Lamaj F, Fanizza G, Grando MS (2008) Berry and phenology-related traits in grapevine (*Vitis vinifera* L.): from Quantitative Trait Loci to underlying genes. BMC Plant Biology 8:38

Crespan M, Milani N (2001) The Muscats: a molecular analysis of synonyms, homonyms and genetic relationships within a large family of grapevine cultivars. Vitis 40:23–30

da Silva FG, Iandolino A, Al-Kayal F, Bohlmann MC, Cushman MA, Lim H, Ergul A, Figueroa R, Kabuloglu EK, Osborne C, Rowe J, Tattersall E, Leslie A, Xu J, Baek J, Cramer GR, Cushman JC, Cook DR (2005) Characterizing the grape transcriptome. Analysis of expressed sequence tags from multiple Vitis species and development of a compendium of gene expression during berry development. Plant Physiol 139:574–597

Deluc, L.G., Grimplet, J., Wheatley, M.D., TillEtt, R.L., Quilici, D.R., Osborne, C. et al. (2007) Transcriptomic and metabolite analyses of Cabernet Sauvignon grape berry development. BMC Genomics 8: 429.

Dixon R.A. and Paiva N.L (1995) Stress-lnduced Phenylpropanoid Metabolism. Plant Cell, 7: 1085-1097

Doligez A, Audiot E, Baumes R, This P (2006) QTLs for muscat flavour and monoterpenic odorant content in grapevine (*Vitis vinifera* L.). Mol Breeding 18:109–125

Don RH, Cox PT, Wainwright BJ, Baker K, Mattick JS (1991) 'Touchdown' PCR to circumvent spurious priming during gene amplification. Nucleic Acids Res 19:4008

Ebang-Oke JP, de Billerbeck GM, Ambid C (2003) Temporal expression of the Lis gene from *Vitis vinifera* L., cv. Muscat de Frontignan. In: Le Quéré JL, Etiévant PX (eds) Proceedings of the 10th Weurman Flavour Research Symposium "Flavour research at the dawn of the twenty-first century", Beaune (France), 25–28 June 2002. Lavoisier, Paris, France, pp 321–325

El-Kereamy A, Chervin C, Roustan J-P, Cheynier V, Souquet J-M, Moutounet M, Raynal J, Ford C, Latche A, Pech J-C, Bouzayen M: Exogenous ethylenestimulates the long-term expression of genes related to anthocyanin biosynthesis in grape berries. Physiol Plant 2003, 119:175-18

Estevéz JM, Cantero A, Romero C, Kawaide H, Jiménez LF, Kuzuyama T, Seto H, Kamiya Y, León P (2000) Analysis of the expression of CLA1, a gene that encodes the

1-deoxyxylulose 5-phosphate synthase of the 2-C-methyl-D-erythritol-4-phosphate pathway in Arabidopsis. Plant Physiol 124:95–103

Estévez JM, Cantero A, Reindl A, Reichler S, Leo P (2001) 1-deoxy-D-xylulose-5-phosphate synthase, a limiting enzyme for plastidic isoprenoid biosynthesis in plants. J Biol Chem 276:22901–22909

Gong YF, Liao ZH, Guo BH, Sun XF, Tang KX (2006) Molecular cloning and expression profile analysis of Ginkgo biloba *DXS* gene encoding 1-deoxy-D-xylulose 5-phosphate synthase, the first committed enzyme of the 2-C-methyl-D-erythritol 4-phosphate pathway. Planta Med 72:329–335

Grando MS, Bellin D, Edwards KJ, Pozzi C, Stefanini M, Velasco R (2003) Molecular linkage maps of *Vitis vinifera* L. and *V. riparia* Mchx. Theor Appl Genet 106:1213–1224.

Grimplet J, Deluc LG, Tillett RL, Wheatley MD, Schlauch KA, Cramer GR, Cushman JC (2007) Tissue-specific mRNA expression profiling in grape berry tissues. BMC Genomics 8:187 doi:10.1186/1471-2164-8-187

Guardiola J, Iborra JL, Rodenas L, Canovas M (1996) Biotransformation from geraniol to nerol by immobilized cells (V. vinifera). Appl Biochem Biotechnol 56:169–180

Günata Z, Biron C, Sapis JC, Bayonove C (1989) Glycosidase activities in sound and rotten grapes in relation to hydrolysis of grape monoterpenyl glycosides. Vitis 28:191-197

Hoballah, M.E., Stuurman, J., Turlings, T.C., Guerin, P.M., Connetable, S. and Kuhlemeier, C. (2005) The composition and timing of flower odour emission by wild Petunia axillaris coincide with the antennal perception and nocturnal activity of the pollinator Manduca sexta. Planta 222, 141–150.

Hahn FM, Eubanks LM, Testa CA, Blagg BSJ, Baker JA, Poulter CD (2001) 1-Deoxy-D-xylulose 5-phosphate synthase, the gene product of open reading frame (ORF) 2816 and ORF 2895 in Rhodobacter capsulatus. J Bacteriol 183:1–11

Han YS, Roytrakul S, Verberne MC, van der Heijden R, Linthorst HJM, Verpoorte R (2003) Cloning of a cDNA encoding 1-deoxy-D-xylulose 5-phosphate synthase from Morinda citrifolia and analysis of its expression in relation to anthraquinone accumulation. Plant Sci 164:911–917

Huang X, Madan A (1999) CAP3: a DNA sequence assembling program. Genome Res 9:868–877

Jaillon O, Aury JM, Noel B, Policriti A, Clepet C, Casagrande A, Choisne N, Aubourg S, Vitulo N, Jubin C, Vezzi A, Legeai F, Hugueney P, Dasilva C, Horner D, Mica E, Jublot D, Poulain J, Bruyère C, Billault A, Segurens B, Gouyvenoux M, Ugarte E, Cattonaro F, Anthouard V, Vico V, Del Fabbro C, Alaux M, Di Gaspero G, Dumas V, Felice N, Paillard S, Juman I, Moroldo M, Scalabrin S, Canaguier A, Le Clainche I, Malacrida G, Durand E, Pesole G, Laucou V, Chatelet P, Merdinoglu D, Delledonne M, Pezzotti M, Lecharny A, Scarpelli C, Artiguenave F, Pè ME, Valle G, Morgante M, Caboche M, Adam-Blondon AF, Weissenbach J, Quétier F, Wincker P (2007) The grapevine genome sequence suggests ancestral hexaploidization in major angiosperm phyla. Nature 449:463–467

Kasahara, H., Hanada, A., Kuzuyama, T., Takagi, M., Kamiya, Y., and Yamaguchi, S. (2002). Contribution of the mevalonate and methylerythritol phosphate pathways to the biosynthesis of gibberellins in Arabidopsis. J. Biol. Chem. 277, 45188–45194.

Khemvong S, Suvachittanont W (2005) Molecular cloning and expression of a cDNA encoding 1-deoxy-D-xylulose-5-phosphate synthase from oil palm Elaeis guineensis Jacq. Plant Sci 169:571–578

Kim BR, Kim SU, Chang YJ (2005) Differential expression of three 1-deoxy-D-xylulose-5-phosphate synthase genes in rice. Biotechnol Lett 27:997–1001

Kim SM, Kuzuyama T, Chang YJ, Song KS, Kim SU (2006) Identification of class 2 1-deoxy-D-xylulose 5-phosphate synthase and 1-deoxy-D-xylulose 5-phosphate reductoisomerase genes from Ginkgo biloba and their transcription in embryo culture with respect to ginkgolide biosynthesis. Planta Med 72:234–240

Kimura S., Chikagawa Y., Kato M., Maeda K., Ozeki Y. (2007) Upregulation of the promoter activity of the carrot (*Daucus carota*) phenylalanine ammonia-lyase gene (DcPAL3) is caused by new members of the transcriptional regulatory proteins, DcERF1 and DcERF2, which bind to the GCC-box homolog and act as an activator to the DcPAL3 promoter. Journal of Plant Research (5)121: 499-508

Kolosova, N., Sherman, D., Karlson, D. and Dudareva, N. (2001) Cellular and subcellular localization of S-adenosyl-Lmethionine: benzoic acid carboxyl methyltransferase, the

enzyme responsible for biosynthesis of the volatile ester methylbenzoate in snapdragon flowers. Plant Physiol. 126, 956–964

Lander ES, Botstein D (1989) Mapping mendelian factors underlying quantitative traits using RFLP linkage maps. Genetics 121:185–199

Lange BM, Ghassemian M (2003) Genome organization in Arabidopsis thaliana: a survey for genes involved in isoprenoid and chlorophyll metabolism. Plant Mol Biol 51:925–948

Lange BM, Wildung MR, McCaskill D, Croteau R (1998) A family of transketolases that directs isoprenoid biosynthesis via a mevalonate-independent pathway. Proc Natl Acad Sci USA 95:2100–2104

Li W, Godzik A (2006) Cd-hit: a fast program for clustering and comparing large sets of protein or nucleotide sequences. Bioinformatics 22:1658–1659

Lichtenthaler HK (1999) The 1-deoxy-D-xylulose-5-phosphate pathway of isoprenoid biosynthesis in plants. Annu Rev Plant Physiol Plant Mol Biol 50:47–65

Lois LM, Rodríguez-Concepción M, Gallego F, Campos N, Boronat A (2000) Carotenoid biosynthesis during tomato fruit development: regulatory role of 1-deoxy-D-xylulose 5-phosphate synthase. Plant J 22:503–513

Luan F, Wüst M (2002) Differential incorporation of 1-deoxy-D-xylulose into (3S)-linalool and geraniol in grape berry exocarp and mesocarp. Phytochemistry 60:451–459

Luan F, Mosandl A, Münch A, Wüst M (2005) Metabolism of geraniol in grape berry mesocarp of *Vitis vinifera* L. cv. Scheurebe: demonstration of stereoselective reduction, E/Z-isomerization, oxidation and glycosylation. Phytochemistry 66:295–303

Lücker J, Bowen P, Bohlmann J (2004) *Vitis vinifera* terpenoid cyclases: functional identification of two sesquiterpene synthase cDNAs encoding (+)-valencene synthase and (-)-germacrene D synthase and expression of mono- and sesquiterpene synthases in grapevine flowers and berries. Phytochemistry 65:2649–2659

Mahmoud SS, Croteau RB (2002) Strategies for transgenic manipulation of monoterpene biosynthesis in plants. Trends Plant Sci 7:366–373

Martin DM, Bohlmann J (2004) Identification of *Vitis vinifera* (-)-α-terpineol synthase by in silico screening of full-length cDNA ESTs and functional characterization of recombinant terpene synthase. Phytochemistry 65:1223–1229

Mateo JJ, Jiménez M (2000) Monoterpene in grape juice and wines. J Chromatogr 881:557–567

Mathieu S, Terrier N, Procureur J, Bigey F, Günata Z (2005) A Carotenoid Cleavage Dioxygenase from *Vitis vinifera* L.: functional characterization and expression during grape berry development in relation to C13-norisoprenoid accumulation. J Exp Bot 56:2721–2731

Morgante M, Salamini F (2003) From plant genomics to breeding practice. Curr Opin Biotech 14:214–219

Morreel K, Goeminne G, Storme V, Sterck L, Ralph J, Coppieters W, Breyne P, Steenackers M, Georges M, Messens E, Boerjan W (2006) Genetical metabolomics of flavonoid biosynthesis in Populus: a case study. Plant J 47:224–237

Murakami S, Kondo Y, Nakano T, Sato F (2000) Protease activity of CND41, a chloroplast nucleoid DNA-binding protein, isolated from cultured tobacco cells. FEBS Lett 468:15–18

Nakano T, Murakami S, Shoji T, Yoshida S, Yamada Y, Sato F (1997) A novel protein with DNA binding activity from tobacco chloroplast nucleoids. Plant Cell 9:1673–1682

Nakano T, Nagata N, Kimura T, Sekimoto M, Kawaide H, Murakami S, Kaneko Y, Matsushima H, Kamiya Y, Sato F, Yoshida S (2003) CND41, a chloroplast nucleoid protein that regulates plastid development, causes reduced gibberellin content and dwarfism in tobacco. Physiol Plantarum 117:130–136

Paran I, Zamir D (2003) Quantitative traits in plants: beyond the QTL. Trends Genet 19:303–306

Pflieger S, Lefebvre V, Causse M (2001) The candidate gene approach in plant genetics: a review. Mol Breed 7:275–291

Phillips MA, Walter MH, Ralph SG, Dabrowska P, Luck K, Urós EM, Boland W, Strack D, Rodríguez-Concepción M, Bohlmann J, Gershenzon J (2007) Functional identification and differential expression of 1-deoxy-D-xylulose 5-phosphate synthase

in induced terpenoid resin formation of Norway spruce (Picea abies). Plant Mol Biol 65:243-257

Pilati S, Perazzolli M, Malossini A, Cestaro A, Dematte L, Fontana P, Dal Ri A, Viola R, Velasco R, Moser C (2007) Genome-wide transcriptional analysis of grapevine berry ripening reveals a set of genes similarly modulated during three seasons and the occurrence of an oxidative burst at vèraison. BMC Genomics 8:428

Price AH (2006) Believe it or not, QTLs are accurate! Trends Plant Sci 11:213-216

Remington DL, Ungerer MC, Purugganan MD (2001) Map-based cloning of quantitative trait loci: progress and prospects. Genet Res Camb 78:213–218

Ribérau-Gayon P, Boidron JN, Terrier A (1975) Aroma of muscat grape varieties. J Agric Food Chem 23:1042–1047

Ribéreau-Gayon P, Glories Y, Maujean A, Dubourdieu D (2000) The chemistry of wine: stabilization and treatments. In: Wiley J and Sons Ltd (eds) Handbook of enology volume 2, pp 187–206

Rodríguez-Concepción M, Boronat A (2002) Elucidation of the methylerythritol phosphate pathway for isoprenoid biosynthesis in bacteria and plastids. A metabolic milestone achieved through genomics. Plant Physiol 130:1079–1089

Salamov A, Solovyev V (2000) Ab initio gene finding in Drosophila genomic DNA. Genome Res 10:516–522

Salvi S, Tuberosa R (2005) To clone or not to clone plant QTLs: present and future challenges. Trends Plant Sci 10:297–304

Sánchez-Fernández R, Davies TG, Coleman JO, Rea PA (2001): The Arabidopsisthaliana ABC protein superfamily, a complete inventory.J Biol Chem 2001, 276:30231-30244

Scienza A., Versini G., Romano F.A. (1989). Considerations sur l'influence du genotipe et du milieu sur la synthese des aromes dans les raisins – cas particulier du Chardonnay. Proceed. Intern. Symp. on 'The aromatic substances in grapes and wines', San Michele all'Adige, June 25-27, 1987, A. Scienza & G. Versini Eds., Manfrini, Calliano (TN), pp. 9-54

Schaffer R.J, Friel E.N., Souleyre E.J.F., Bolitho K., Thodey K., Ledger S., Bowen J.H., Ma J-H., Nain B., Cohen D,, Gleave A.P., Crowhurst R.N., Janssen B.J., Yao J-L. Newcomb R.D. (2007). A genomics approach reveals that aroma production in apple is

controlled by ethylene predominantly at the final step in each biosynthetic pathway. Plant Physiology, 144: 1899-1912

Schmitz-Hoerner, R. and Weissenbock, G. (2003) Contribution of phenolic compounds to theUV-Bscreening capacity of developing barley primary leaves in relation toDNAdamage and repair under elevated UV-B levels. Phytochemistry 64, 243–255.

Sanguinetti CJ, Dias Neto E, Simpson AJ (1994) Rapid silver staining and recovery of PCR products separated on polyacrylamide gels. Biotechniques 17:914–921

Sevini F, Marino R, Grando MS, Moser S, Versini G (2004) Mapping candidate genes and QTLs for aroma content in grape. Acta Hortic 652:439-446

Slaughter JC: The naturally occurring furanones: formation and function from pheromone to food. Biol Rev Camb Philos Soc 1999, 74:259-276.

Small I, Peeters N, Legeai F, Lurin C (2004) Predotar: A tool for rapidly screening proteomes for N-terminal targeting sequences. Proteomics 4:1581–1590

Strauss CR, Wilson B, Gooley PR, Williams PJ (1986) Role of monoterpenes in grape and wine flavour. In: Parliament T, Croteau R (eds) Biogeneration of aromas. American Chemical Society, Washington DC, pp 222–242

Van Ooijen JW, Boer MP, Jansen RC, Maliepaard C (2002) MapQTL® 4.0 Software for the calculation of QTL positions on genetic maps. Plant Research International, Wageningen, the Netherlands

Veau B, Courtois M, Oudin A, Chénieux JC, Rideau M, Clastre M (2000) Cloning and expression of cDNAs encoding two enzymes of the MEP pathway in Catharanthus roseus. BBA-Gene Struct Expr 1517:159–163

Velasco R, Zharkikh A, Troggio M, Cartwright DA, Cestaro A, Pruss D, Pindo M, FitzGerald LM, Vezzulli S, Reid J, Malacarne G, Iliev D, Coppola G, Wardell B, Micheletti D, Macalma T, Facci M, Mitchell JT, Perazzolli M, Eldredge G, Gatto P, Oyzerski R, Moretto M, Gutin N, Stefanini M, Chen Y, Segala C, Davenport C, Demattè L, Mraz A, Battilana J, Stormo K, Costa F, Tao Q, Si-Ammour A, Harkins T, Lackey A, Perbost C, Taillon B, Stella A, Solovyev V, Fawcett J, Sterck L, Vandepoele K, Grando MS, Toppo S, Moser C, Lanchbury J, Bogden R, Skolnick M, Sgaramella V, Bhatnagar SK, Fontana P, Gutin A, Van de Peer Y, Salamini F, Viola R

(2007) A high quality draft consensus sequence of the genome of a heterozygous grapevine variety. PLoSONE 2(12):e1326

Versini G, Dalla Serra A, Dell'Eva M, Scienza A, Rapp A (1988) Evidence of some glycosidically bound new monoterpenes and norisoprenoids in grapes. In: Schreier P (ed) Bioflavour '87. W de Gruyter, Berlin, Germany, pp 161-170

Versini G, Dalla Serra A, Monetti A, De Micheli L, Mattivi F (1993) Free and bound grape aroma profiles variability within the family of muscat-called varieties. In: Bayonove C, Crouzet J, Flanzy C, Martin JC, Sapis JC (eds) Proceedings of the International Symposium ''Connaissance aromatique des cépages et qualité des vins'', Montpellier (France), 9–10 February 1993. Revue Française d'Oenologie, Lattes, France, pp 12–21

Wagner R (1967) Etude de quelques disjonctions dans des descendances de Chasselas, Muscat Ottonel et Muscat à petits grains. Vitis 6:353–363

Walter MH, Fester T, Strack D (2000) Arbuscolar mycorrhizal fungi induce the non-mevalonate methylerythritol phosphate pathway of isoprenoid biosynthesis correlated with accumulation of the 'yellow pigment' and other apocarotenoids. Plant J 21:571–578

Walter MH, Hans J, Strack D (2002) Two distantly related genes encoding 1-deoxy-D-xylulose 5-phosphate synthases: differential regulation in shoots and apocarotenoid-accumulating mycorrhizal roots. Plant J 31:243–254

Winefield, C; Cartwright, J; Mitchell, N; Trought, M; Jordan, B. (2006) Characterisation of the biochemical pathway responsible for the formation of glutathione–aroma compound conjugates from Sauvignon blanc grapes Proceedings of the 8th International Congress of Plant Molecular Biology. Adelaide, Australia.

Winter D., Vinegar B., Nahal H., Ammar R., Wilson G., Provart N.J. (2007) An Electronic Fluorescent Pictograph" Browser for Exploring and Analyzing Large-Scale Biological Data Sets. PLoS ONE 2(8): e718 doi:10.1371/journal.pone.0000718

Winterhalter P. and Rouseff R. (2000) Carotenoid-derived aroma compounds: an introduction, in: Proceedings of the 219th ACS National Meeting, San Francisco, CA, 2000.

Wungsintaweekul J, Sirisuntipong T, Kongduang D, Losuphanporn T, Ounaroon A, Tansakul P, De-Eknamkul (2008) Transcription profiles analysis of genes encoding 1-deoxy-D-xylulose 5-phosphate synthase and 2C-methyl-D-erythritol 4-phosphate synthase in plaunotol biosynthesis from Croton stellatopilosus. Biol Pharm Bull 31:842-85

Zubieta C, Ross JR, Koscheski P, Yang Y, Pichersky E, Noel JP (2003) Structural basis for substrate recognition in the salicylic acid carboxyl methyltransferase family. Plant Cell 2003, 15:1704-1716.82

Ringraziamenti

Desidero ringraziare la Dr.ssa Stella Grando ed il Dr. Claudio Bonghi per l'appoggio, la fiducia e il grandissimo aiuto che mi hanno dato durante il dottorato.

Ringrazio il Dr. Sergio Moser, la Dr.ssa Flavia Gasperi ed il Prof. Giuseppe Versini per gli utilissimi consigli ed il supporto che mi hanno dato nell'interpretazione dei dati relativi all'analisi dei terpeni. Ringrazio il Dr. Mario Malacarne ed Emanuela Betta per il loro fondamentale aiuto nelle analisi chimiche. La Dr.ssa Costantini Laura che mi ha aiutato nella stesura del primo capitolo della tesi. Un particolare ringraziamento ad Alessandro, Paolo e Marco per il sostegno ed i loro preziosissimi consigli bioinformatici.

Desidero ringraziare Il Dr. Fabio Massimo Rizzini per l'aiuto che mi ha dato durante il mio periodo di permanenza nei laboratori del Dipartimento di Agronomia Ambientale e Scienze di Produzioni vegetali del Prof. Angelo Ramina, il quale ringrazio per la disponibilità datami.

Ringrazio Francesco Emanuelli per la stima e l'amicizia, non sarei stato in grado superare certi ostacoli senza il suo sostegno. Ringrazio Maddalena Sordo per il supporto morale e la pazienza.

Ringrazio tutti gli amici/colleghi di S.Michele: Massimo, Alberto, Luca, Flavia, Jessica, Sara L., Moreno, Giusy, Giulia, Pamela, Sara C., Alessandra, Silvia, Paolo e Domenico con i quali ho condiviso molti momenti di gioia.

Ringrazio i miei genitori che nonostante il mio carattere insopportabile mi son sempre vicini.

Inoltre ringrazio le due persone che porto sempre con me nel cuore, alle quali ho dedicato questa tesi: mio fratellino Mattia e Silvia. Vi ringrazio di esistere.